GEM TN-92-220

SSCintCal Meeting - SSCL

Jim Reidy, Editor
University of Mississippi

October 22-23, 1992

Abstract:

Agenda and presentations of the GEM SSCintCal Meeting held at the SSC Laboratory on October 22 and 23, 1992. Agenda items are: Overview of SSCintCal; Report from Bill Willis' Committee; SSCintCal R&D Goals for Next Year; Institutional Responsibilities; Discussion with Bill Willis; Institutional Responsibilities Continued; Discussion of Engineering Responsibilities; Discussion of GEM-Calorimeter Optimization; Simulation Results; and Future Plans for Simulation.

10/22/92 R&D

9:00 Overview of SSCintCAL (Paar/Sulak)
Discussion.

9:15 Report from Bill Willis' committee (Branson/Sulak)
Discussion.

9:45 SSCintCAL R&D goals for next year
Engineering (Rennich)
Simulation (Carey, Kamyshkov, Moore)
Testbeam plans (Yost)
Prototype work (Paar/Sulak)
Radiation Damage (Young)
Discussion.

10:30 Break

11:00 Institutional responsibilities (Paar/Sulak)
Tasks for each Institution
Budget for each Institution

12:00 Lunch

13:00 Discussion with Bill Willis

14:00 Institutional responsibilities, continued

15:00 Discussion of engineering responsibilities (Rennich)

16:00 Break

16:30 Discussion of GEM-Calorimeter optimization
SSCintCAL position on noble liquid hadron calorimeter and fiber logs
Studies and action items

18:00 Dinner
Continue discussions

10/23/92 R&D

9:00 Simulation Results
GEM calorimeter (Kamyshkov, Savin, Shmakov et al)
BU stack (Carey et al, Moore et al)
Fiber/absorber ratio and e/h (Wigmans)
Muon issues (McNeil)
Calorimeter optimization (all)

11:00 Future plans for simulation (all)
Integration with em and muon detectors

12:30 Lunch

Open period

SSCintCAL R & D Tasks for 4/1/93-3/31/93

A full scale integrated em and had cal prototype must be designed, constructed, and tested during the next year. Radiation damage, simulation, and engineering should go on in parallel. Other issues like readout, optical coupling, testbeam will be driven by the prototype program.

The instsitutionalk assignments of the various tasks follow below.

Cu procurement	BU
Cu groving	BU
Fiber procurement and quality control	UCSD
Fiber mirroring	TTU
Calibration system	UCSD, FairU, UTenn
Longitudinal segmentation issues	UCSD
Tower assembly	BU, UCSD
Cosmic ray testing of modules	UCSD, TTU, UMiss
Testbeam infrastructure	BU, FairU, IowaU, LSU, ORNL, TTU, UCSD, UMiss, UTenn
PM development	IowaU, FairU, UCSD
PM base development and HV distribution	IowaU, USFQ
Pre-amp shaper development	BU, ORNL
Optical coupling	TTU, UMiss
Detector optimization and MC simulation	BU, UMiss, ORNL, TTU
Radiation hardness studies	ORNL, UMiss, UFlor
Systems integration	BU, ORNL, TAM
Muon system issues and integration	BU, LSU
Massless gap detector	UMiss, ORNL

BUDGET

	10/24/92	last yr	#PhD-FTEs	$$ / PhD-FTE
BU	255 [2] + 210	320	0.5 + 3.2	510 + 66
FairU	40 * [1]	40	0.5	80
UFlor	20	0	0.2	100
IowaU	117	65	1.5	78
LSU	20	20	?	?
UMiss	165 *	53	3.0	55
MSU	20	69	?	?
ORNL	350 [2] + 88 *[2]	100	6.0 + 1.0	60 + 88
UTenn	50	29	?	?
TAM	35	0	?	?
TTU	105 [3]	65	1.5	70
UCSD	50 [2] + 220	94	0.5 + 3.0	100 + 73
	--- +	--- +	--- +	--- +
Total	305 + 1090	855	7.0 + 14.0	305 + 77

Footnotes:

1. received $70k interim funding
2. will be a separate proposal
3. received $60k interim funding

Willis' New Calorimeter Design

a). Shown by Willis

b). Study Responsibility for SSCintCal

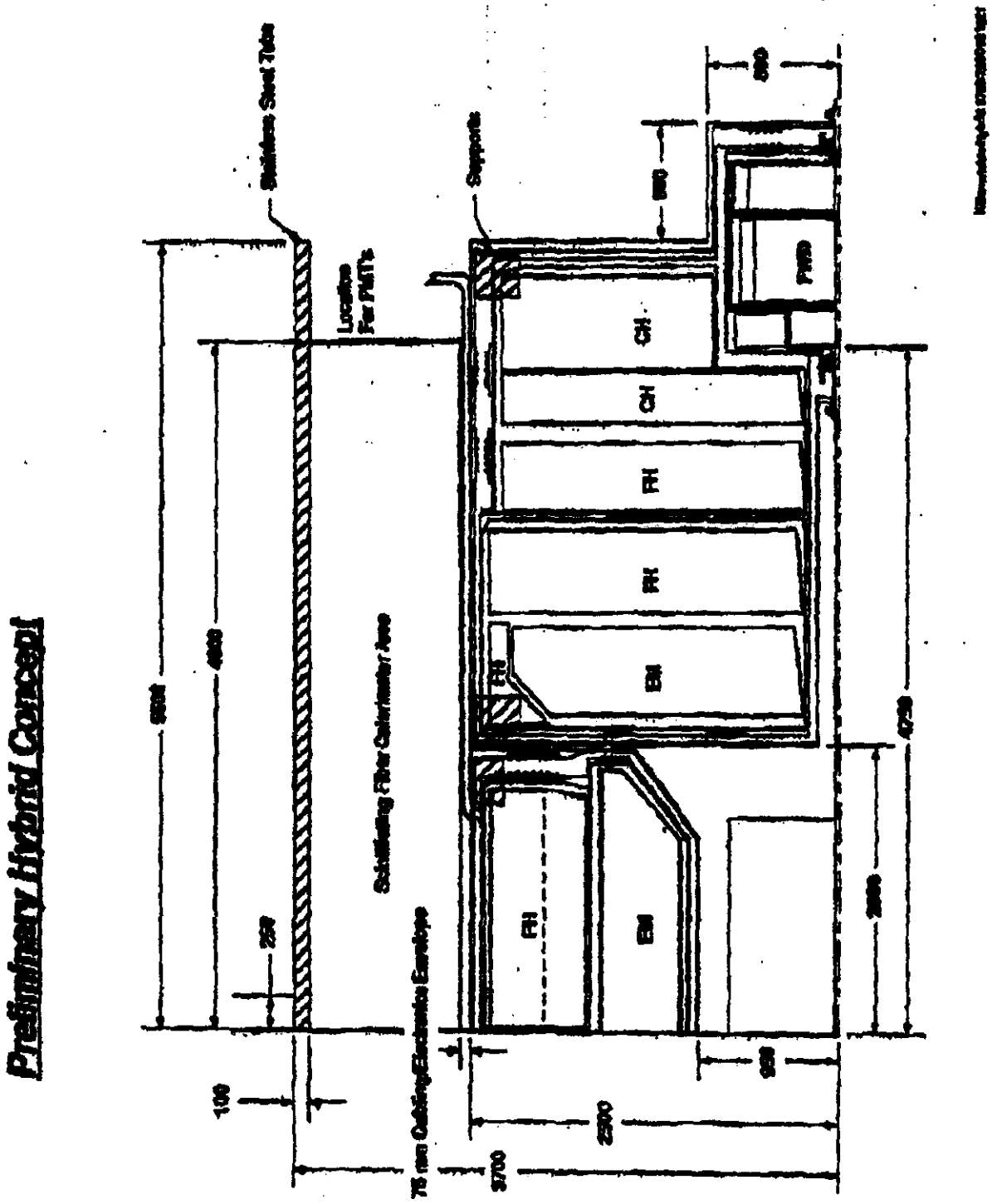
Preliminary Hybrid Concept
Stainless Steel Tube
Supports
Location For PMT's
Scintillating Fiber Calorimeter Area
75 mm Cabling/Electronics Envelope
CH
CH
FH
FH
EM
FH
EM
FWD
100
2500
3700

(a) 7

INTEGRATED

Preliminary Hybrid Concept

JR, YK n-occupancy
ORNL inner radius
ORNL corner (A) and E_T
R cost

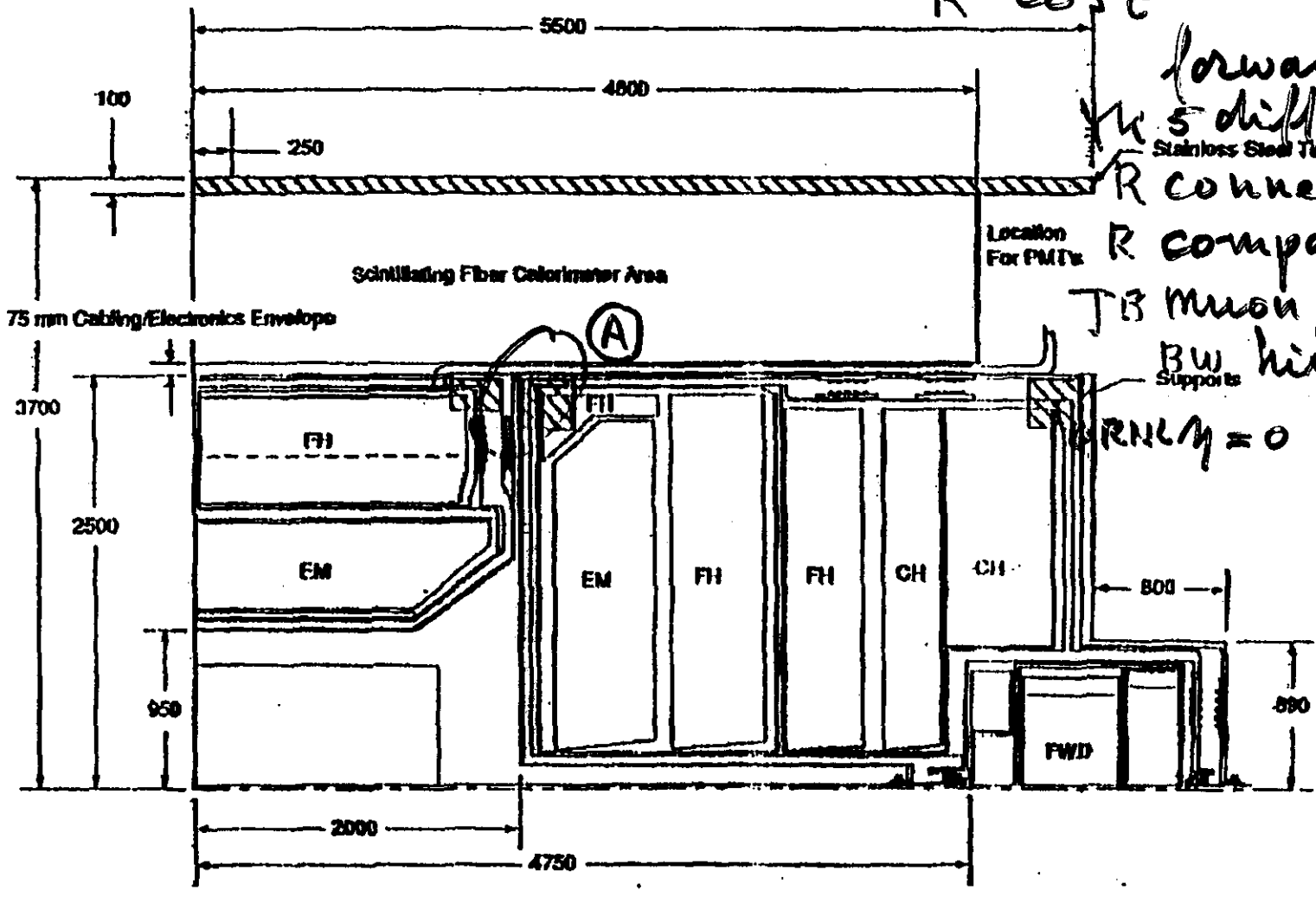

forward region
YK 5 diff had as $f(\eta)$
R connectors
R compactness
JB muon tracking
BW high luminosit
ORNL $\eta = 0$ dead region

(b)

8

K. Shmakov

Missing E_T in Cryostat Walls

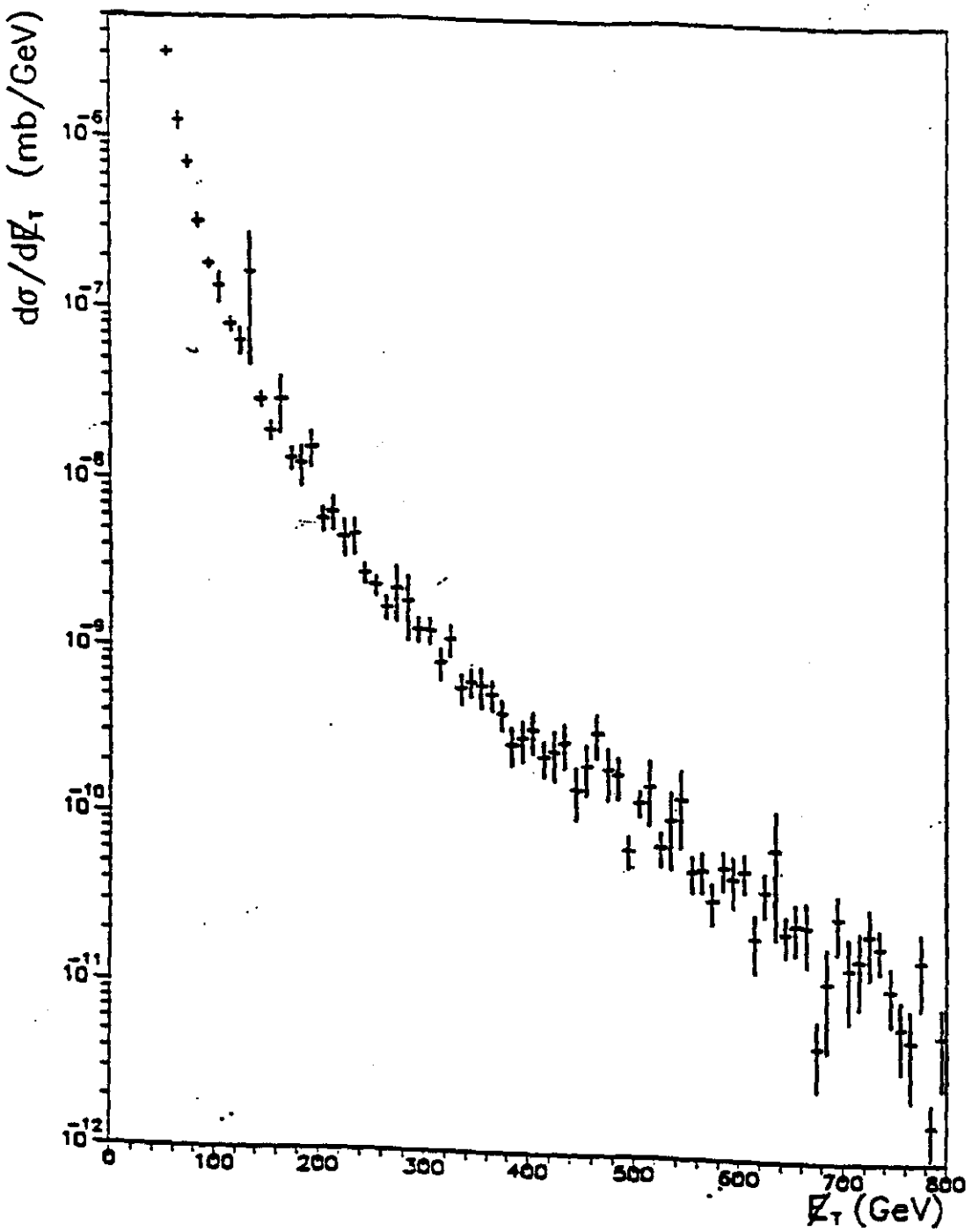

Figure 2.1: True $\not{E}_T$ cross section from neutrinos from heavy quark decays.

Fig. 9

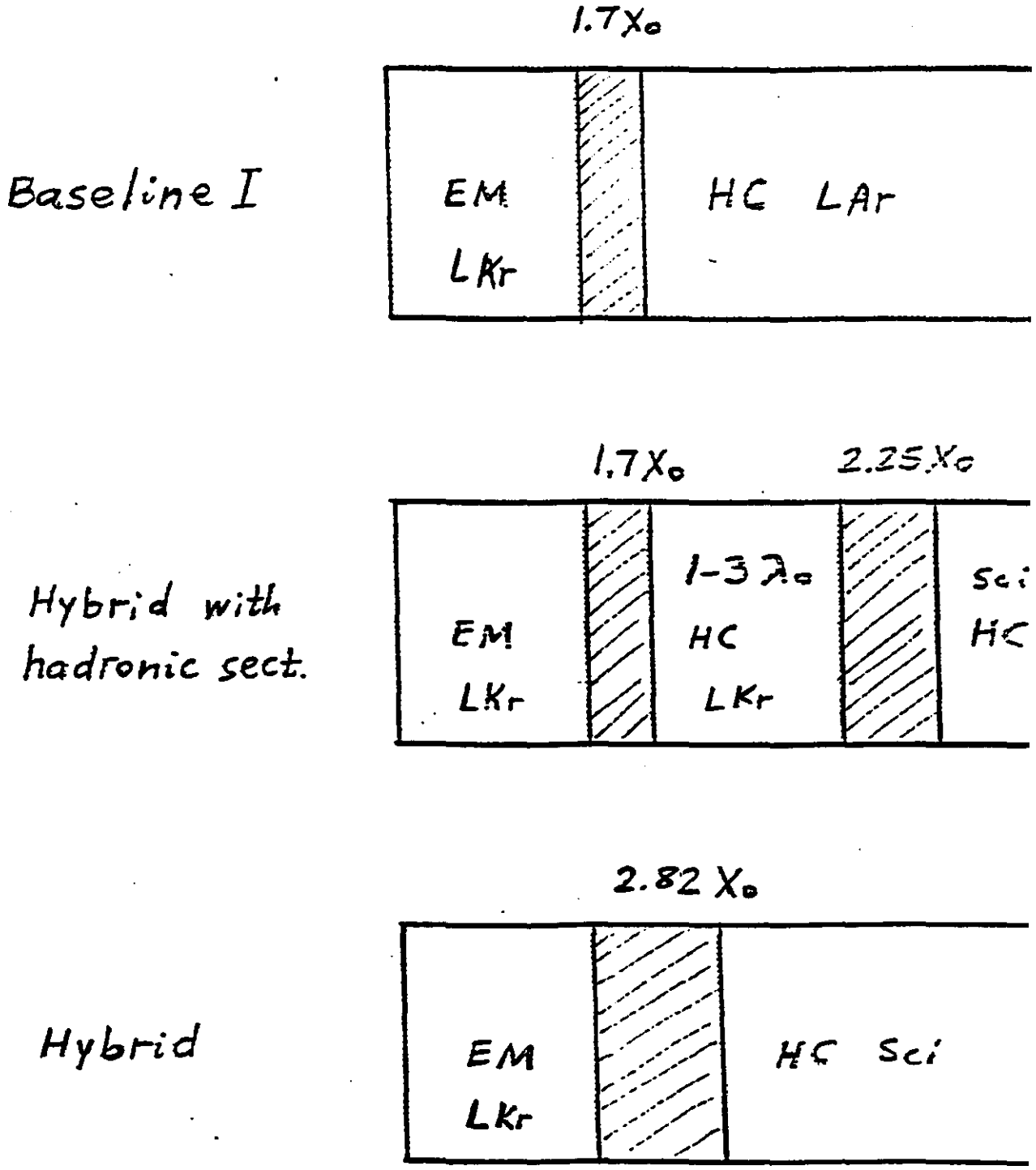

Dead material between E-M and hadronic sections

Fig. 1

50 GeV pions-

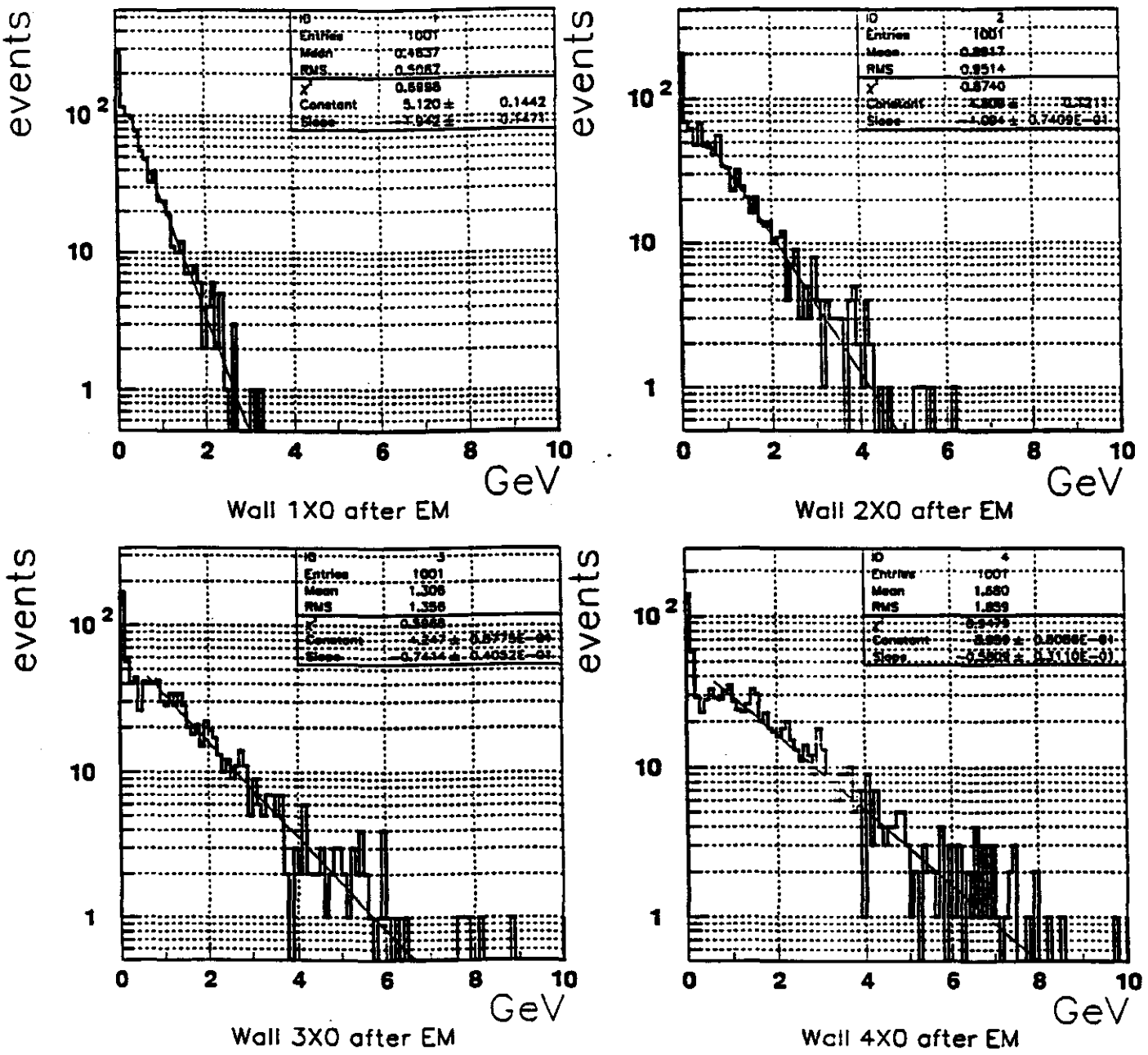

Fig. 4

50 GeV pions-

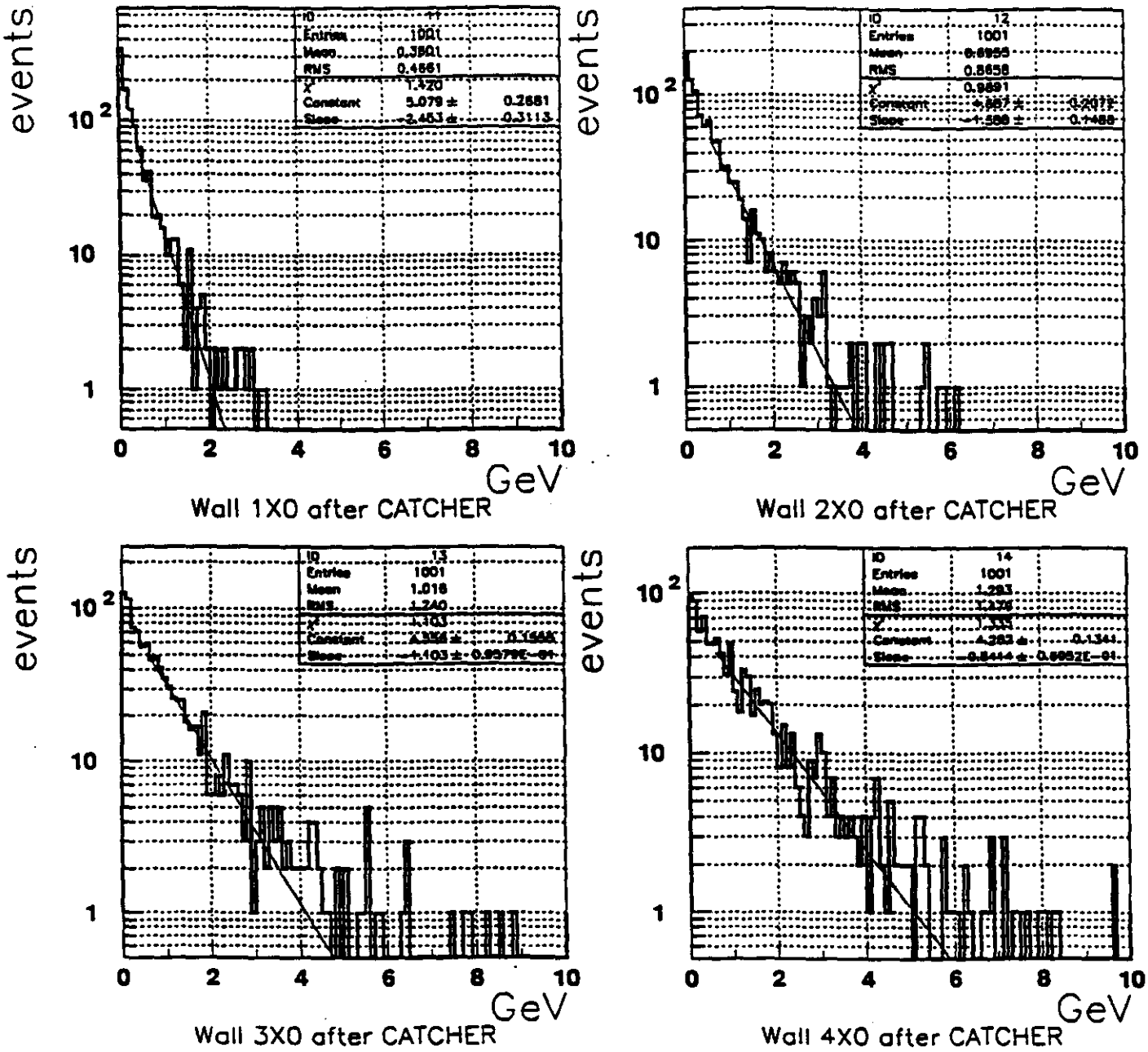

Fig. 5

Parametrisation of the pi- energy loss in dif. (cryostat) walls

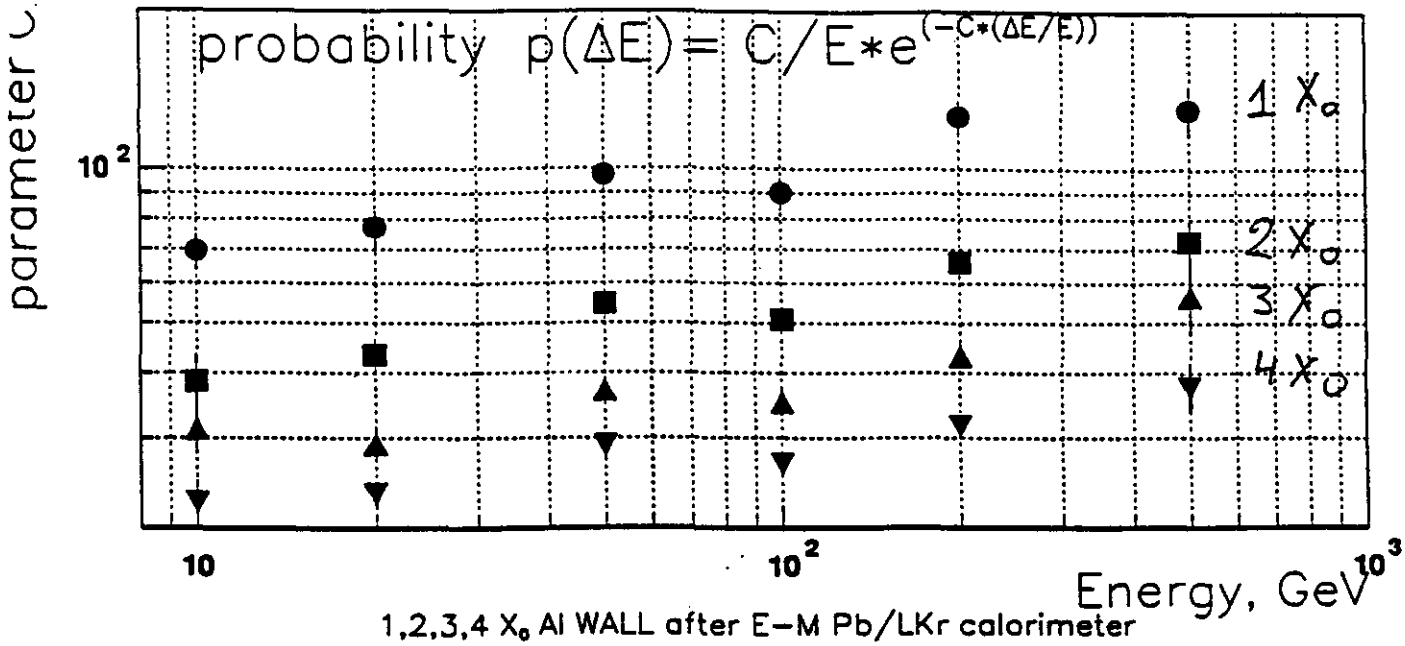

1,2,3,4 X_0 Al WALL after E–M Pb/LKr calorimeter

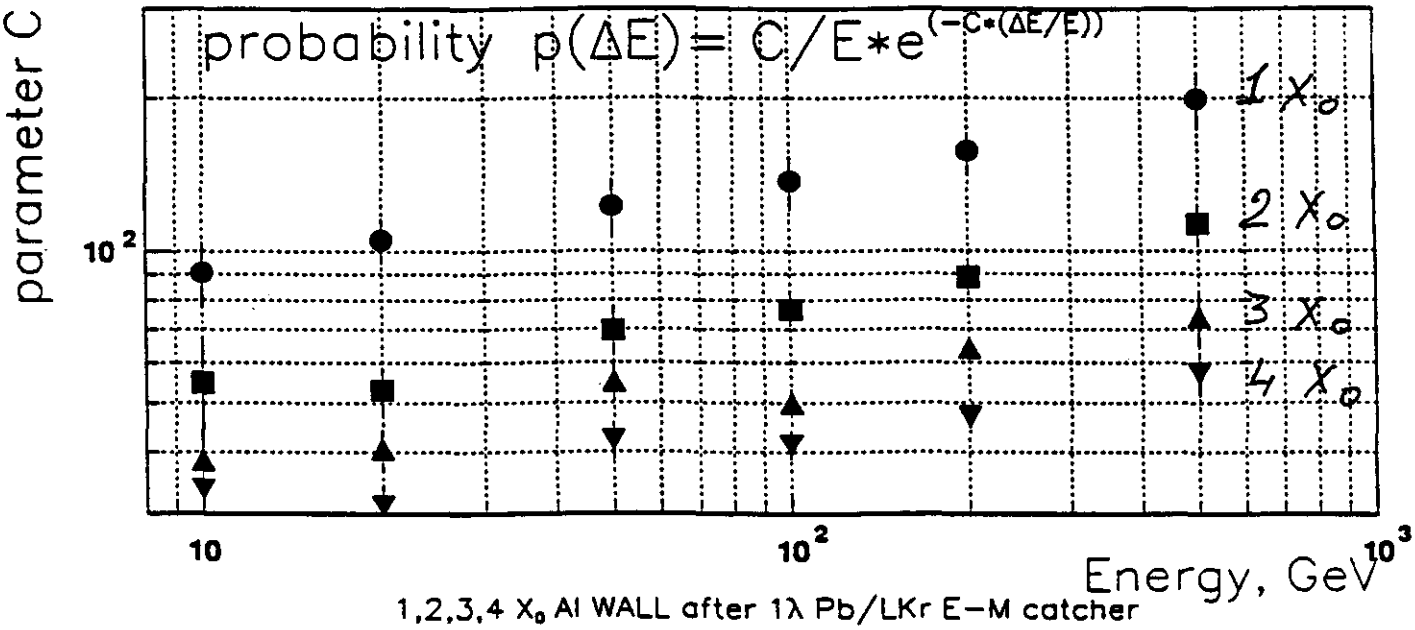

1,2,3,4 X_0 Al WALL after 1λ Pb/LKr E–M catcher

Fig. 8

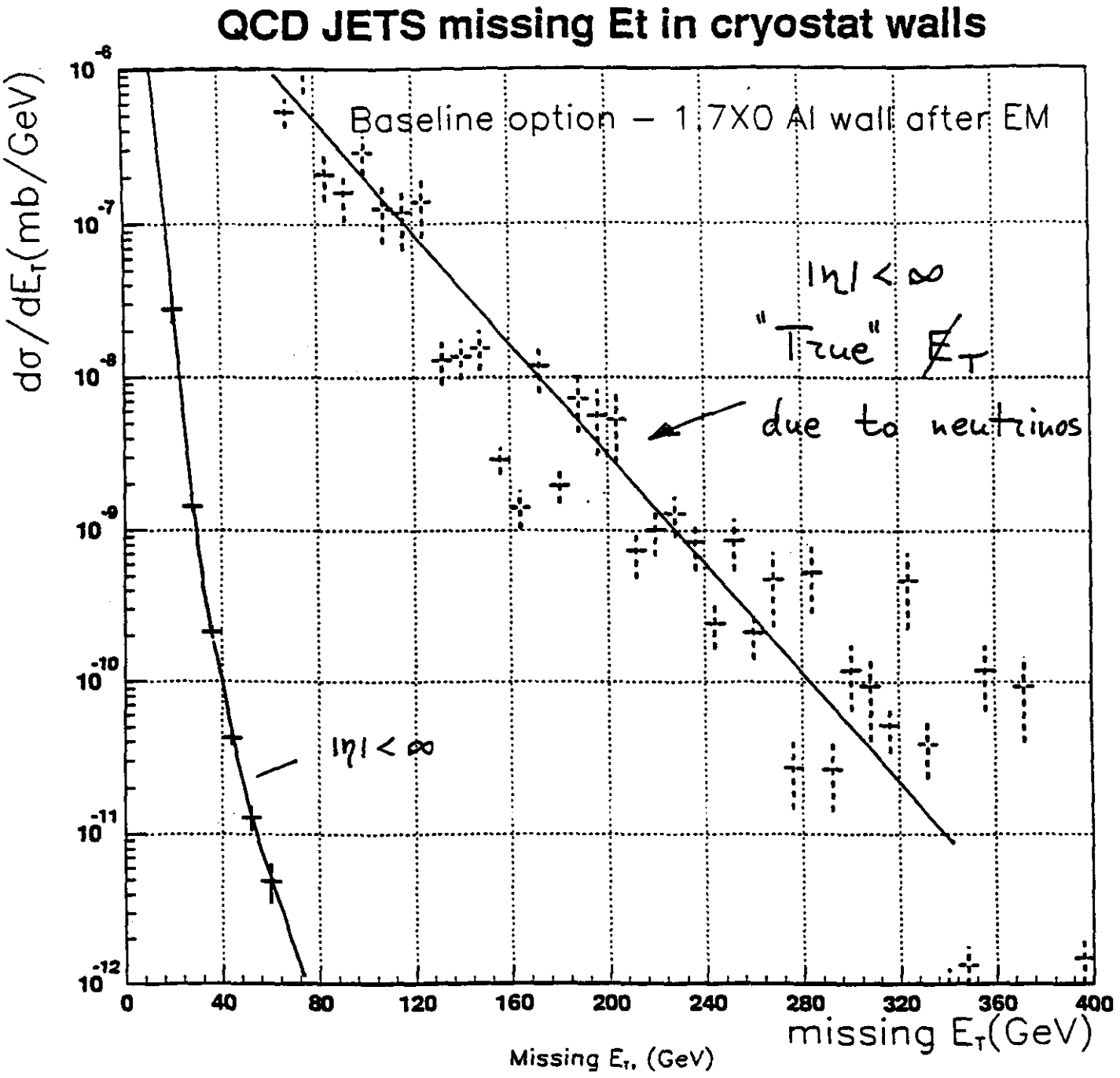
QCD JETS missing Et in cryostat walls
Baseline option – 1.7X0 Al wall after EM
dσ/dE_T(mb/GeV)
|η| < ∞
"True" E̸_T
due to neutrinos
|η| < ∞
missing E_T(GeV)
Missing E_T, (GeV)

Fig. 10

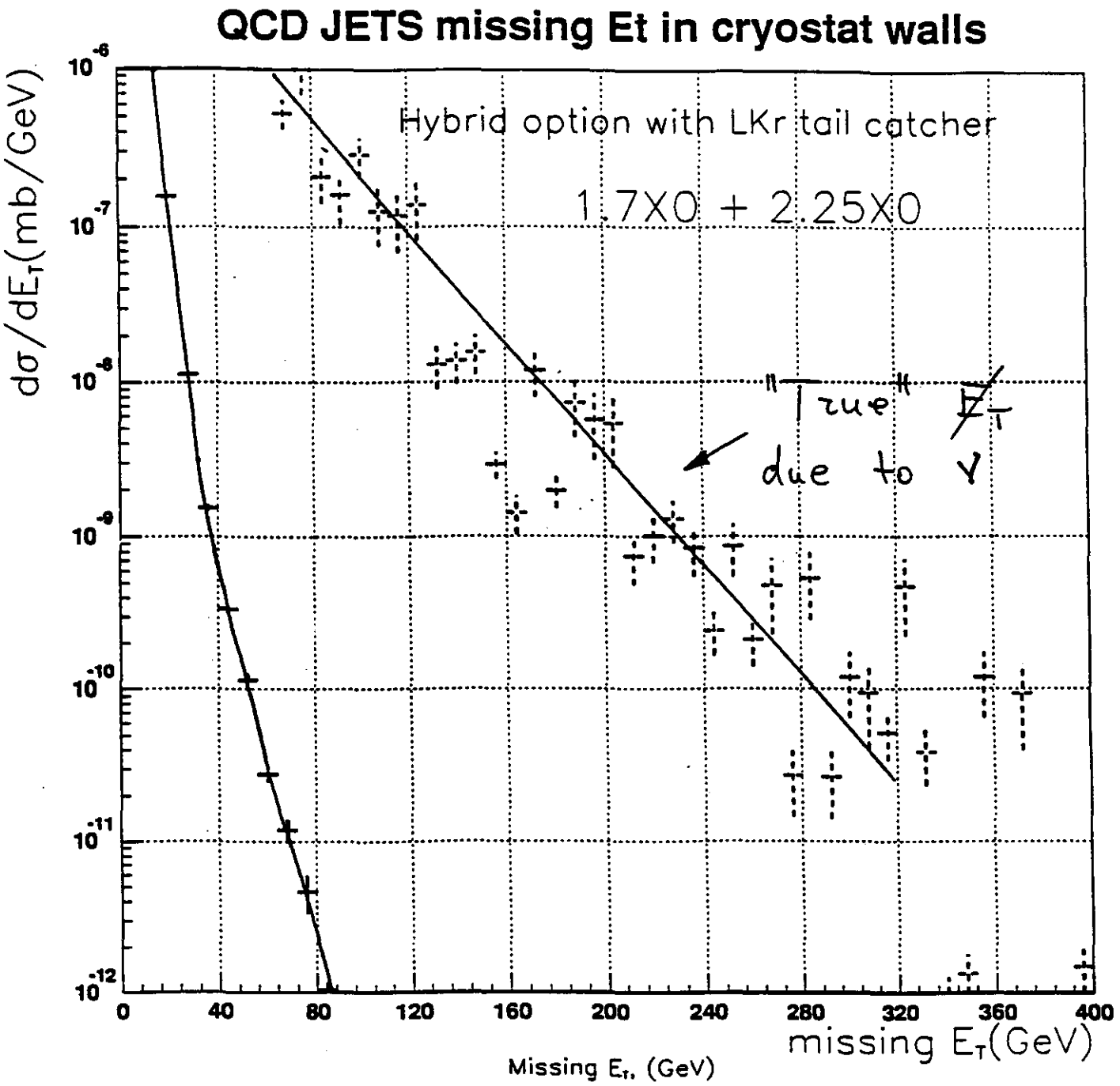
QCD JETS missing Et in cryostat walls
Hybrid option with LKr tail catcher
1.7X0 + 2.25X0
"True" $\not{E}_T$
due to ν
$d\sigma/dE_T$(mb/GeV)
missing E_T(GeV)
Missing E_T, (GeV)

Fig. 11

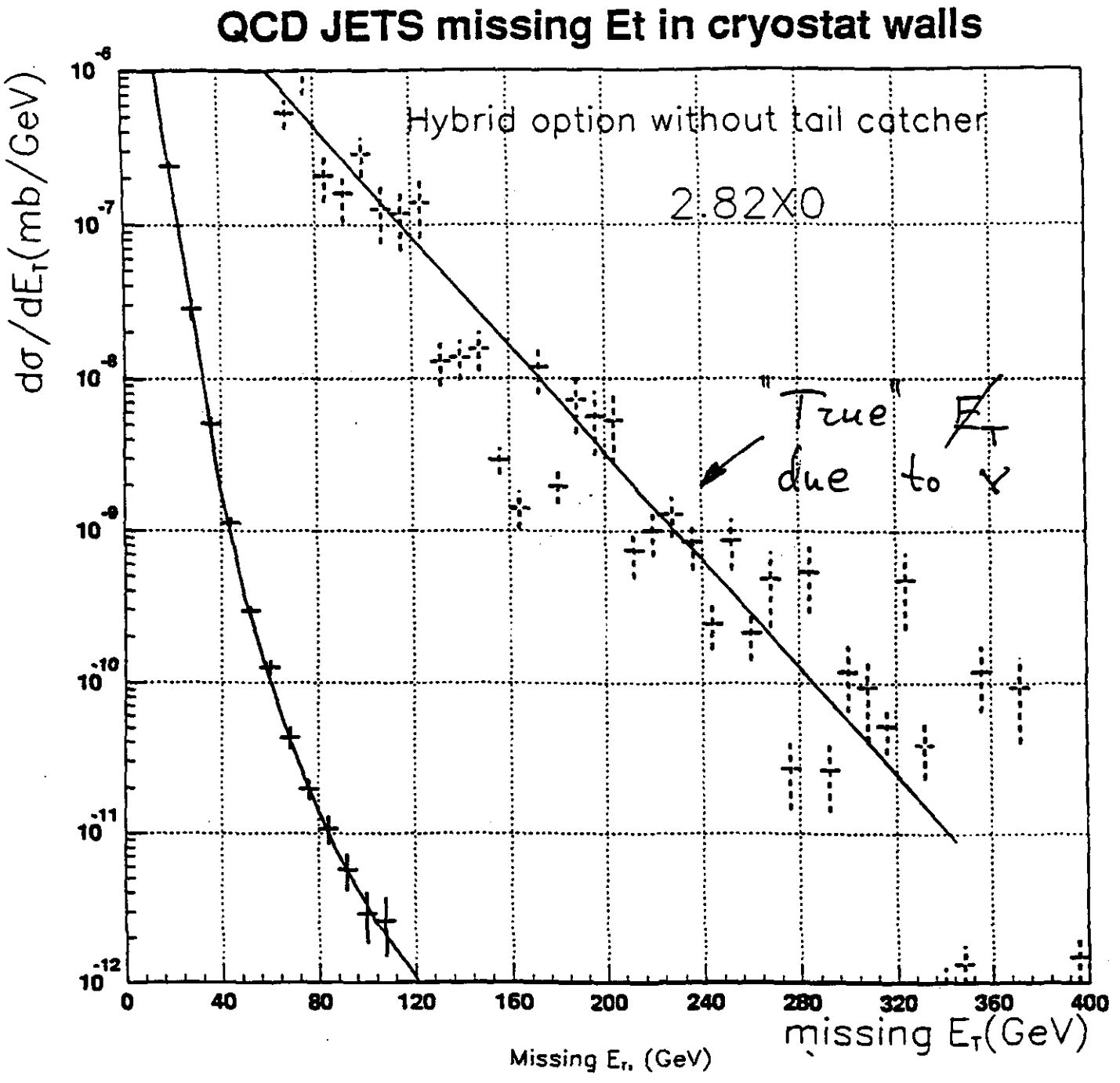
QCD JETS missing Et in cryostat walls
Hybrid option without tail catcher
2.82X0
"True" $\not{E}_T$ due to ν
$d\sigma/dE_T$(mb/GeV)
missing E_T(GeV)
Missing E_T, (GeV)

Fig. 12

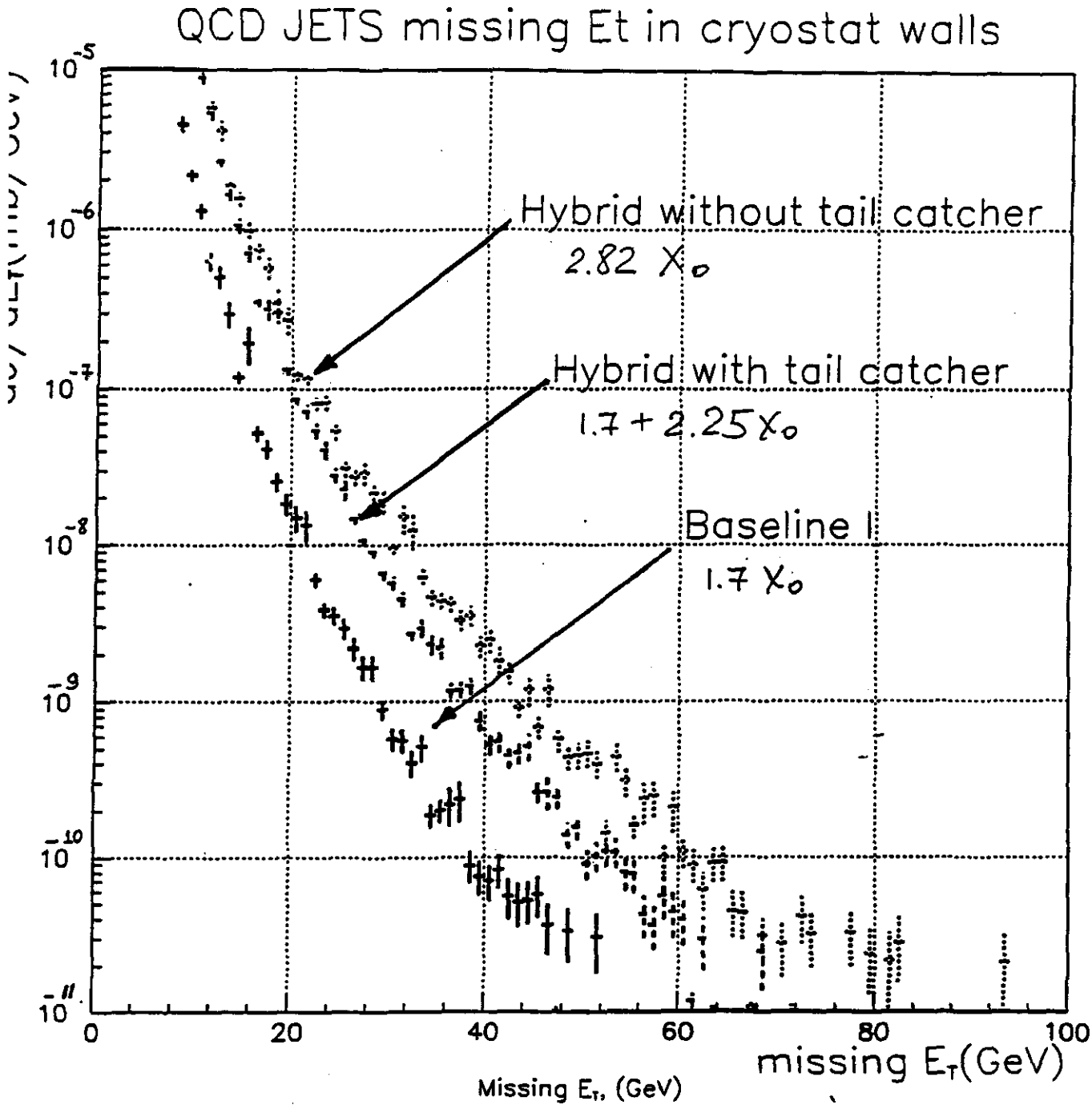
QCD JETS missing Et in cryostat walls
Hybrid without tail catcher
2.82 X_0
Hybrid with tail catcher
1.7 + 2.25 X_0
Baseline I
1.7 X_0
missing E_T(GeV)
Missing E_T, (GeV)

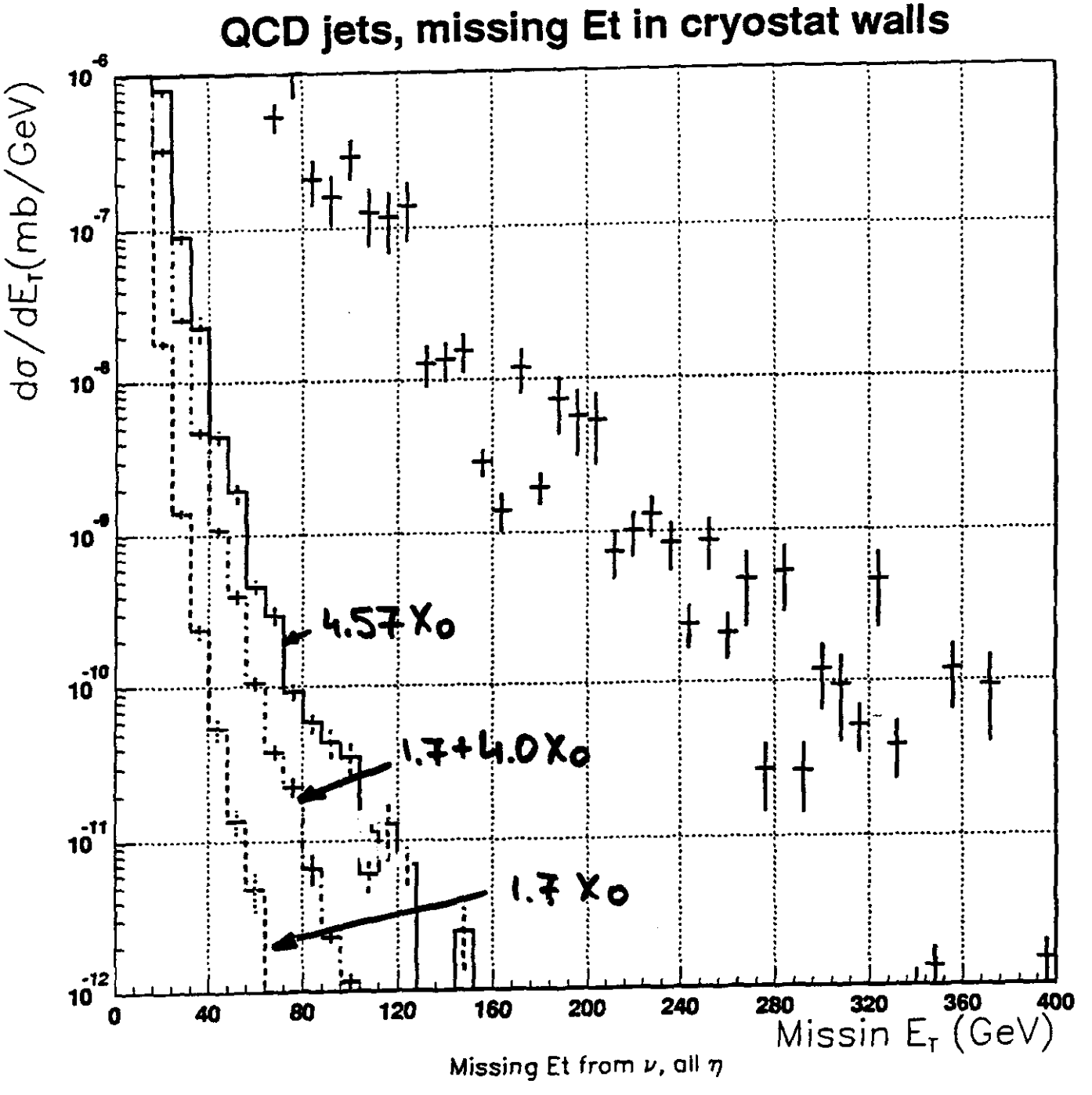
QCD jets, missing Et in cryostat walls
dσ/dE_T(mb/GeV)
10^-6
10^-7
10^-8
10^-9
10^-10
10^-11
10^-12
0
40
80
120
160
200
240
280
320
360
400
Missin E_T (GeV)
4.57 X0
1.7+4.0X0
1.7 X0
Missing Et from ν, all η

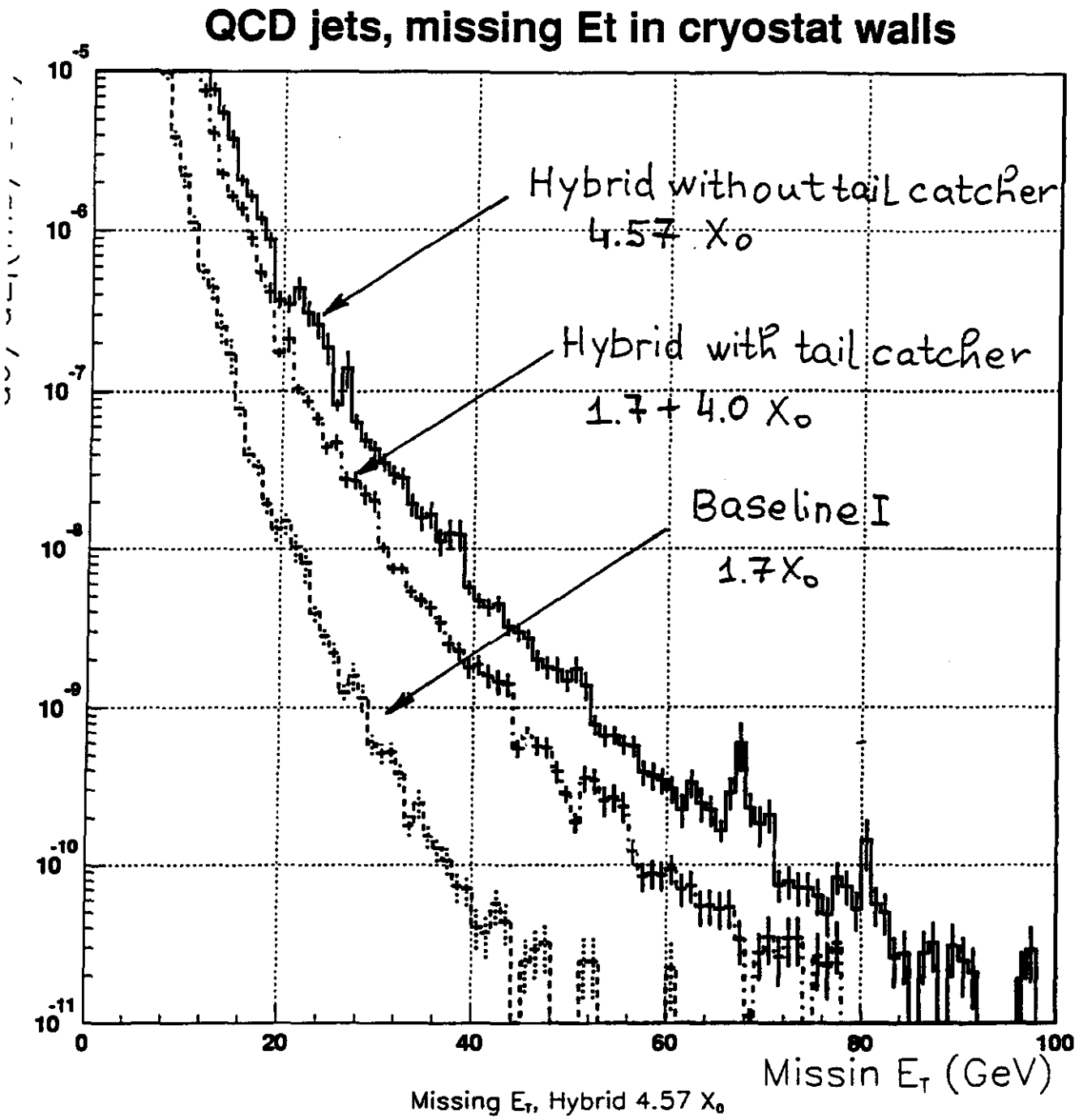
QCD jets, missing Et in cryostat walls
Hybrid without tail catcher
4.57 X₀
Hybrid with tail catcher
1.7 + 4.0 X₀
Baseline I
1.7 X₀
Missin E_T (GeV)
Missing E_T, Hybrid 4.57 X₀

Fitting by exp(-kx) and gauss*exp(-kx)

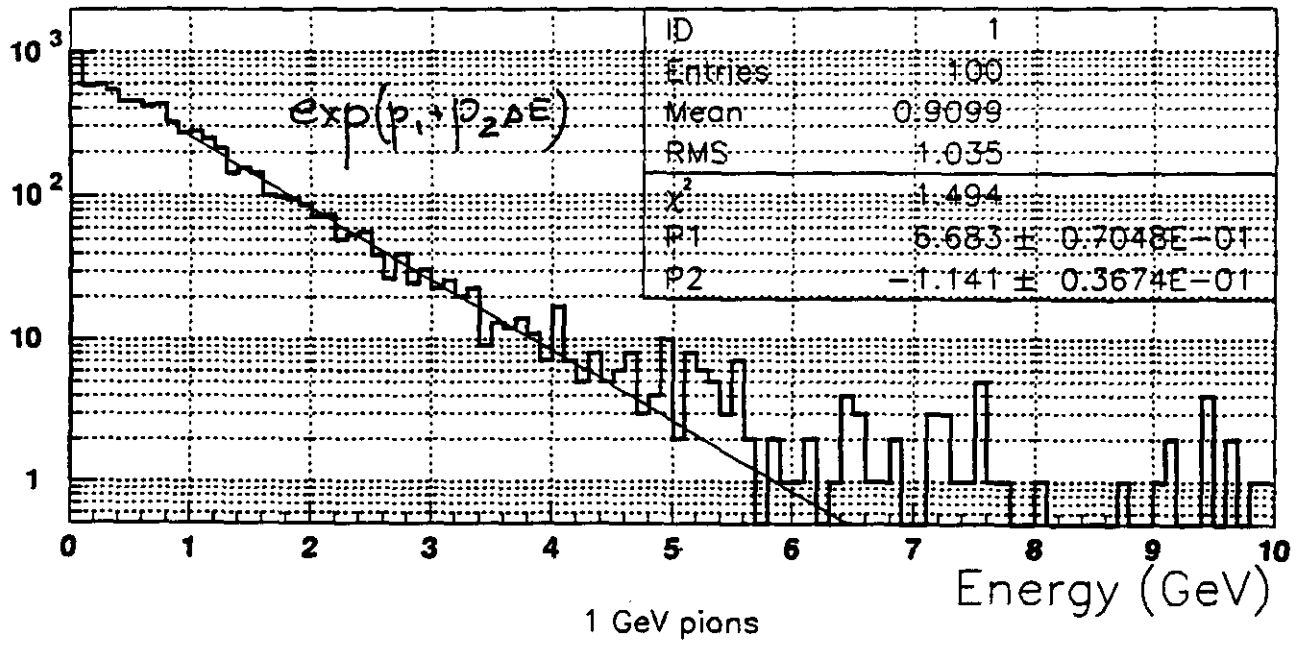

1 GeV pions

Missing E_T due to nongaussian tails in the hadron energy response.

Use the worst case — SSCintCAL test beam data wich has

1) transverzal leakage
2) No e-m calorimeter before.

Fitting by exp(-kx) and gauss*exp(-kx)

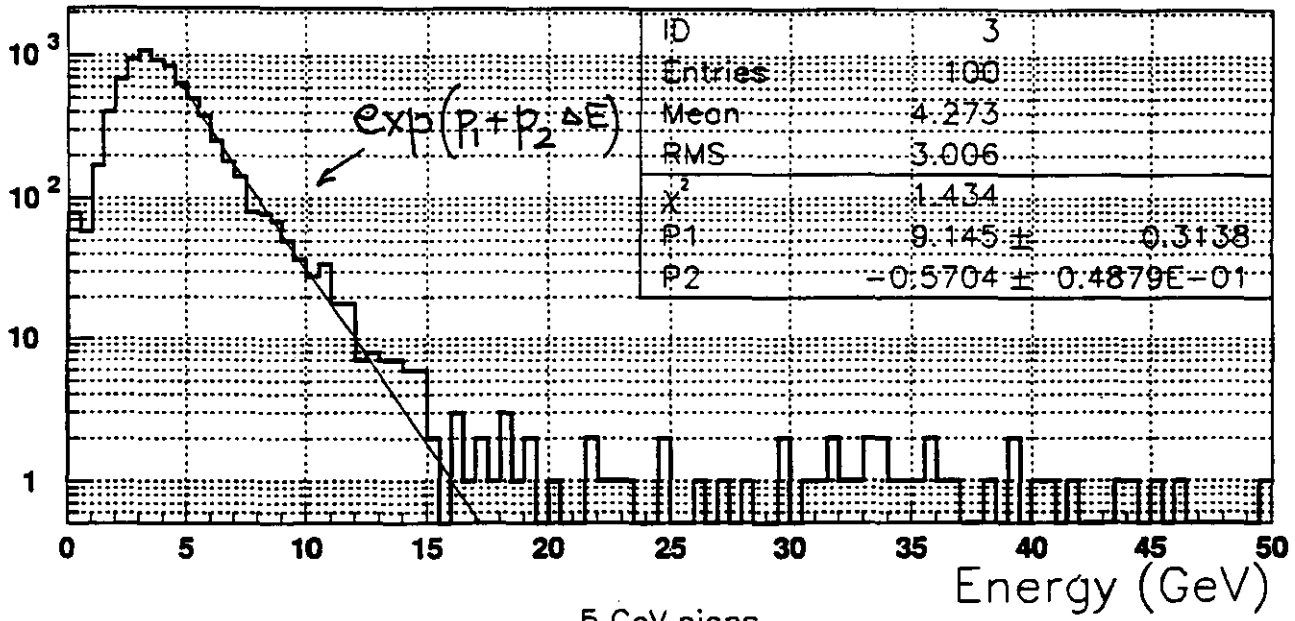

5 GeV pions

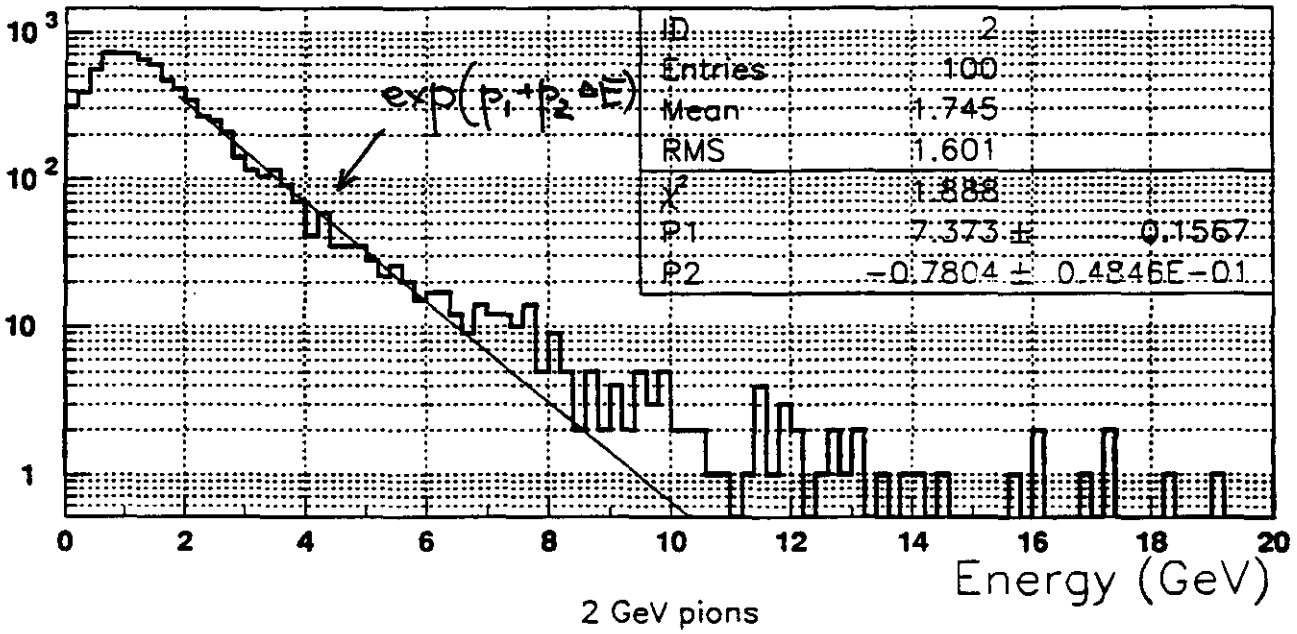

2 GeV pions

Fitting by exp(-kx) and gauss*exp(-kx)

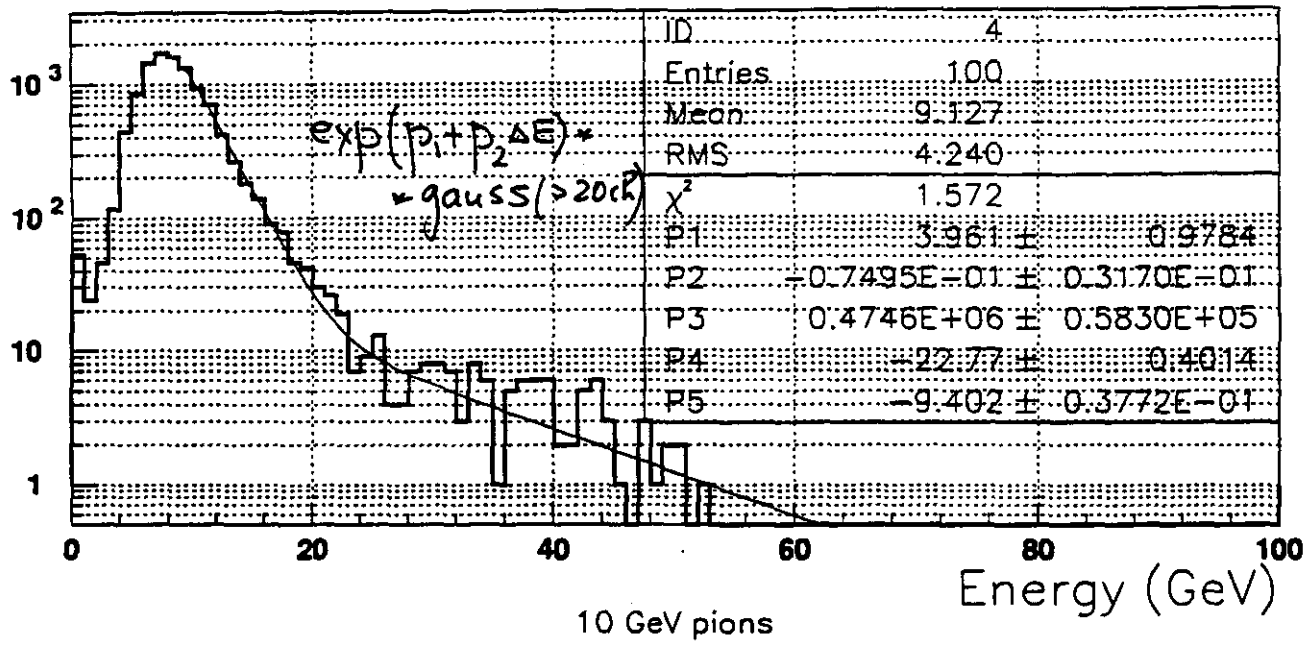

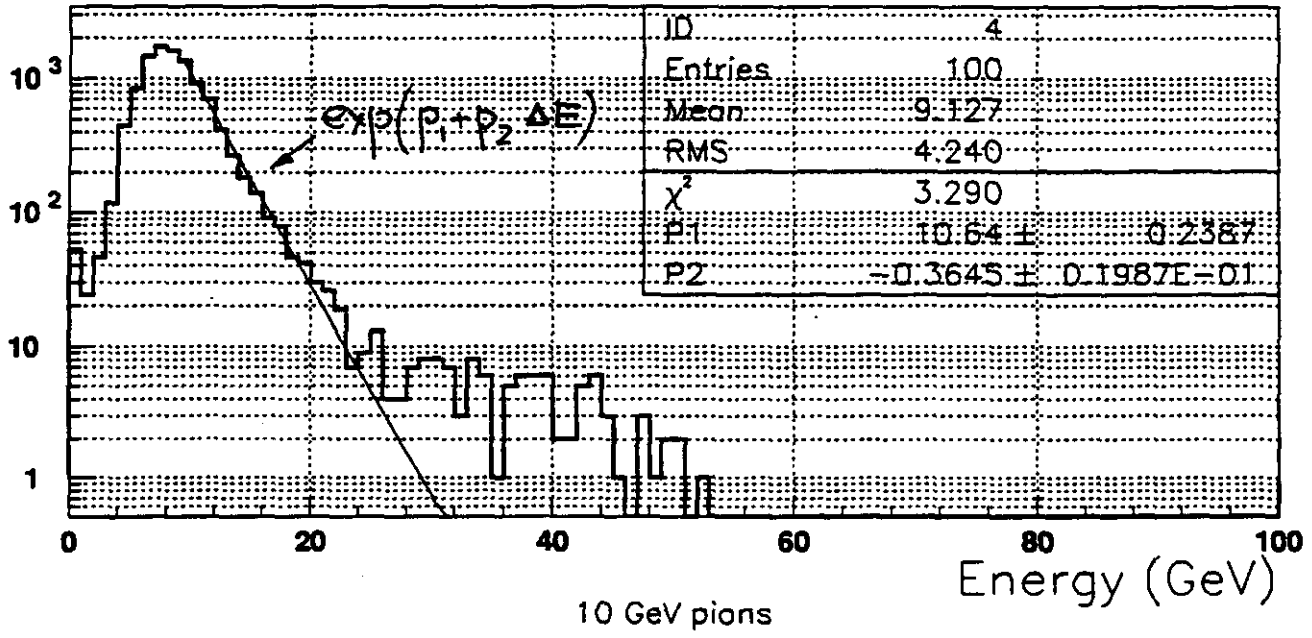

Fitting by exp(-kx) and gauss*exp(-kx)

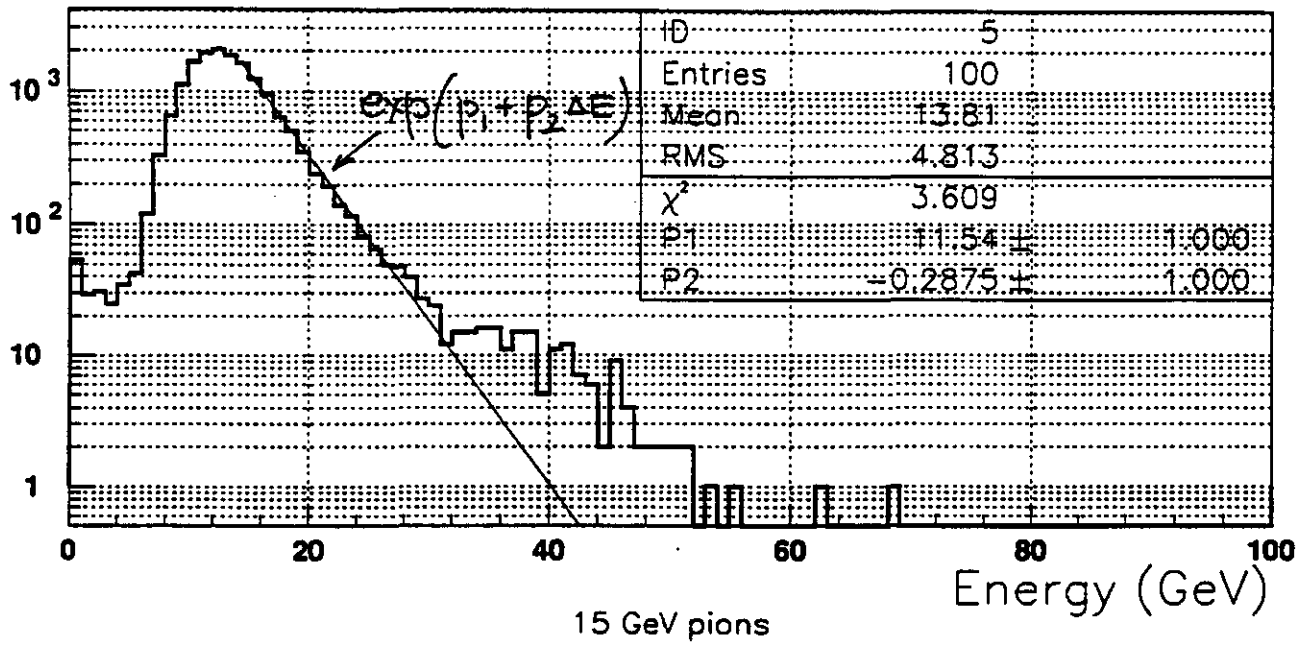

15 GeV pions

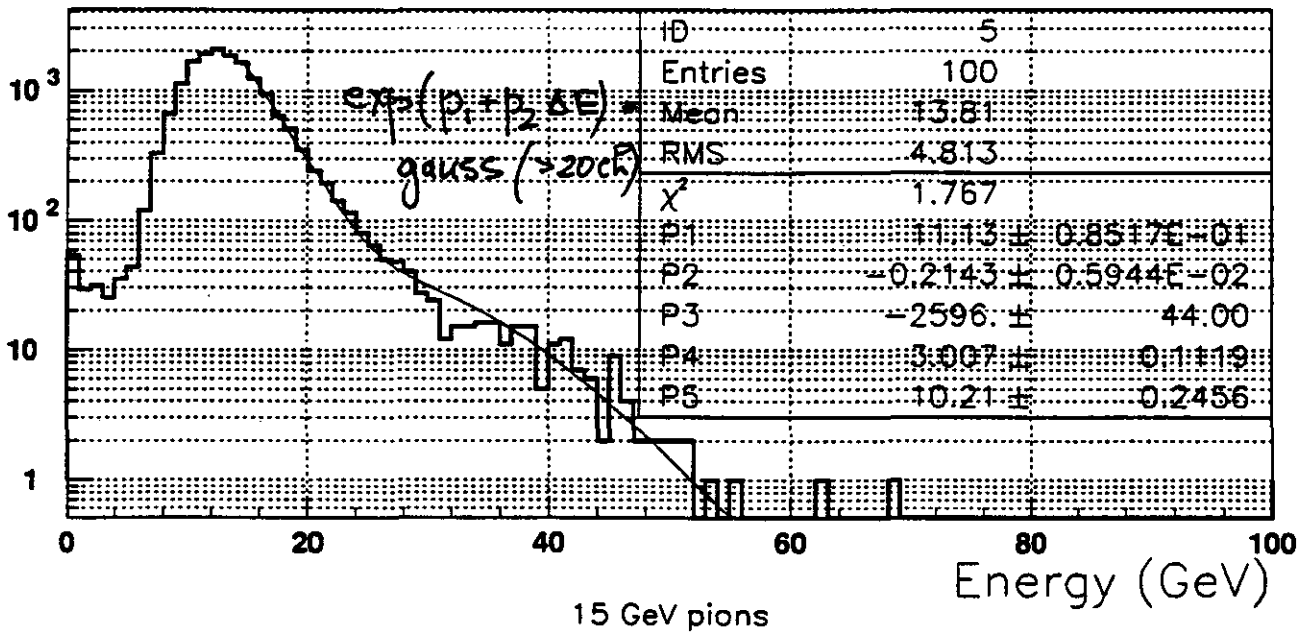

15 GeV pions

Fitting by exp(-kx) and gauss*exp(-kx)

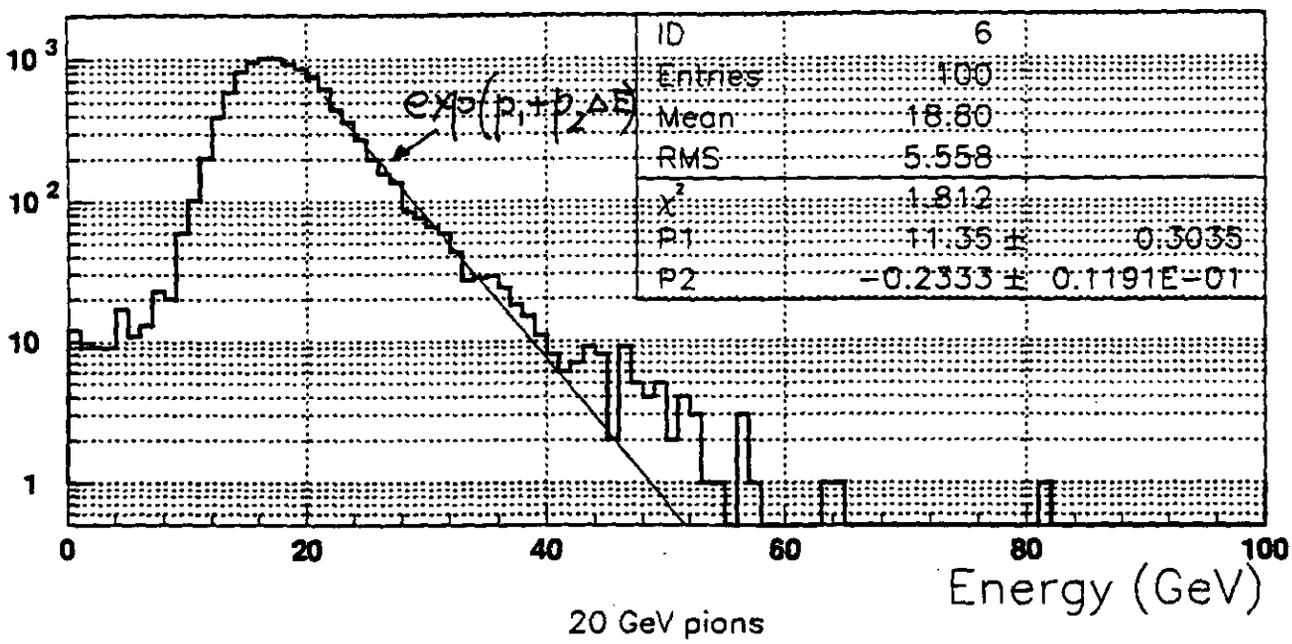

20 GeV pions

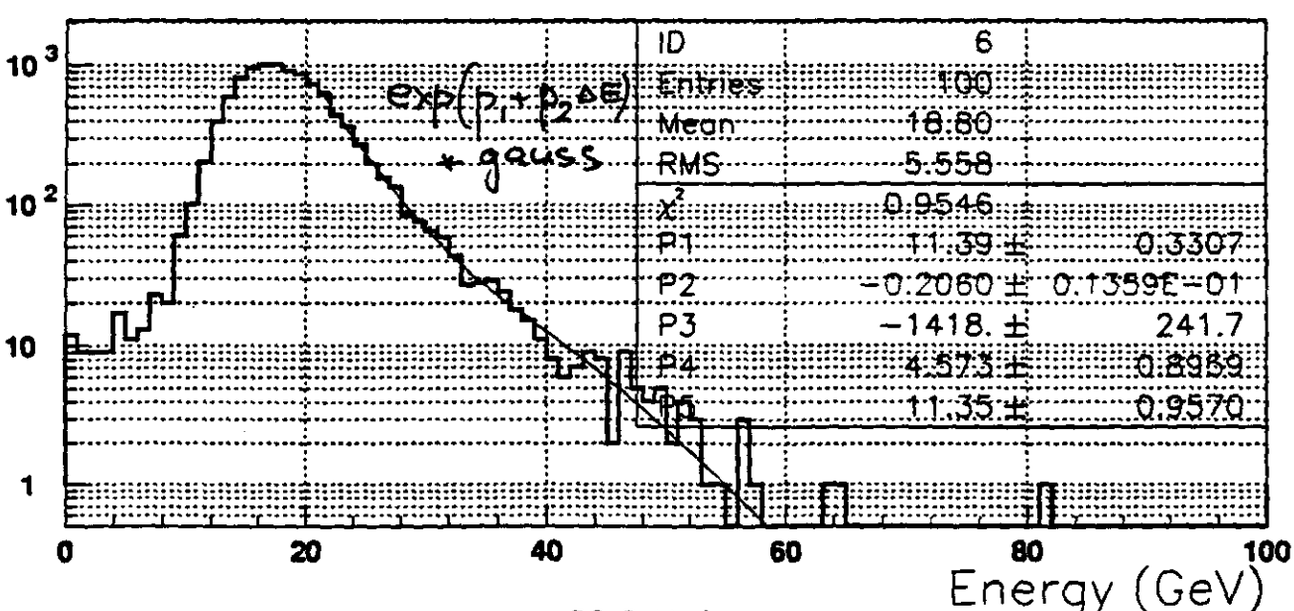

20 GeV pions

Fitting of experimental data tail

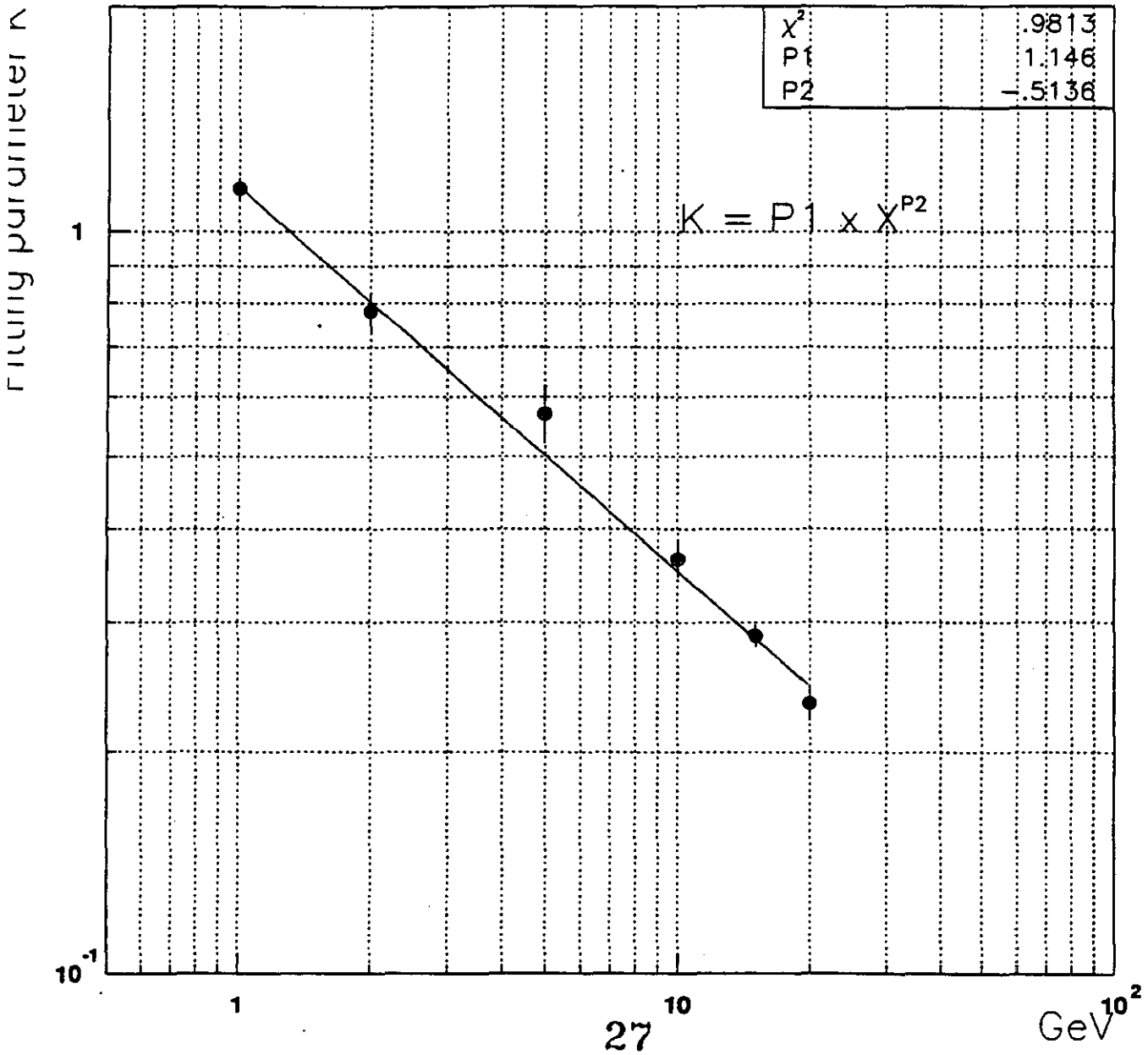

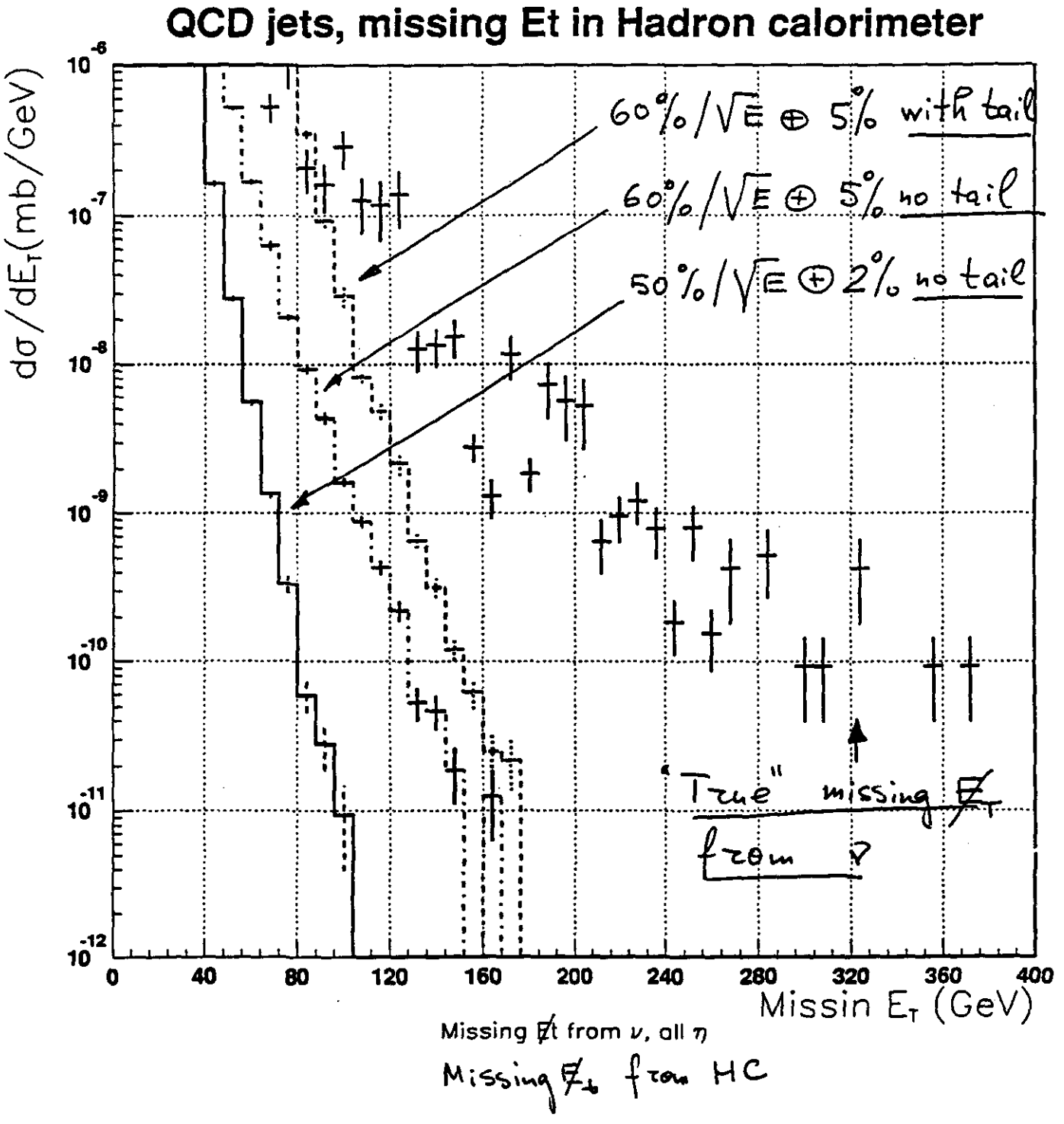
QCD jets, missing Et in Hadron calorimeter
dσ/dE_T(mb/GeV)
60%/√E ⊕ 5% with tail
60%/√E ⊕ 5% no tail
50%/√E ⊕ 2% no tail
"True" missing E̸_T from ν
Missin E_T (GeV)
Missing E̸t from ν, all η
Missing E̸_t from HC

gem

γeμ

Presentation by:

S. Savin

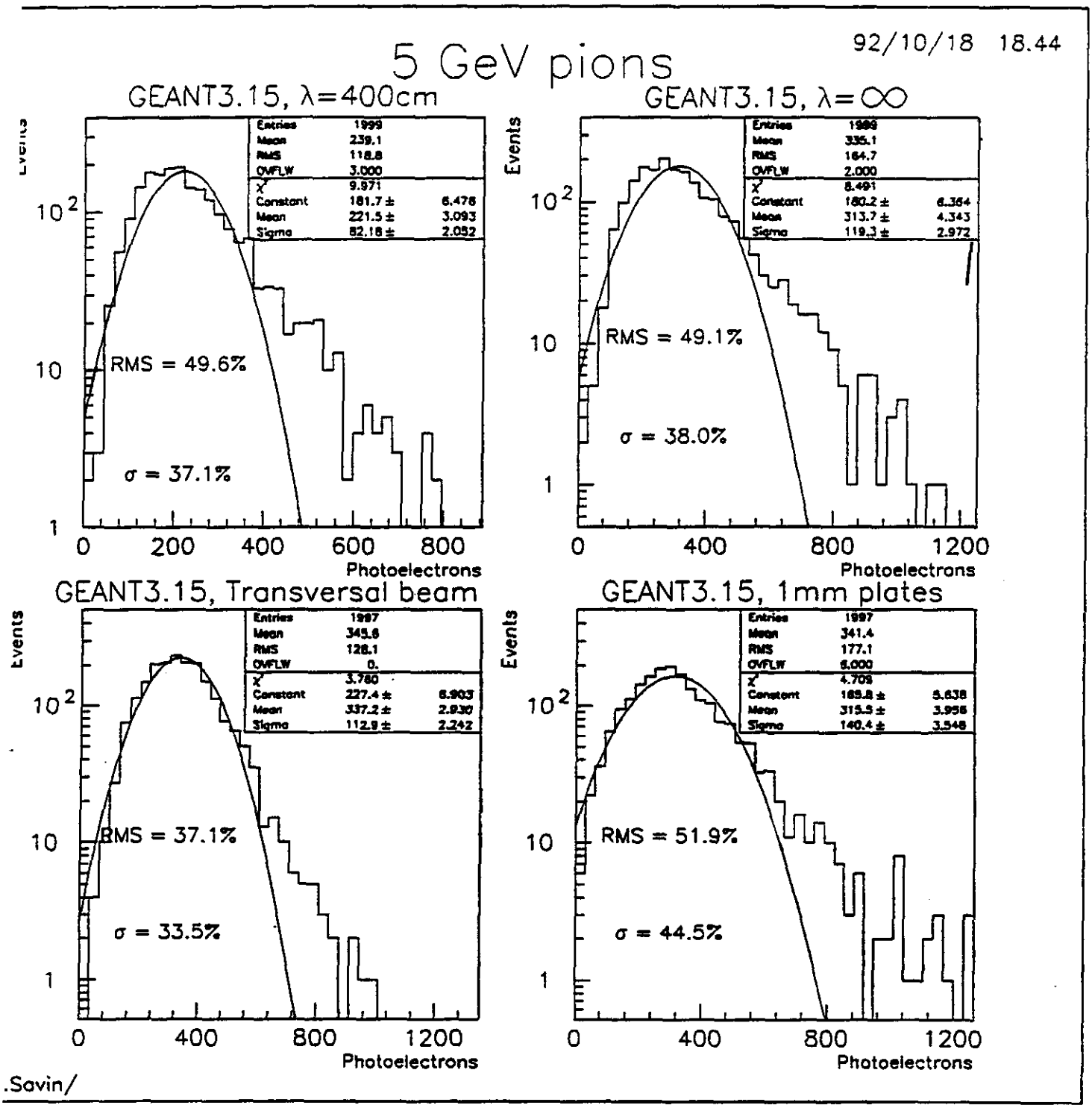
5 GeV pions
92/10/18 18.44
GEANT3.15, λ=400cm
Entries 1999
Mean 239.1
RMS 118.8
OVFLW 3.000
χ² 9.971
Constant 181.7 ± 6.476
Mean 221.5 ± 3.093
Sigma 82.18 ± 2.052
RMS = 49.6%
σ = 37.1%
Photoelectrons
GEANT3.15, λ=∞
Entries 1999
Mean 335.1
RMS 164.7
OVFLW 2.000
χ² 8.491
Constant 180.2 ± 6.364
Mean 313.7 ± 4.343
Sigma 119.3 ± 2.972
RMS = 49.1%
σ = 38.0%
Photoelectrons
GEANT3.15, Transversal beam
Events
Entries 1997
Mean 345.6
RMS 128.1
OVFLW 0.
χ² 3.760
Constant 227.4 ± 6.903
Mean 337.2 ± 2.930
Sigma 112.9 ± 2.242
RMS = 37.1%
σ = 33.5%
Photoelectrons
GEANT3.15, 1mm plates
Events
Entries 1997
Mean 341.4
RMS 177.1
OVFLW 6.000
χ² 4.709
Constant 165.8 ± 5.638
Mean 315.5 ± 3.956
Sigma 140.4 ± 3.548
RMS = 51.9%
σ = 44.5%
Photoelectrons
.Savin/

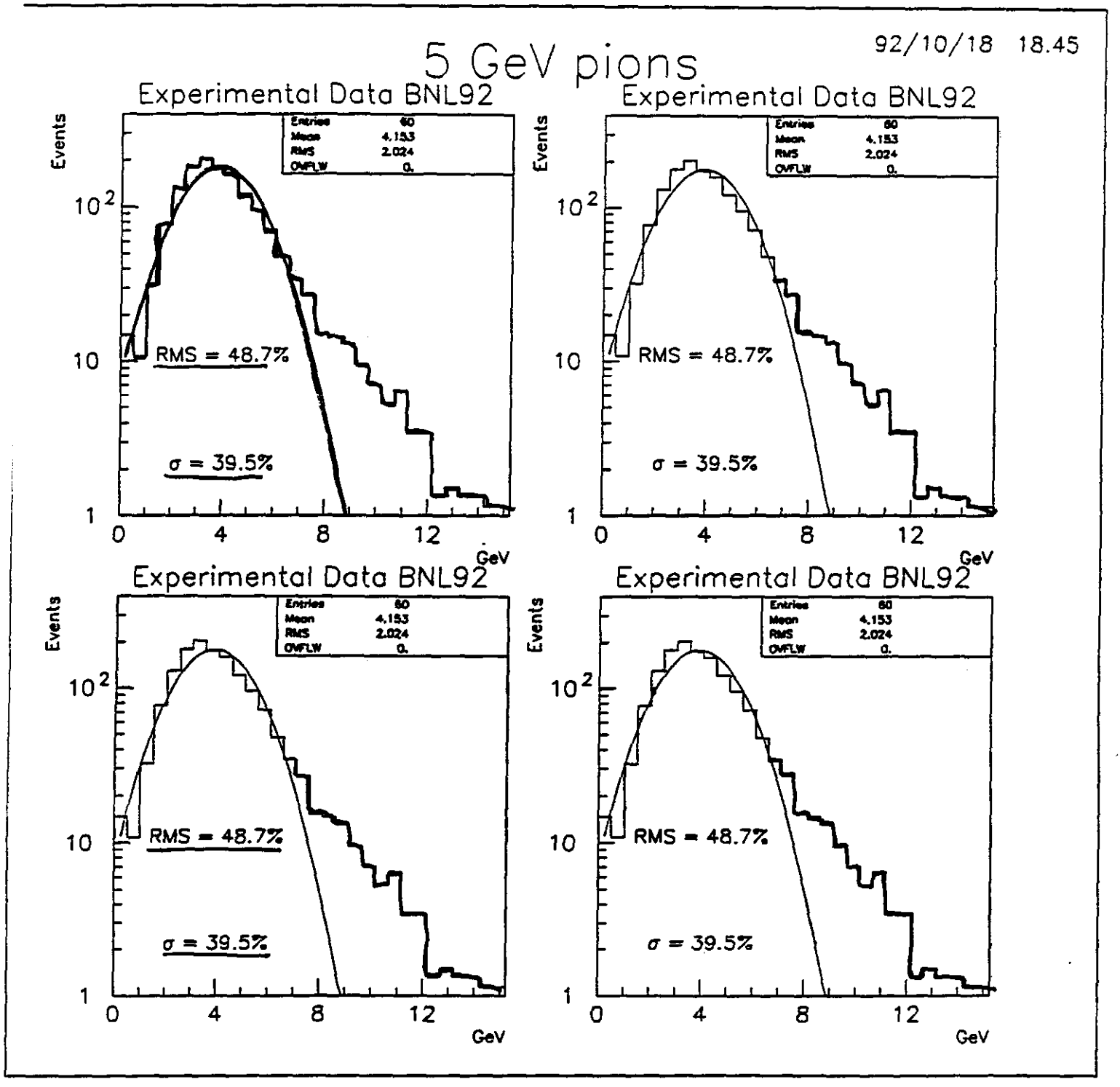
5 GeV pions
92/10/18 18.45
Experimental Data BNL92
Entries 60
Mean 4.153
RMS 2.024
OVFLW 0.
Events
RMS = 48.7%
σ = 39.5%
GeV

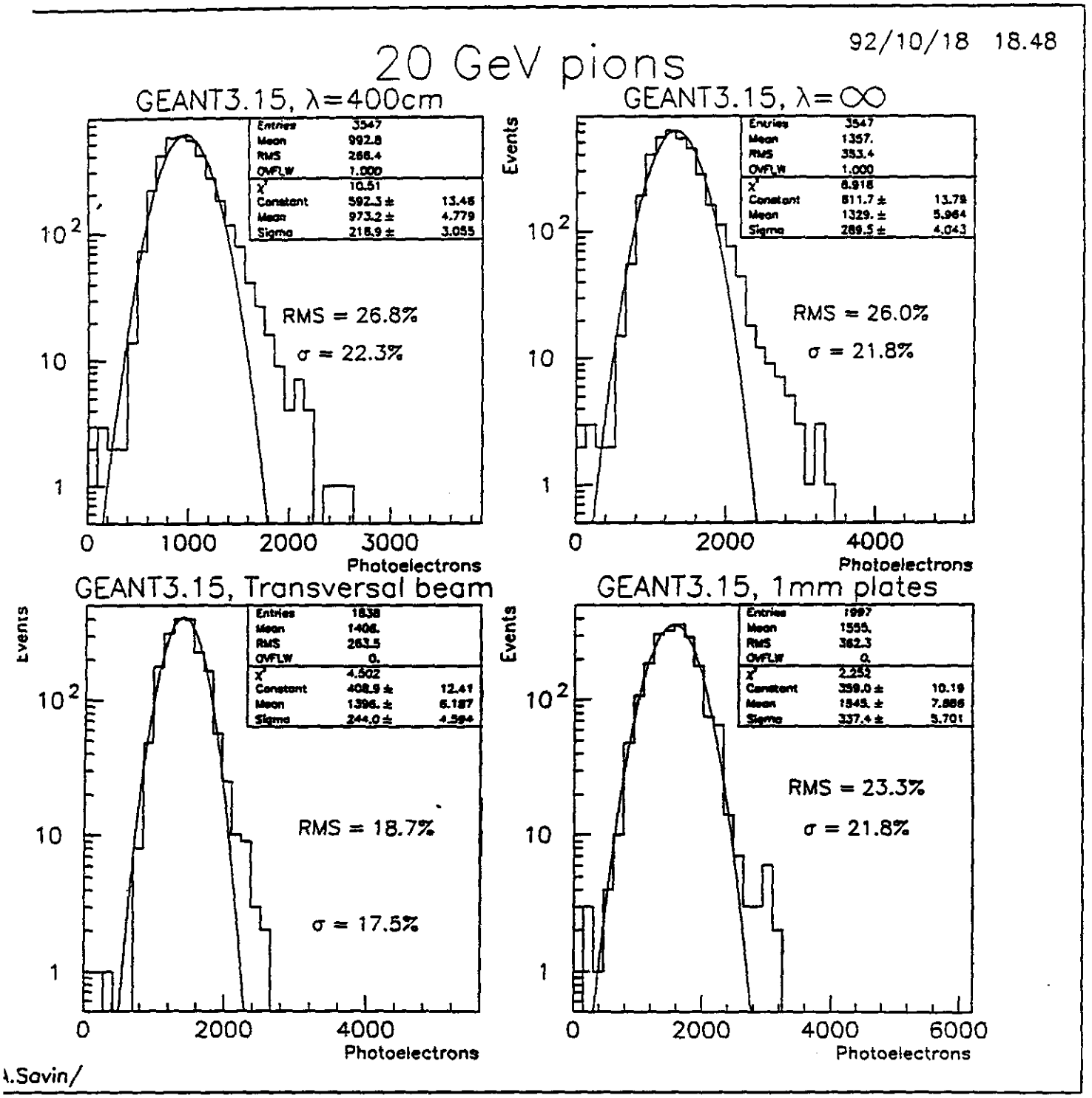
92/10/18 18.48
20 GeV pions
GEANT3.15, λ=400cm
Entries 3547
Mean 992.8
RMS 266.4
OVFLW 1.000
χ² 10.51
Constant 592.3 ± 13.46
Mean 973.2 ± 4.779
Sigma 216.9 ± 3.055
RMS = 26.8%
σ = 22.3%
Photoelectrons
GEANT3.15, λ=∞
Entries 3547
Mean 1357.
RMS 353.4
OVFLW 1.000
χ² 6.916
Constant 611.7 ± 13.79
Mean 1329. ± 5.964
Sigma 289.5 ± 4.043
RMS = 26.0%
σ = 21.8%
Photoelectrons
GEANT3.15, Transversal beam
Entries 1838
Mean 1406.
RMS 263.5
OVFLW 0.
χ² 4.502
Constant 408.9 ± 12.41
Mean 1396. ± 6.187
Sigma 244.0 ± 4.594
RMS = 18.7%
σ = 17.5%
Photoelectrons
GEANT3.15, 1mm plates
Entries 1997
Mean 1555.
RMS 362.3
OVFLW 0.
χ² 2.252
Constant 359.0 ± 10.19
Mean 1545. ± 7.886
Sigma 337.4 ± 5.701
RMS = 23.3%
σ = 21.8%
Photoelectrons
Events
A.Savin/

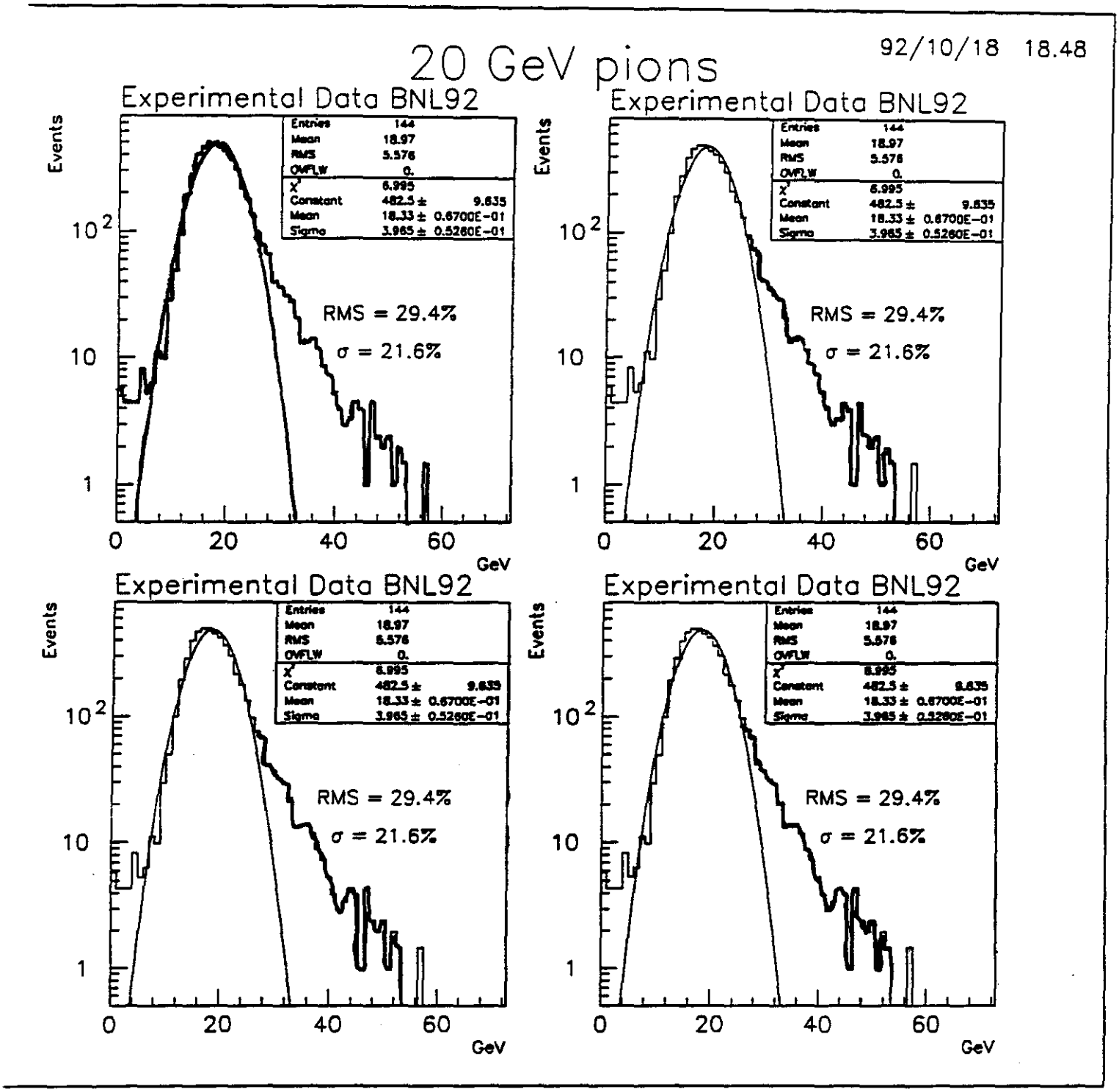
20 GeV pions
92/10/18 18.48
Experimental Data BNL92
Entries 144
Mean 18.97
RMS 5.576
OVFLW 0.
χ² 6.995
Constant 482.5 ± 9.635
Mean 18.33 ± 0.6700E-01
Sigma 3.965 ± 0.5260E-01
RMS = 29.4%
σ = 21.6%
Events
GeV

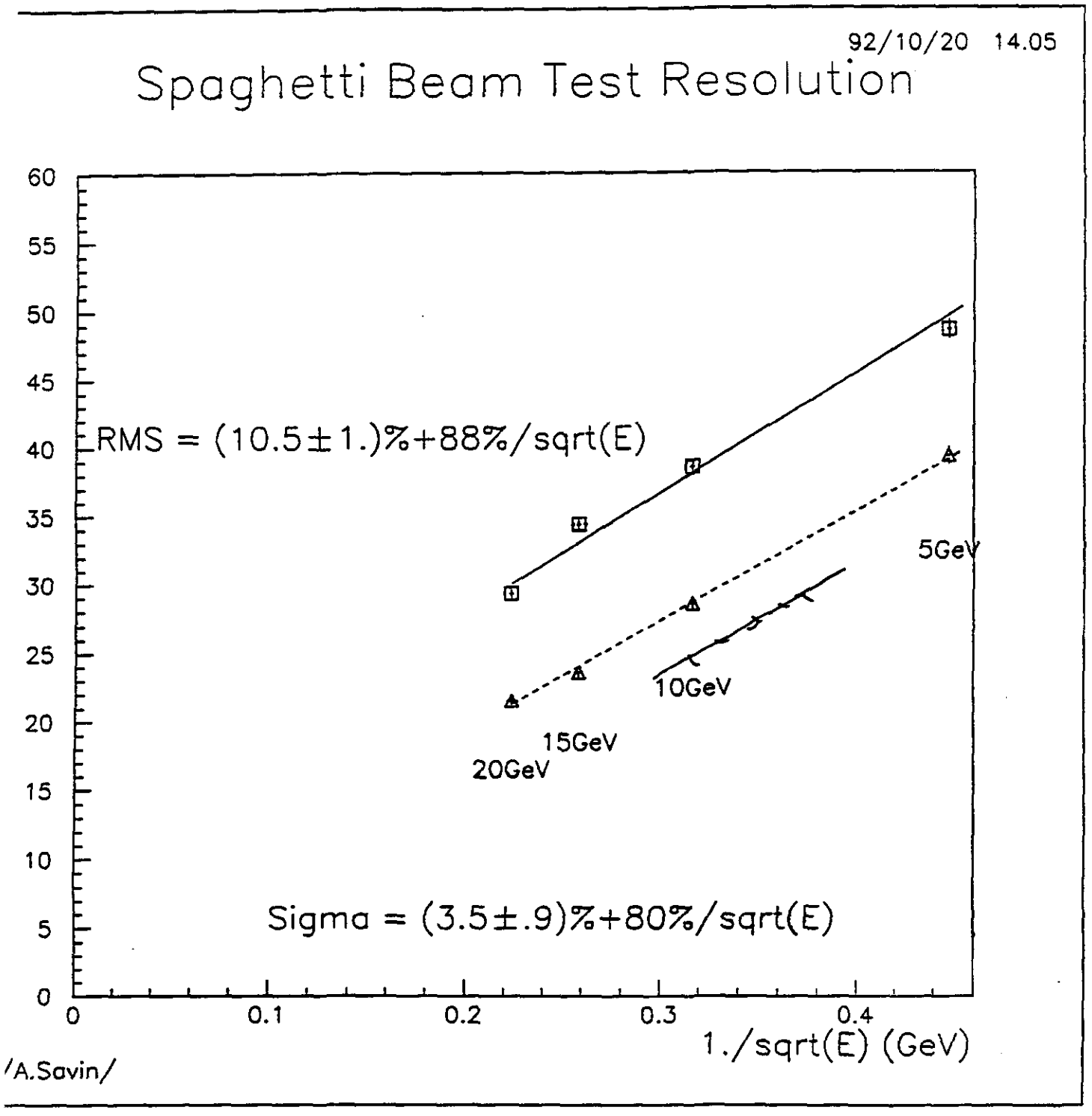
92/10/20 14.05
Spaghetti Beam Test Resolution
RMS = (10.5±1.)%+88%/sqrt(E)
Sigma = (3.5±.9)%+80%/sqrt(E)
5GeV
10GeV
15GeV
20GeV
1./sqrt(E) (GeV)
/A.Savin/

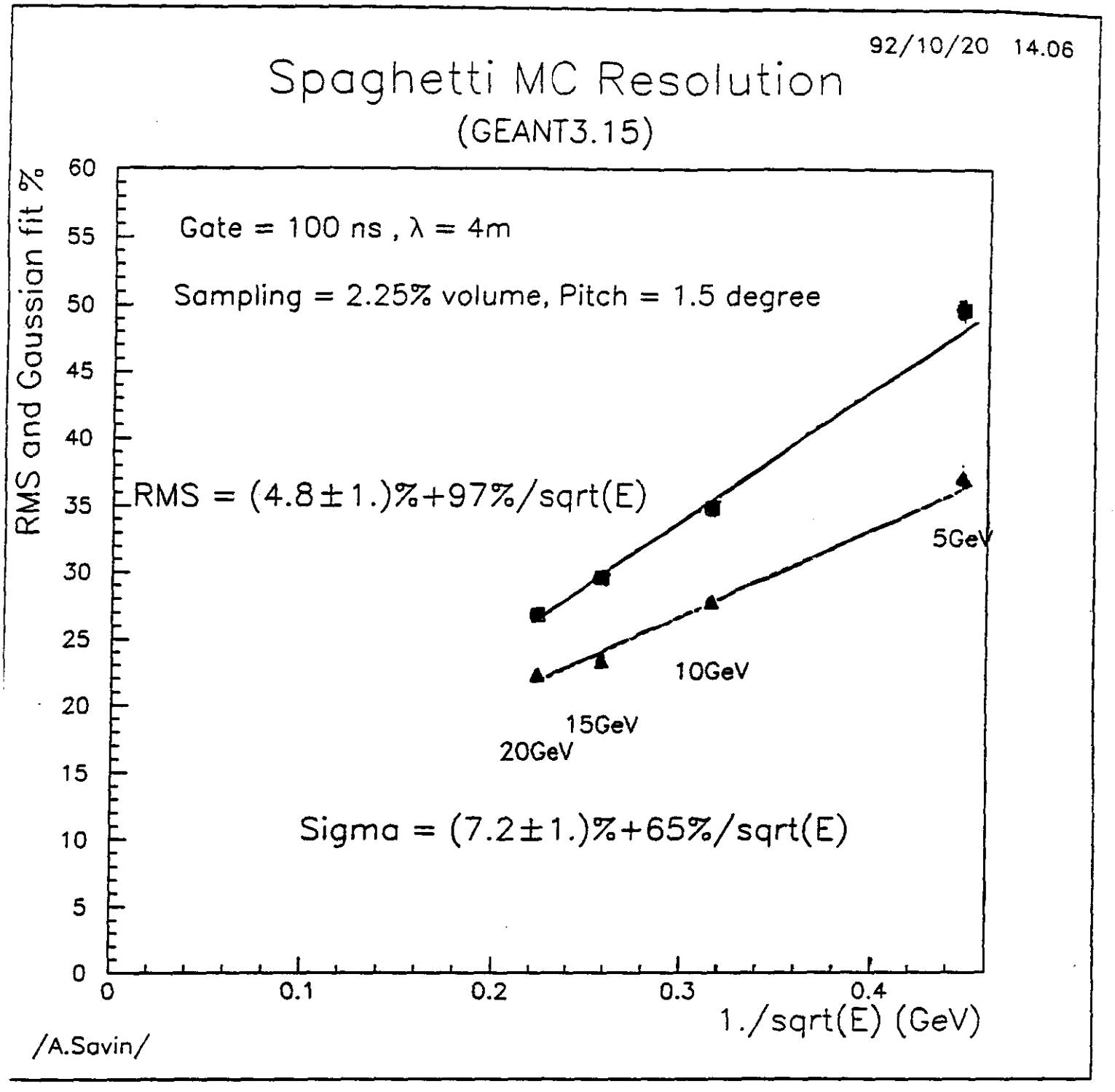
92/10/20 14.06
Spaghetti MC Resolution
(GEANT3.15)
Gate = 100 ns , λ = 4m
Sampling = 2.25% volume, Pitch = 1.5 degree
RMS = (4.8±1.)%+97%/sqrt(E)
Sigma = (7.2±1.)%+65%/sqrt(E)
5GeV
10GeV
15GeV
20GeV
RMS and Gaussian fit %
1./sqrt(E) (GeV)
0
5
10
15
20
25
30
35
40
45
50
55
60
0
0.1
0.2
0.3
0.4
/A.Savin/

Massless Gap for HC , 100 GeV pions

92/10/21 20.35

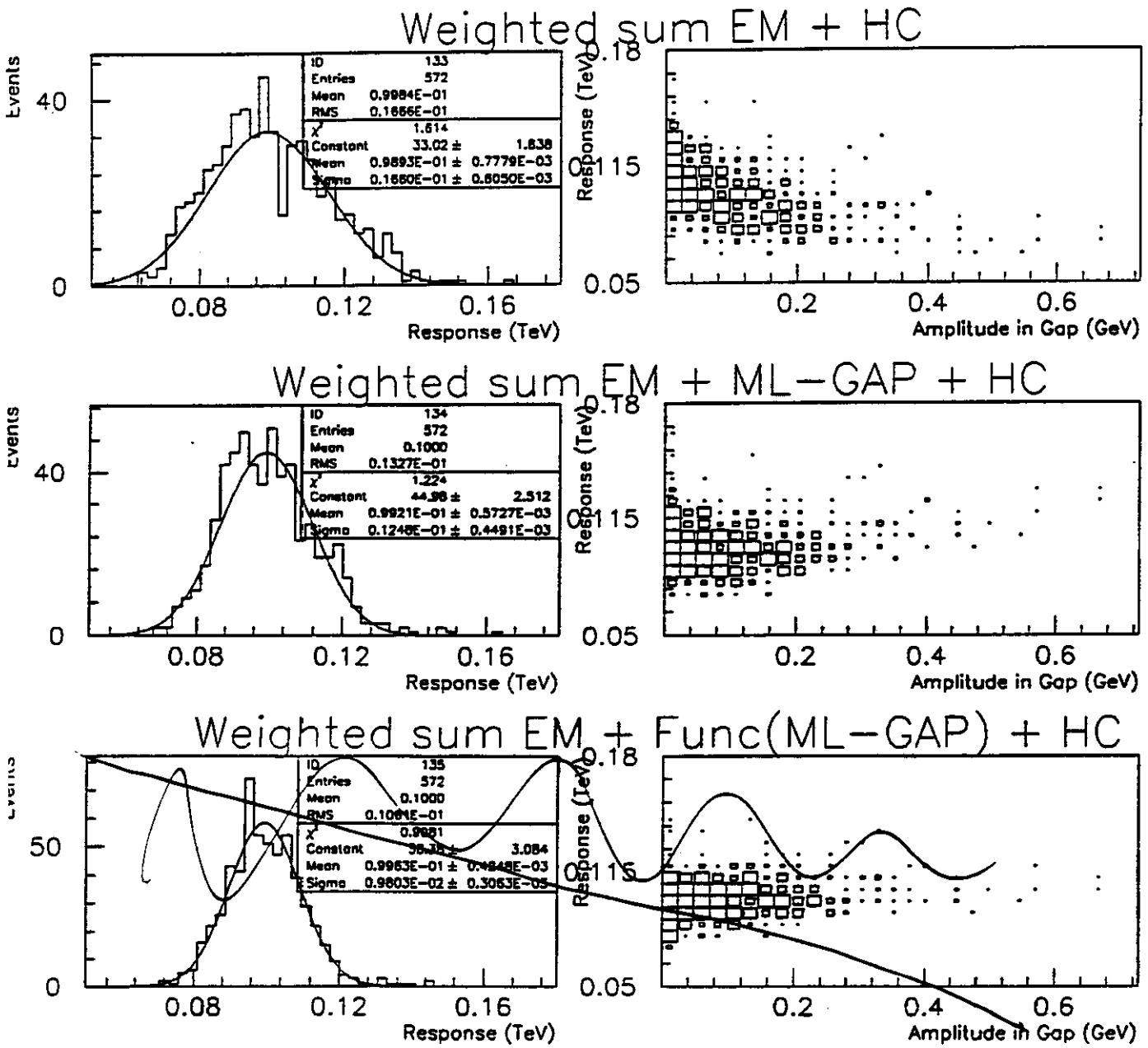

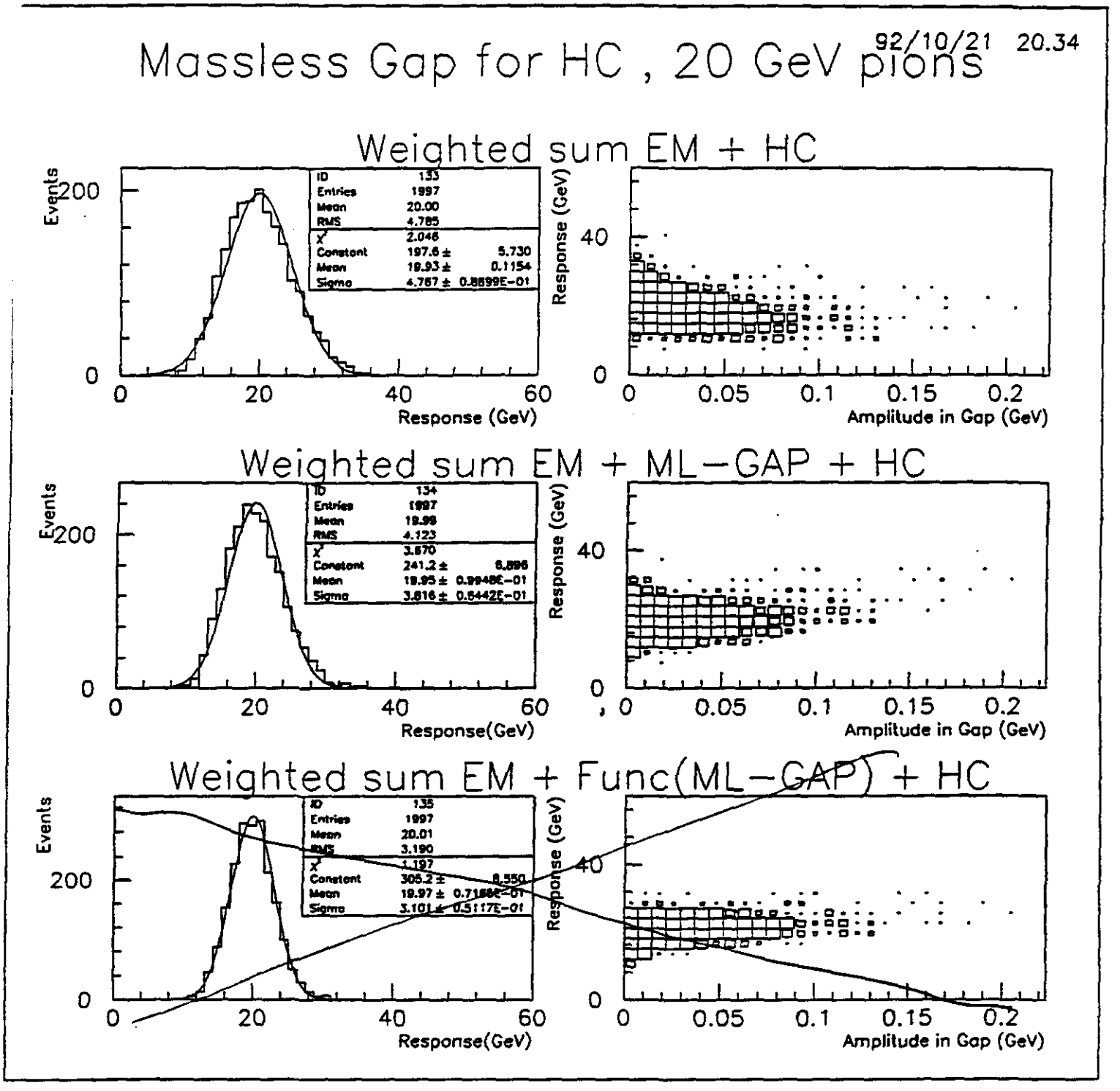
Massless Gap for HC , 20 GeV pions
92/10/21 20.34
Weighted sum EM + HC
ID 133
Entries 1997
Mean 20.00
RMS 4.785
χ² 2.046
Constant 197.6 ± 5.730
Mean 19.93 ± 0.1154
Sigma 4.767 ± 0.8899E-01
Events
Response (GeV)
Amplitude in Gap (GeV)
Weighted sum EM + ML-GAP + HC
ID 134
Entries 1997
Mean 19.98
RMS 4.123
χ² 3.670
Constant 241.2 ± 6.896
Mean 19.95 ± 0.9948E-01
Sigma 3.816 ± 0.6442E-01
Response(GeV)
Weighted sum EM + Func(ML-GAP) + HC
ID 135
Entries 1997
Mean 20.01
RMS 3.190
χ² 1.197
Constant 305.2 ± 8.550
Mean 19.97 ± 0.7188E-01
Sigma 3.101 ± 0.5117E-01

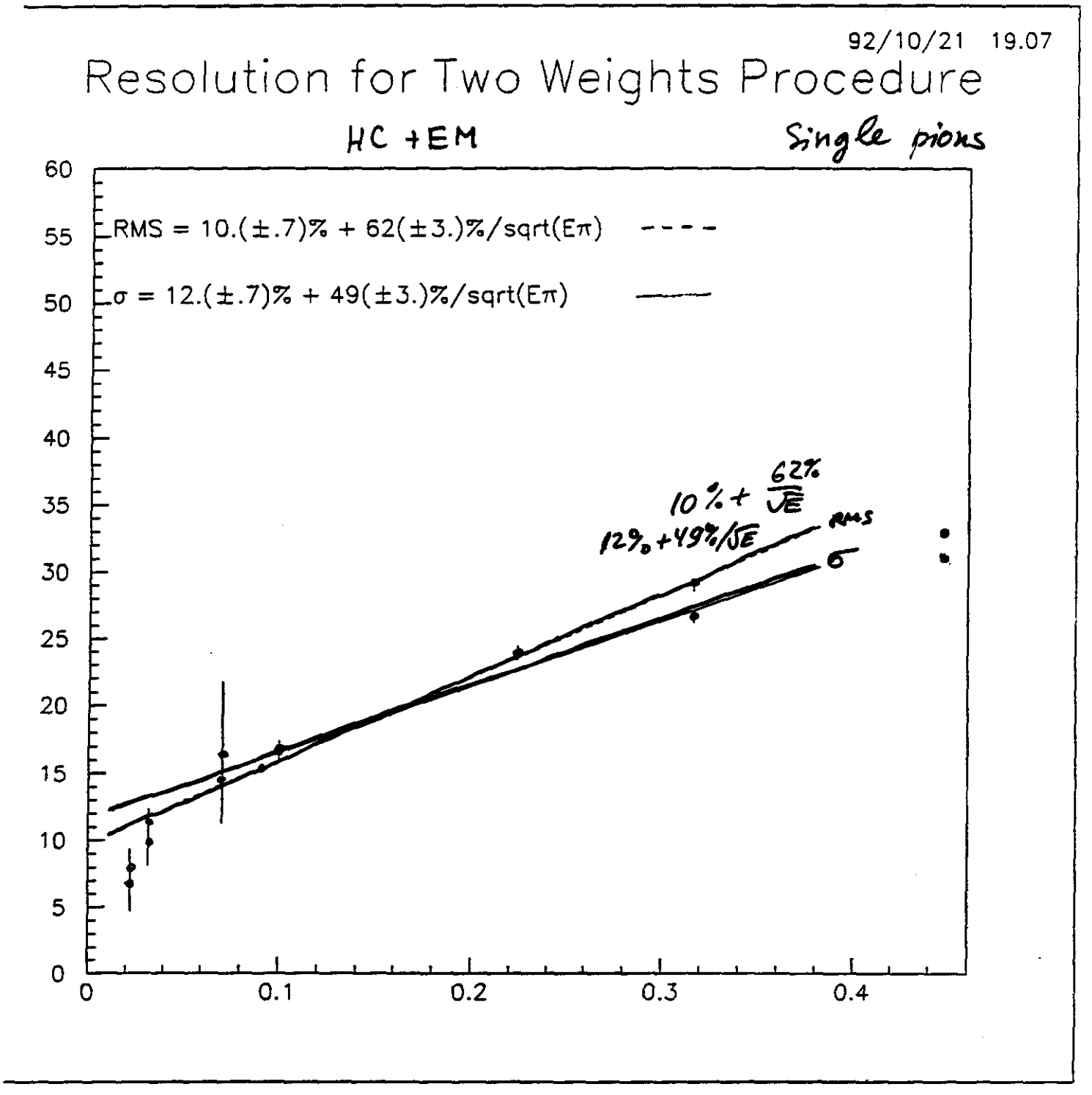
92/10/21 19.07
Resolution for Two Weights Procedure
HC + EM
Single pions
RMS = 10.(±.7)% + 62(±3.)%/sqrt(Eπ)
σ = 12.(±.7)% + 49(±3.)%/sqrt(Eπ)
10% + 62%/√E
12% + 49%/√E
RMS
σ
0
5
10
15
20
25
30
35
40
45
50
55
60
0
0.1
0.2
0.3
0.4

92/10/21 19.07

Resolution for Three Weights Procedure

HC + Massless GAP + EM Single pions

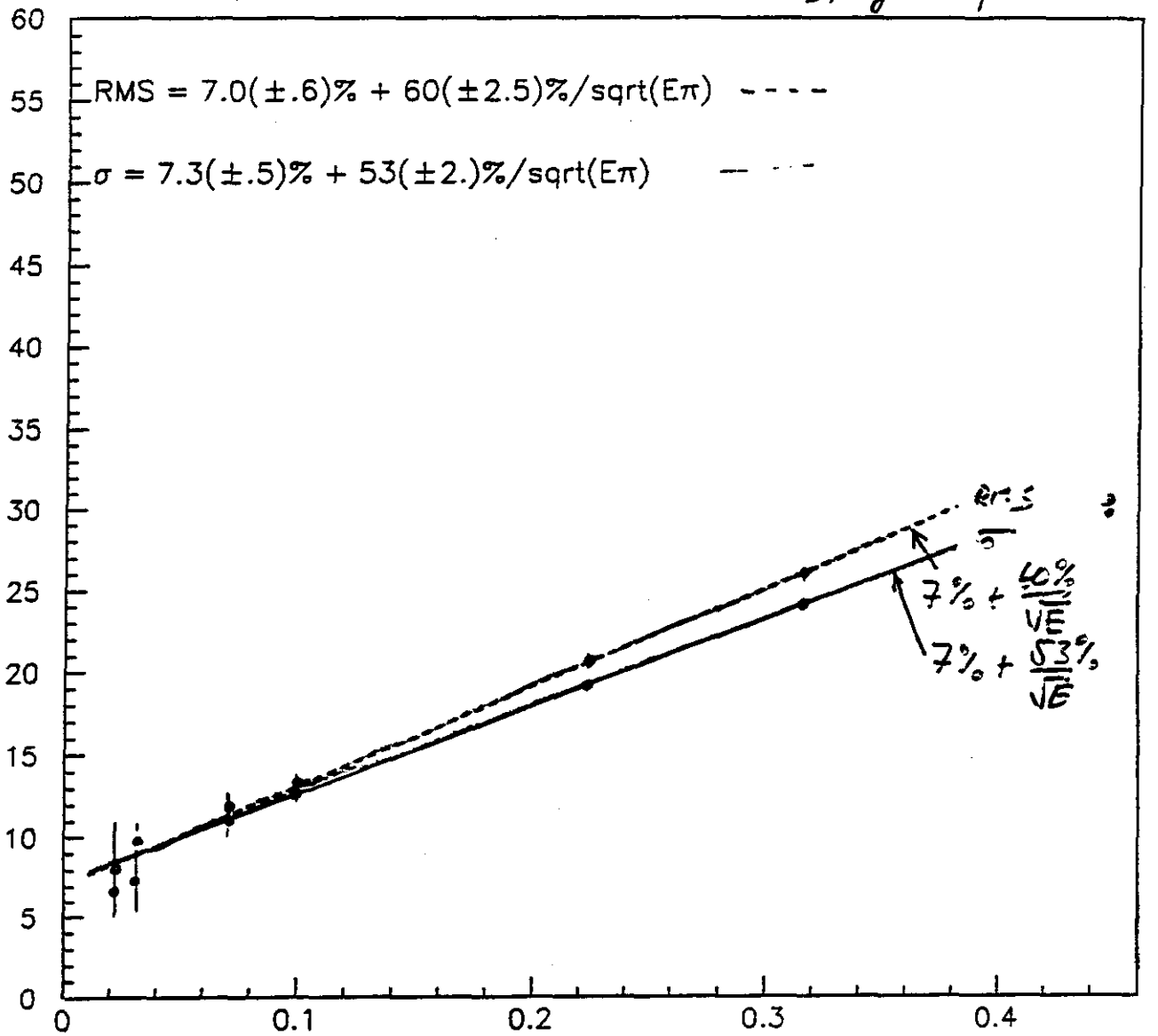

92/10/21 18.55

200 GeV jets

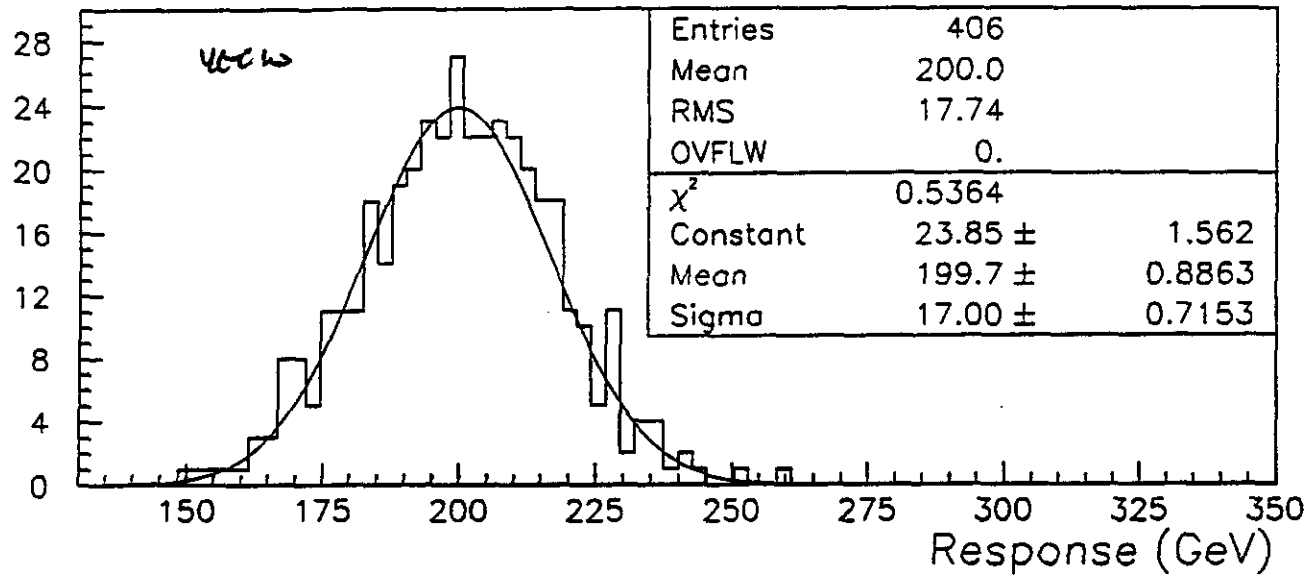

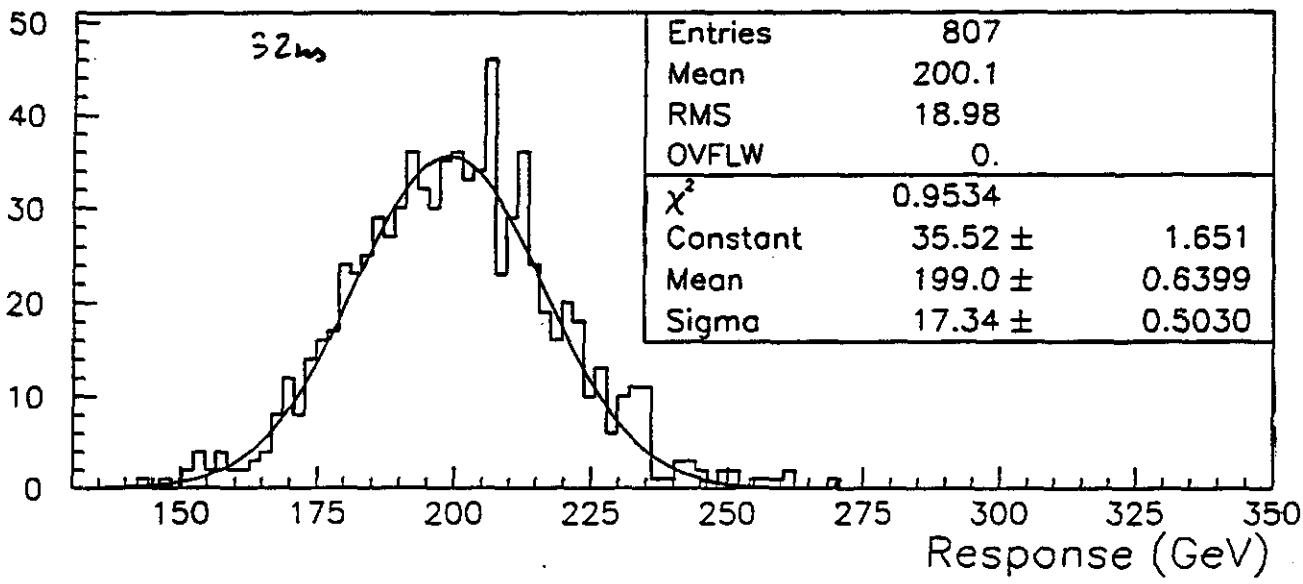

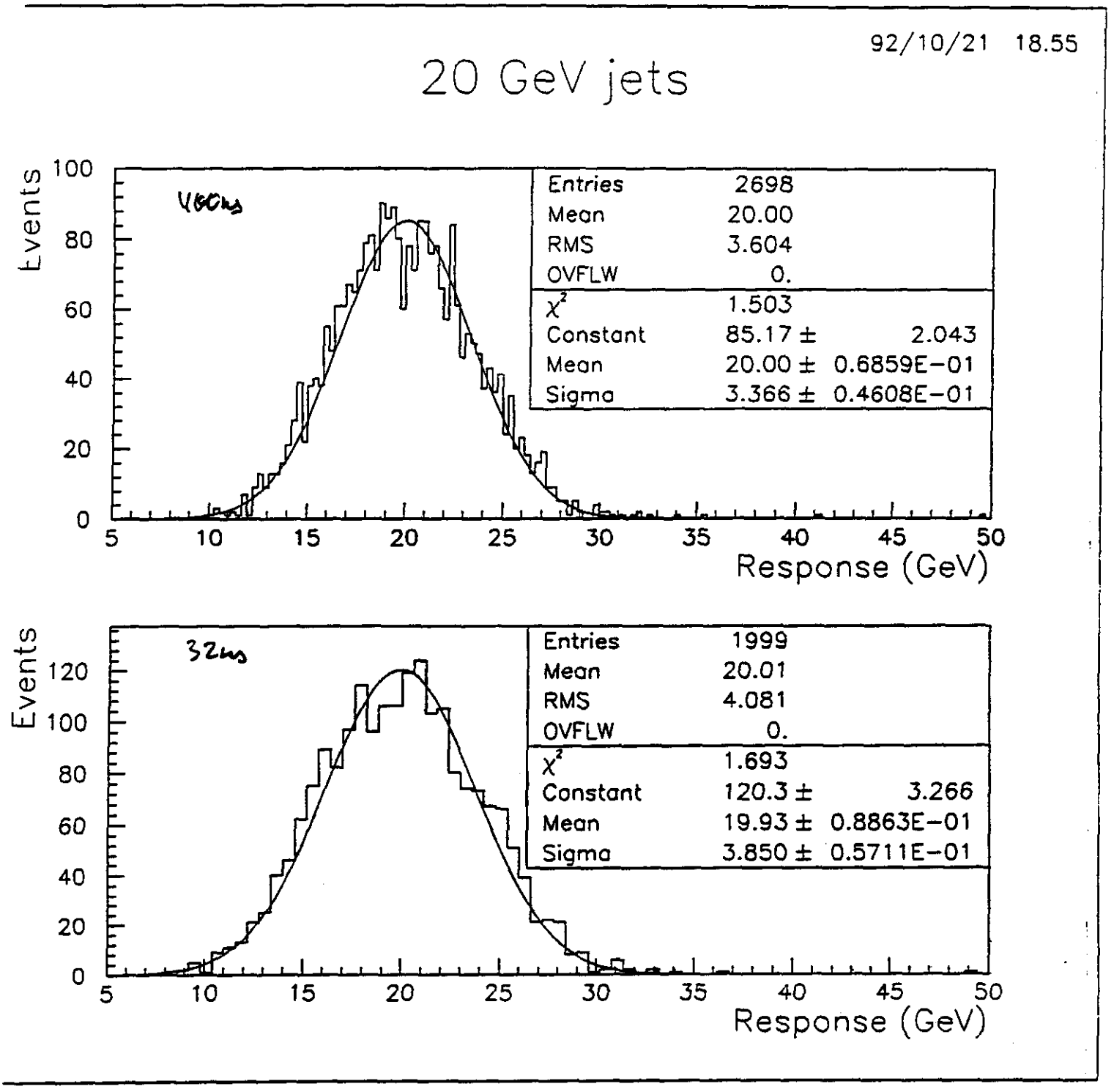
92/10/21 18.55
20 GeV jets
Events
Entries 2698
Mean 20.00
RMS 3.604
OVFLW 0.
χ² 1.503
Constant 85.17 ± 2.043
Mean 20.00 ± 0.6859E−01
Sigma 3.366 ± 0.4608E−01
Response (GeV)
Events
32ns
Entries 1999
Mean 20.01
RMS 4.081
OVFLW 0.
χ² 1.693
Constant 120.3 ± 3.266
Mean 19.93 ± 0.8863E−01
Sigma 3.850 ± 0.5711E−01
Response (GeV)

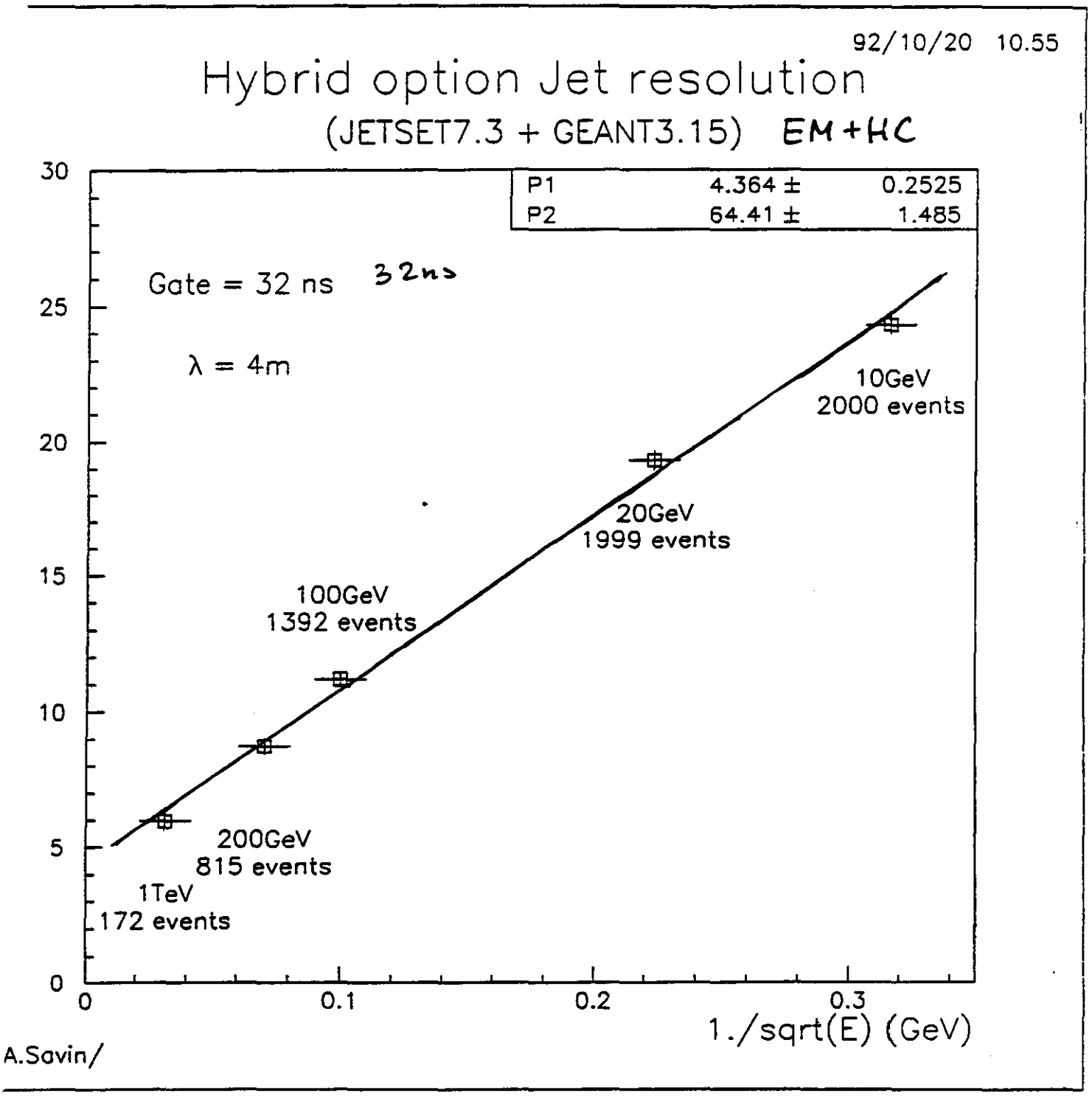
92/10/20 10.55
Hybrid option Jet resolution
(JETSET7.3 + GEANT3.15) EM+HC
P1 4.364 ± 0.2525
P2 64.41 ± 1.485
Gate = 32 ns
32ns
λ = 4m
10GeV
2000 events
20GeV
1999 events
100GeV
1392 events
200GeV
815 events
1TeV
172 events
30
25
20
15
10
5
0
0
0.1
0.2
0.3
1./sqrt(E) (GeV)
A.Savin/

gem

γeμ

Presentation by:

B. Moore

INTEGRATED EM/MASSLESS GAP/HCAL

- EDEP
- ATTENUATION
- ATTENUATION w/MIRRORING
- ATTENUATION w/MIRRORING + FILTERING

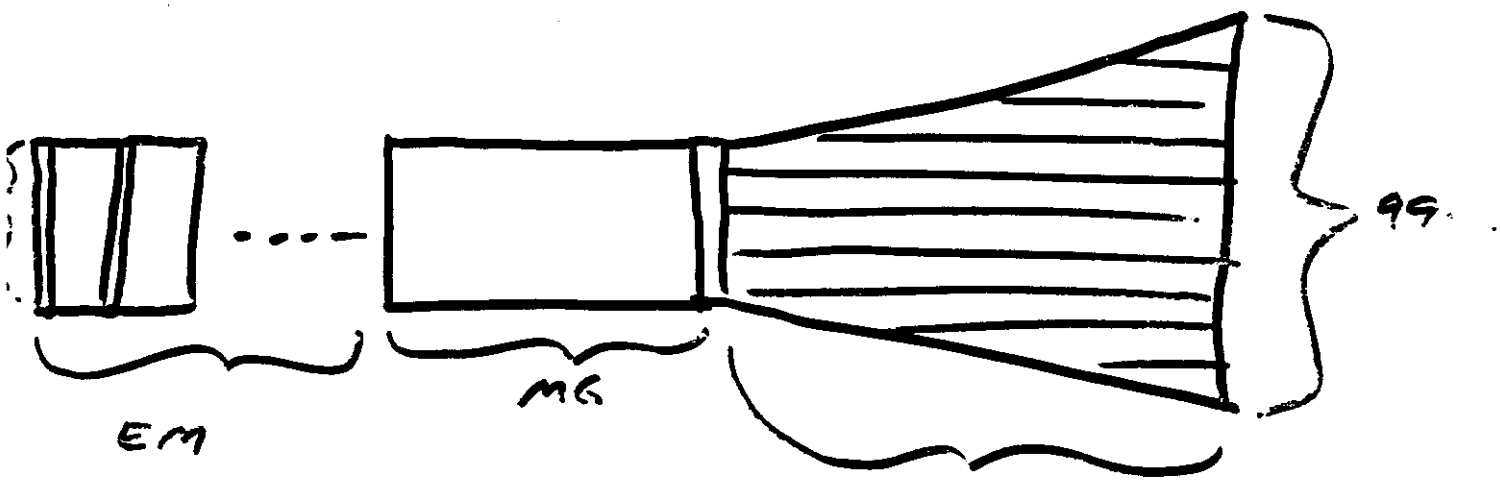

EM	MG	HCAL
0.02 STEEL	31.0 cm Al	
0.14 Pb	0.5 cm PLS	
0.02 STEEL	31.5 cm	160.0 cm
0.14 LKr		Cu w/PLS
0.32 cm		
×		
162 → 51.84 cm		

CALOR 89

1.0 MeV $e^{\pm}$ CUTOFF

0.1 MeV γ CUTOFF

DIAMETER 1mm

SPACING 0.512 cm

~~[illegible]~~

10 GeV π^-, e^-

50 GeV π^-, e^-

TEST BEAM COMPARISON

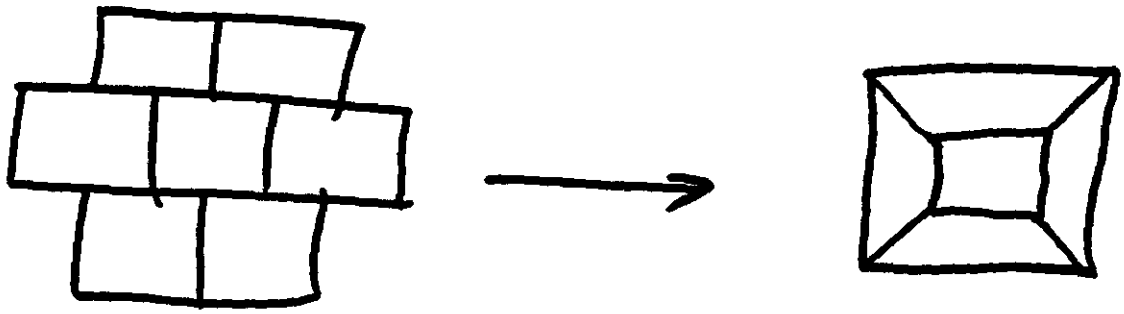

$$\pi \text{ Res} \sim \frac{90\%}{\sqrt{E}}$$

$$e^- \text{ Res} \sim \frac{70\%}{\sqrt{E}}$$

[redacted] 0.7925 cm SPACING

0.125 cm FIBER DIAMETER
0.05 cm PLASTIC CLADDING

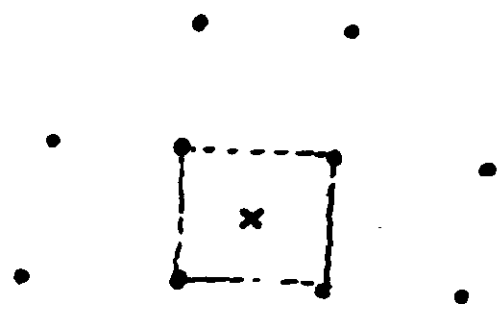

Presentation by:

Yuri Efremenko

(1) So/e

REJECTION.

EANT 3.15

π/e

by

E_{EM}; E_H.

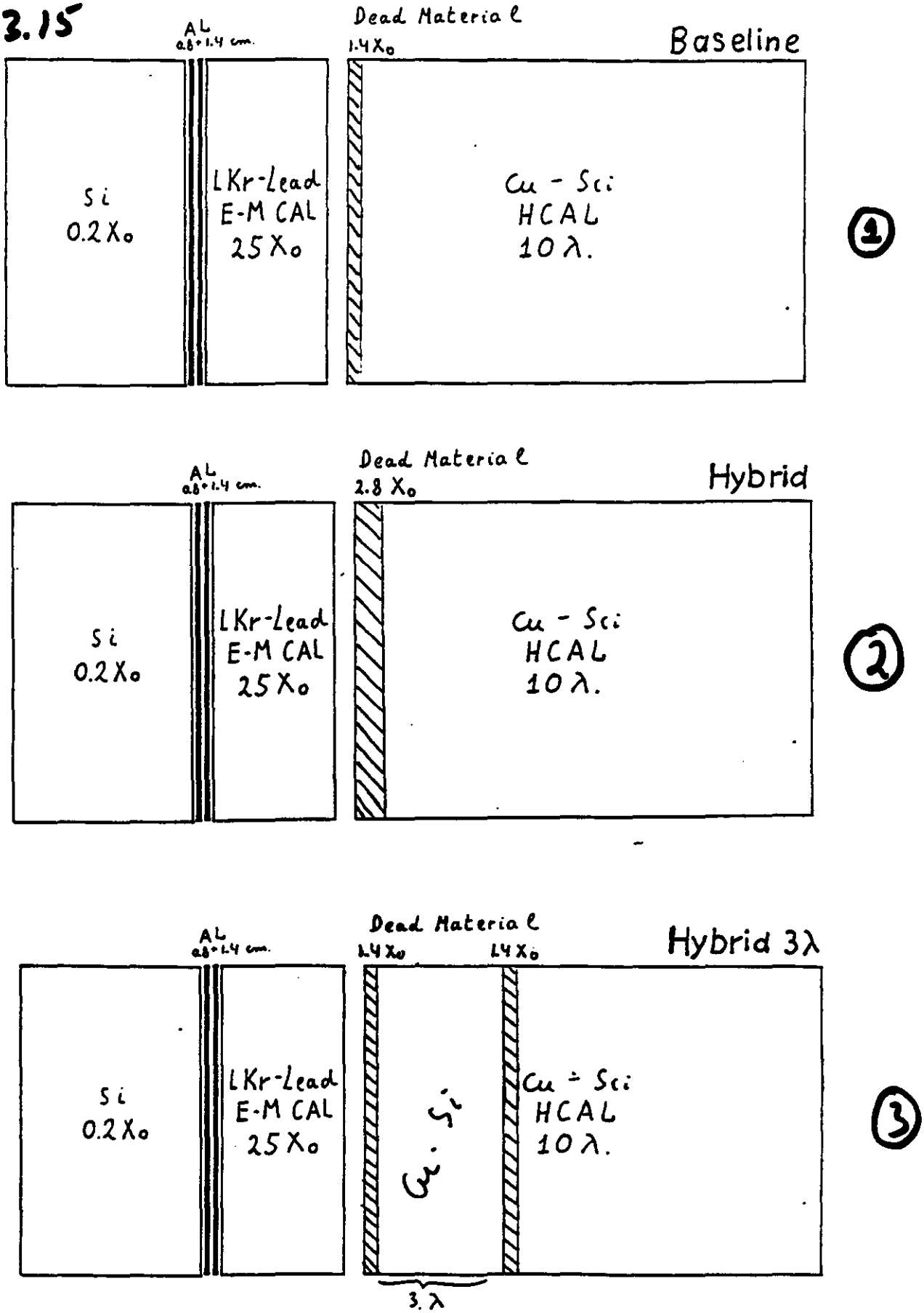

E_e HCAL ① = E_e HCAL ③

Fig 1.

Energy in HCAL, 100 GEV.

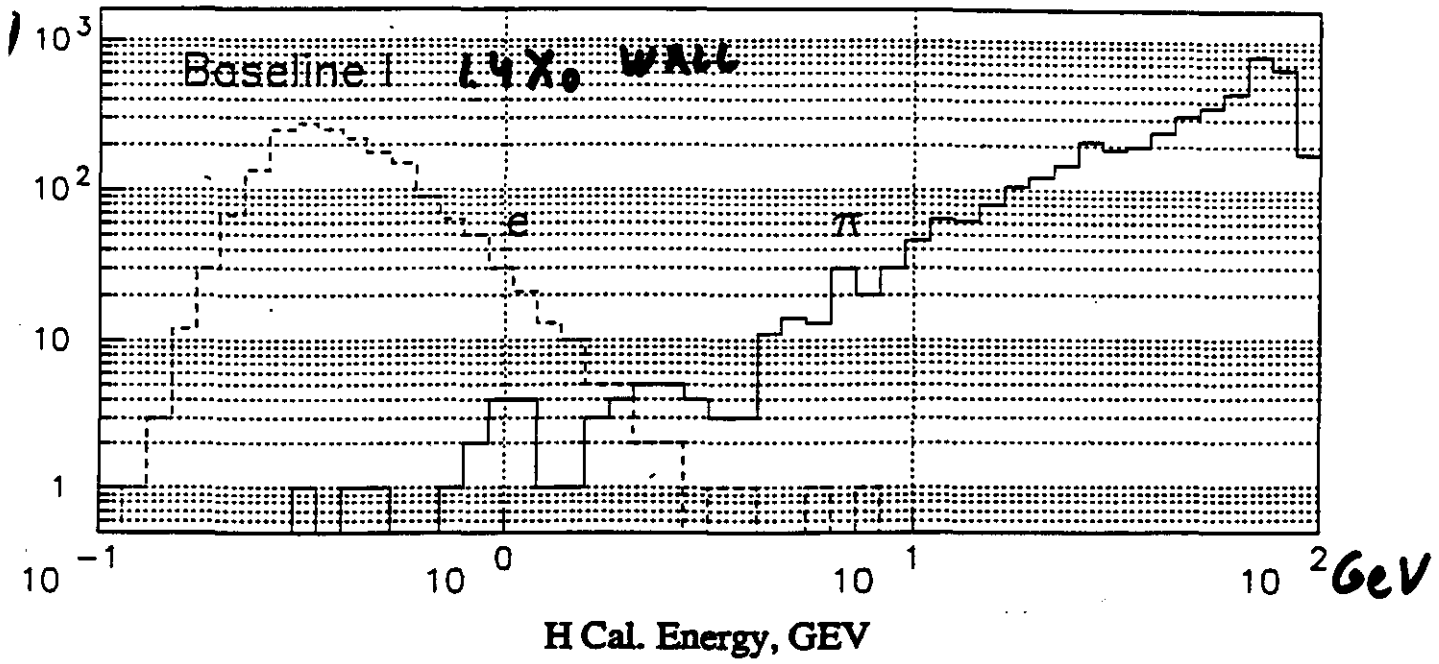

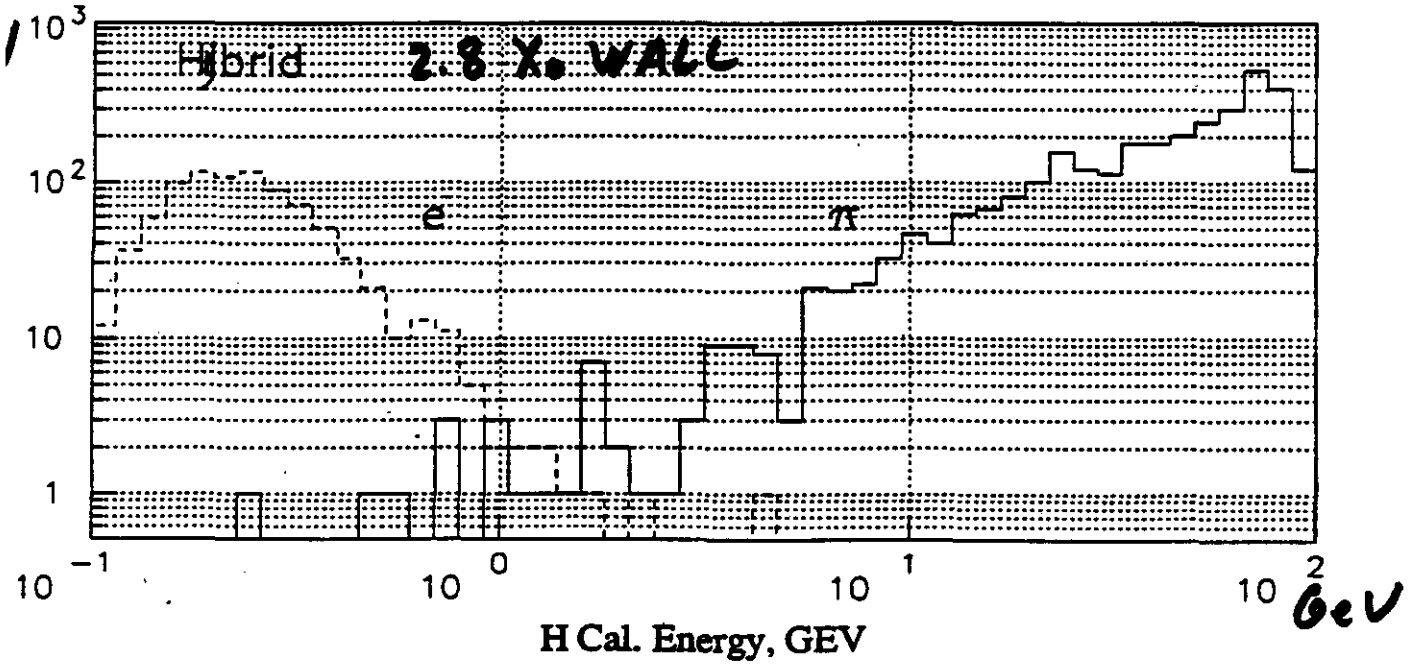

$\frac{dE}{dX}$ (E-M shower) > $\frac{dE}{dX}$ (H shower)

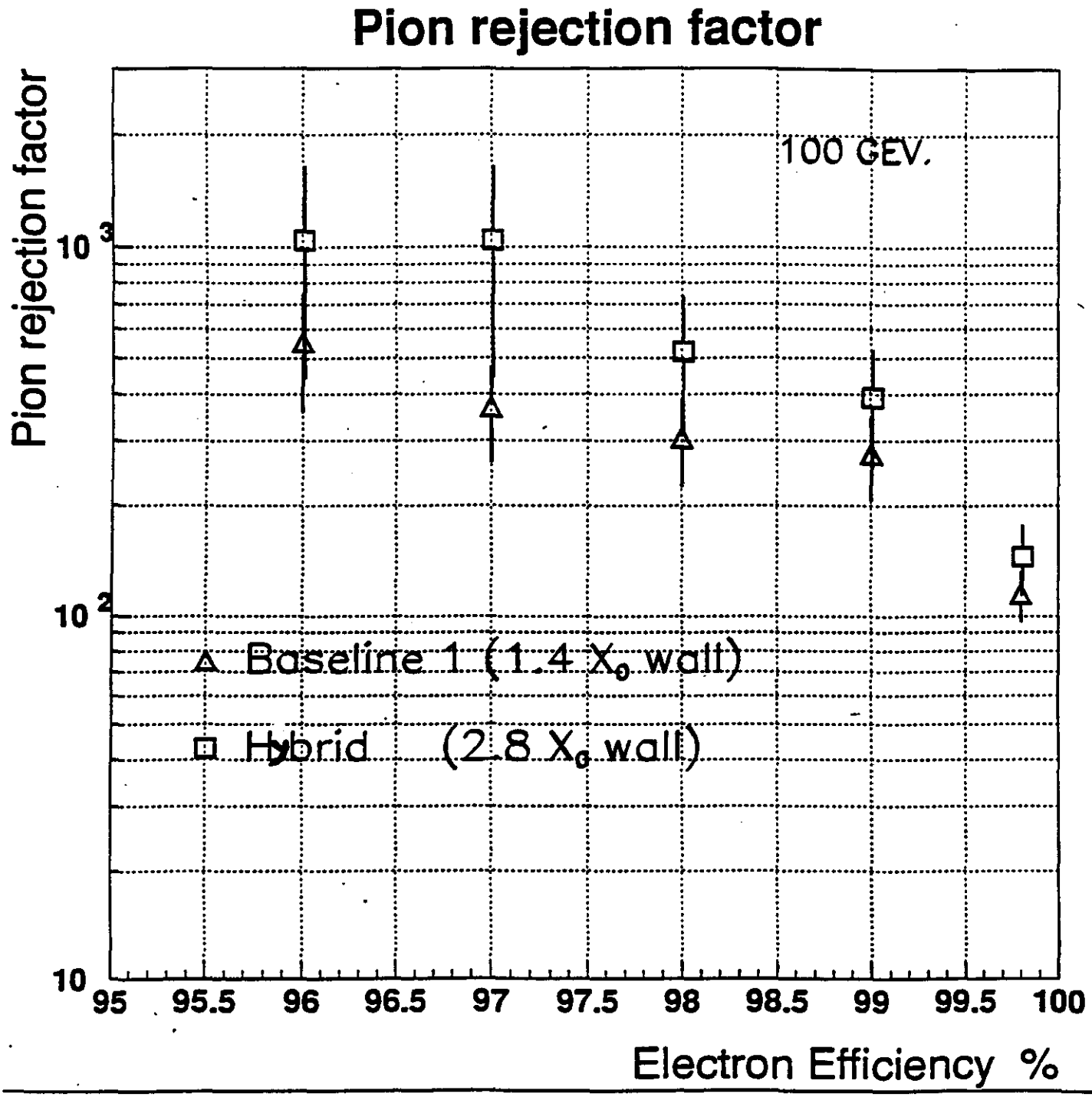

THICK WALL IS BETTER FOR π/e SEPARATION.

Fig. 4.

(2) Dead Material in

in E-M after
preradiator.

Dead Material after pre radiator in E-M calorimeter.

Energy resolution degradation.

GEANT 3.15

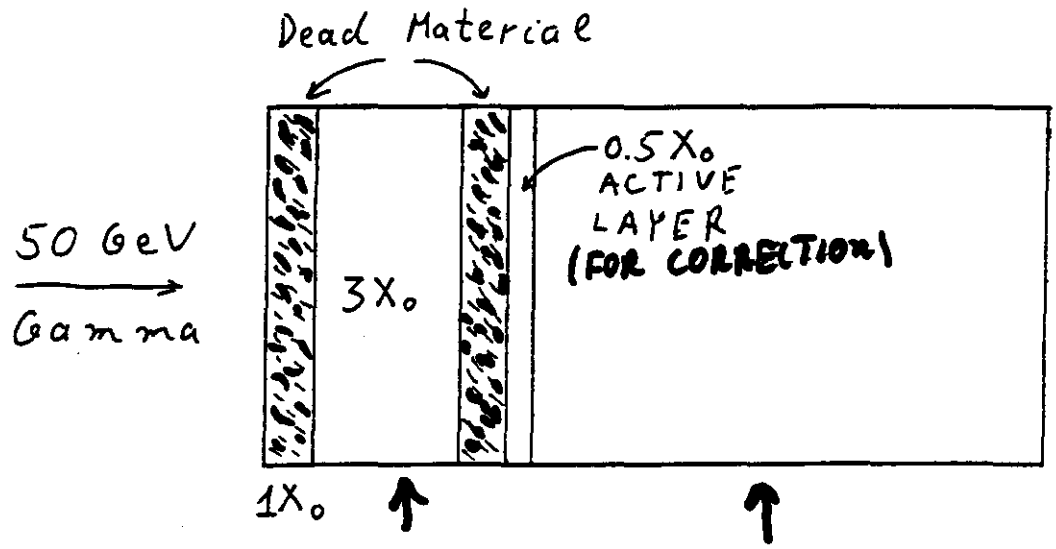

Parallel Plate Accordion
(For example).

50 GEV LKr Par Plate, 3x0, DEAD, OTHER- 0,029.

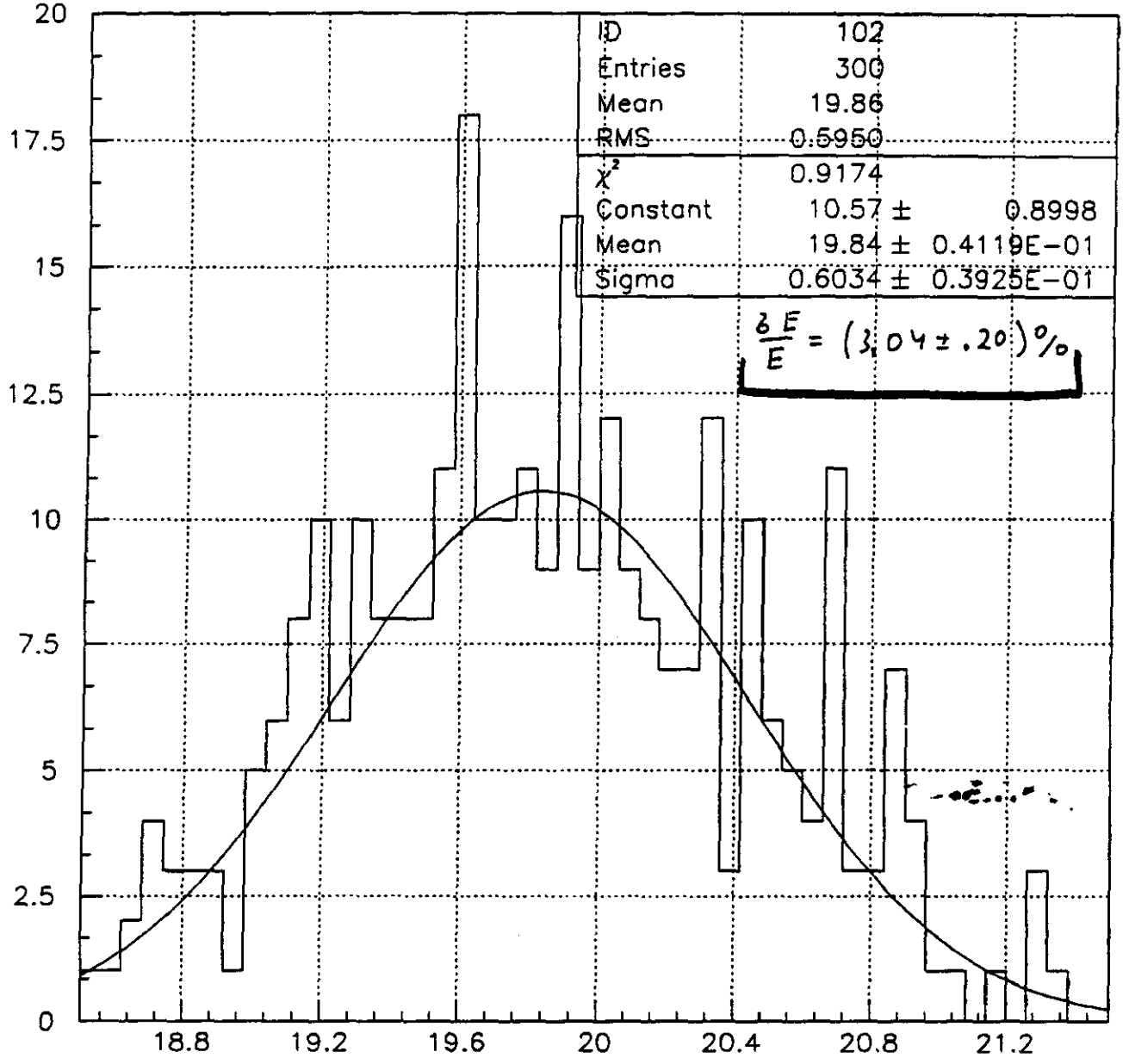

.46 x0 dead material

50 GEV, LKr Par Plate, Dead material after 4X0

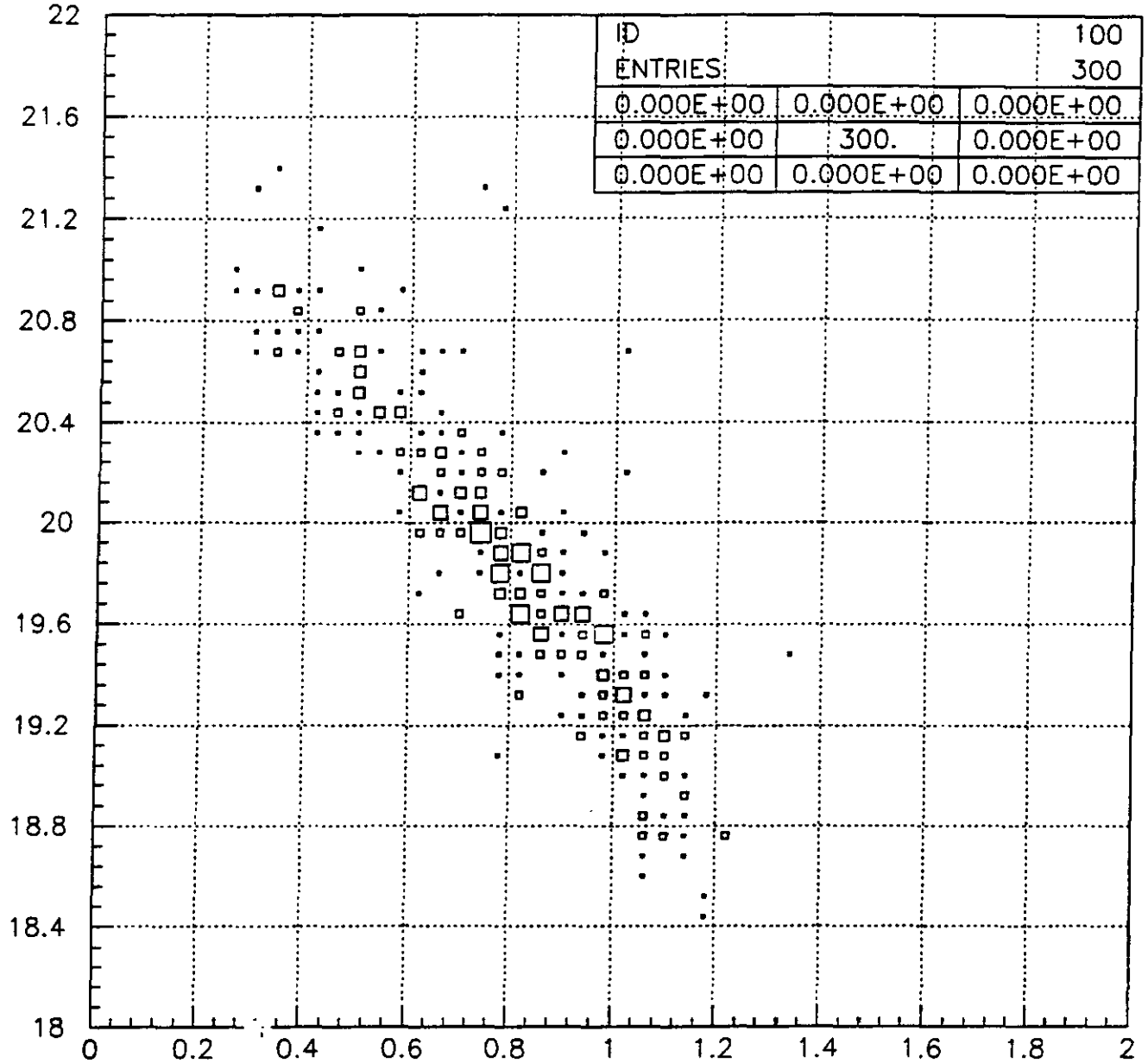

E in cal vs. E in active layer, 0.46 X0 dead

50 GEV LKr Par Plate, 3x0, DEAD, OTHER- 0,029.

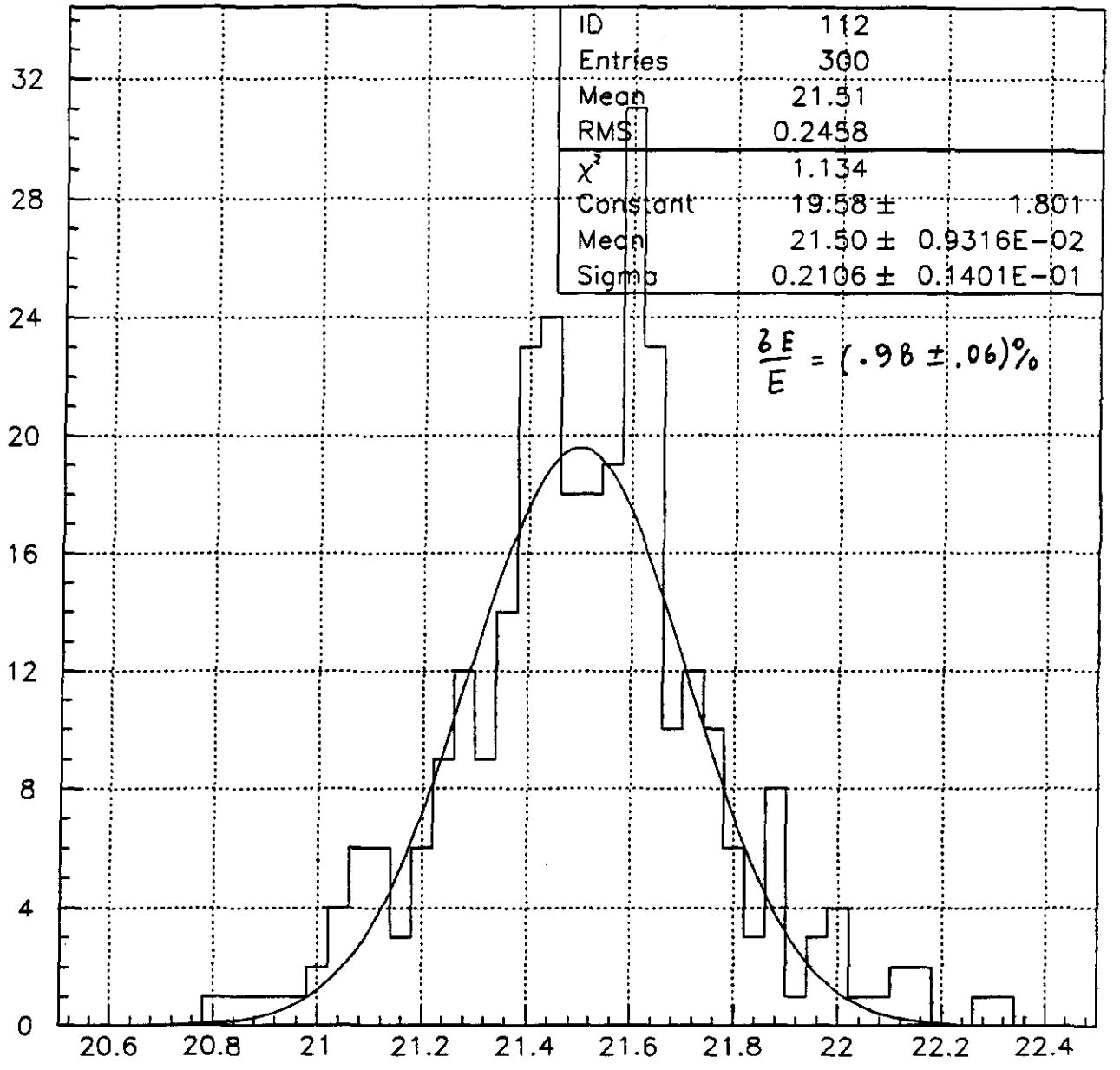

.46 x0 dead material, corrected

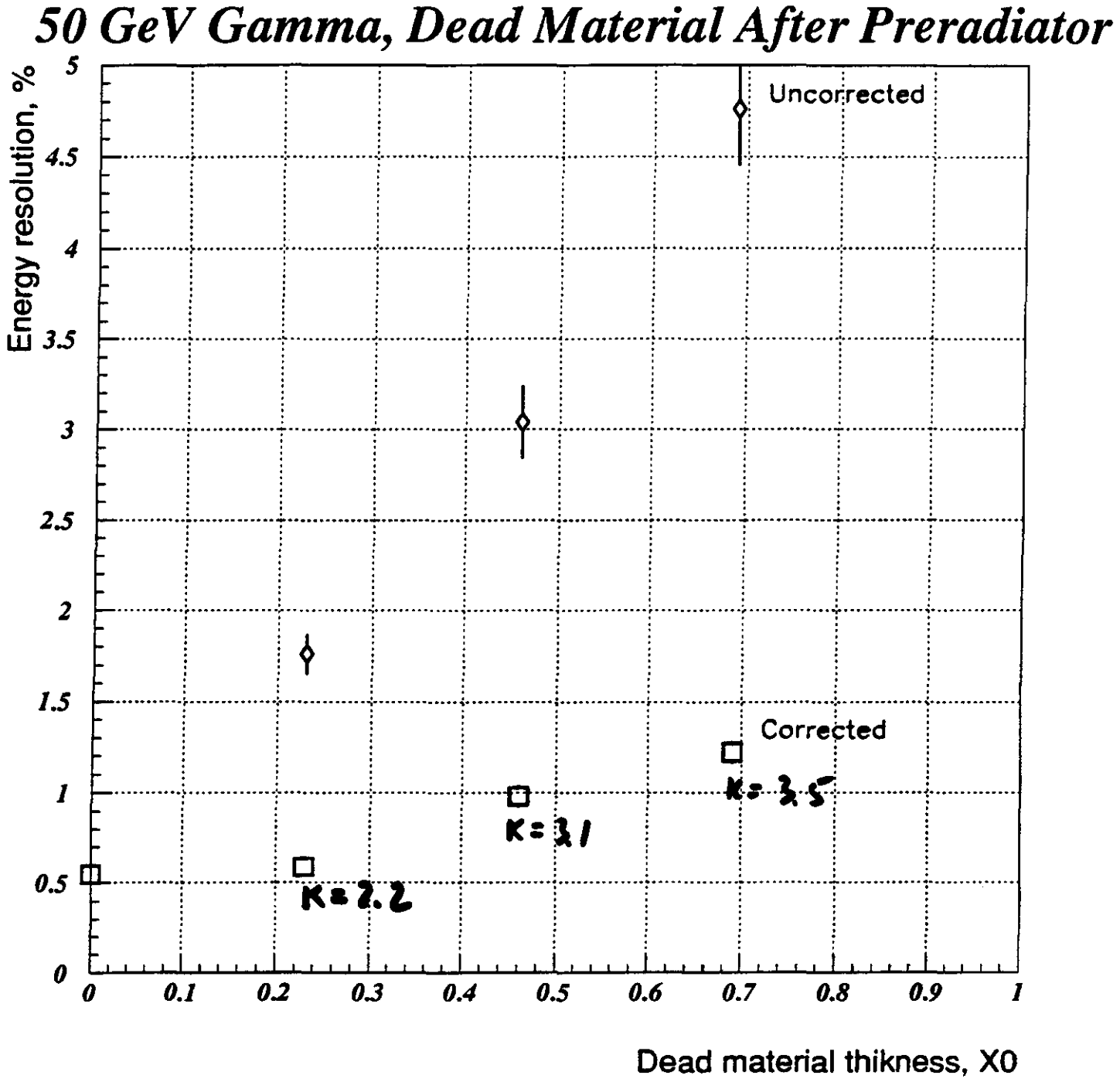

IF ONE WILL HAVE PASSIVE MASS LESS GAP, CORRECTION - WORSE.

K = K (E, THIKNESS, PARTICLE TYPE)

③ Pointing

and $\mu \to \gamma\gamma$

Shmakov.

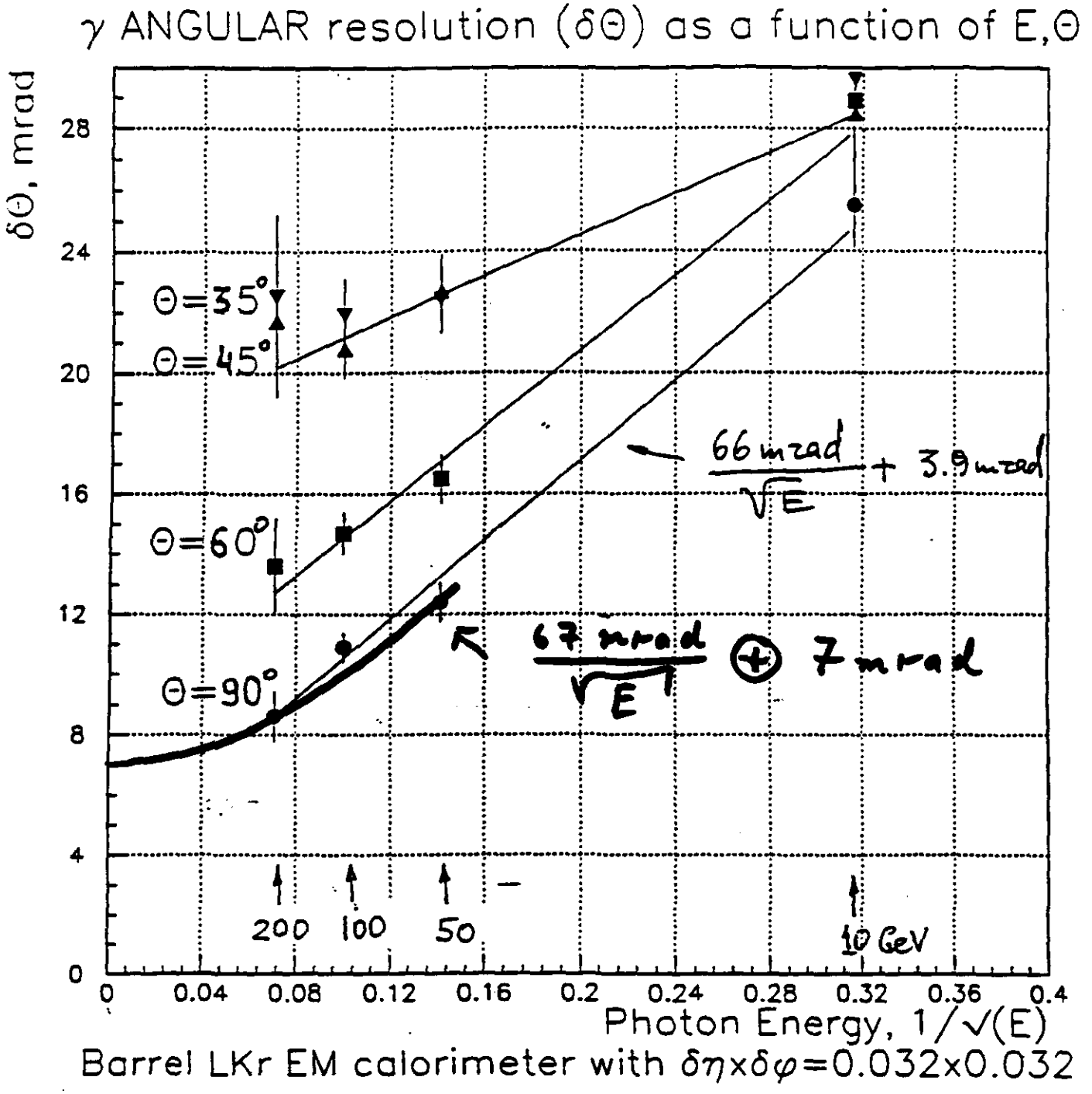
γ ANGULAR resolution (δΘ) as a function of E,Θ
δΘ, mrad
Θ=35°
Θ=45°
Θ=60°
Θ=90°
66 mrad / √E + 3.9 mrad
67 mrad / √E ⊕ 7 mrad
200
100
50
10 GeV
Photon Energy, 1/√(E)
Barrel LKr EM calorimeter with δη×δφ=0.032×0.032

80 GeV HIGS
Sigma(M), GeV

Sigma(E)/E=(5.5/sqrt(E)⊕0.4)%

	Barel Barel	Barel Endcup	Endcup Endcup	Total	Time Discovery
Ideal	0.50+/-.02	0.45+/-.03	0.35+/-.03	0.44+/-.02	1
No vertex	1.30+/-.10	1.48+/-.13	1.56+/-.15	1.55+/-.07	3.56
(67+7)mrad /sqrt(E)	0.68+/-.04	0.96+/-.06	1.29+/-.11	0.92+/-.04	2.10
(43+6)mrad /sqrt(E)	0.63+/-.04	0.88+/-.06	1.25+/-.10	0.84+/-.35	1.82
(35+1)mrad /sqrt(E)	0.57+/-.03	0.60+/-.04	0.80+/-.08	0.64+/-.03	1.45
(67+7)Ba. (35+1)EC /sqrt(E)	0.68+/-.04	0.81+/-.06	0.80+/-.08	0.75+/-.03	1.68

% events 46% 29% 25%

(35+1) => $\frac{35}{\sqrt{E}} \oplus 1$ mrad

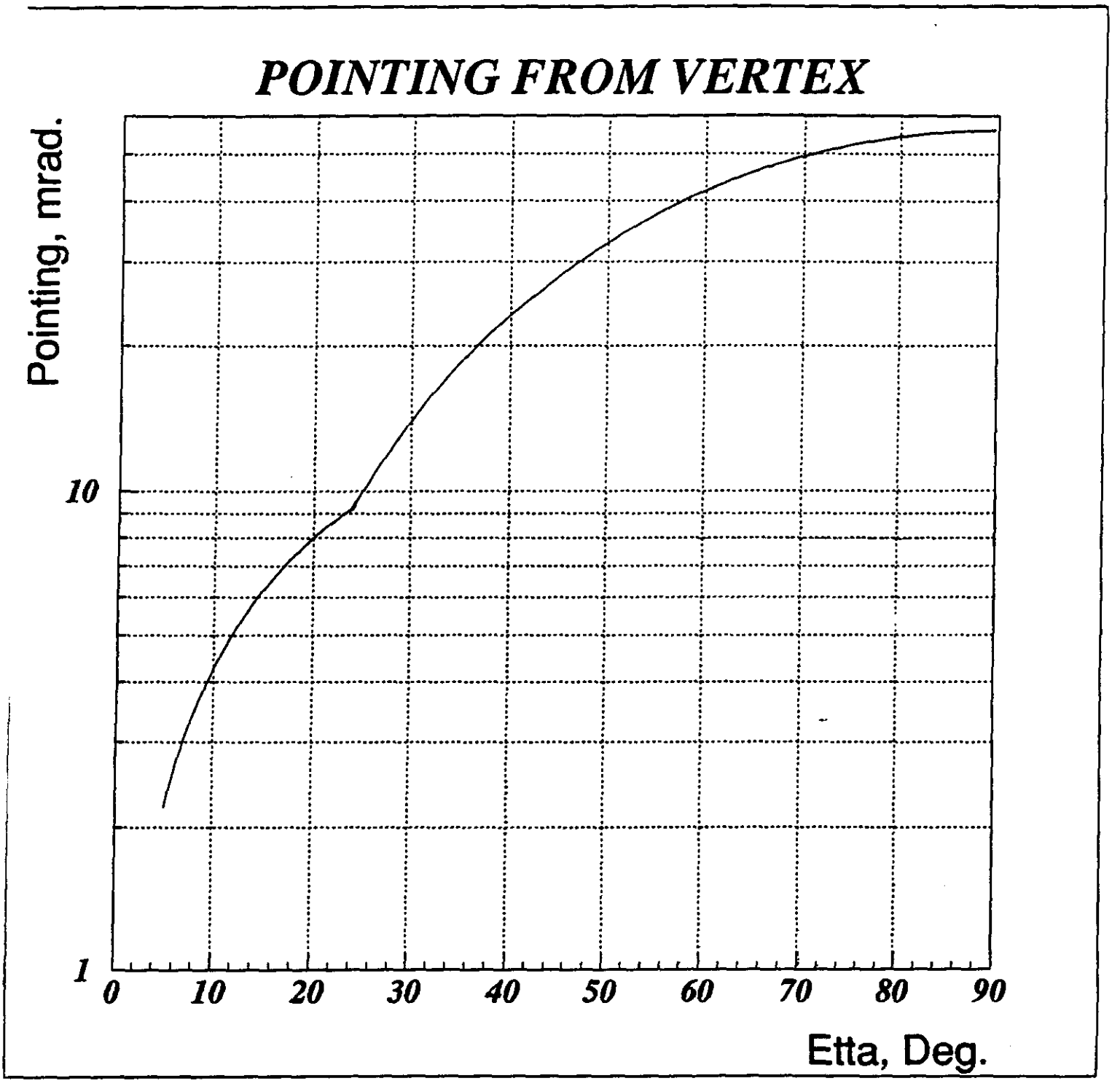
POINTING FROM VERTEX
Pointing, mrad.
10
1
0
10
20
30
40
50
60
70
80
90
Etta, Deg.

$H_0 \to \gamma\gamma$ **decay:**

$$\frac{\delta M_{H_0}}{M_{H_0}} = \frac{1}{2}\sqrt{\left(\frac{\delta E_1}{E_1}\right)^2 + \left(\frac{\delta E_2}{E_2}\right)^2 + \left(\frac{\delta\Theta}{\tan(\frac{\Theta}{2})}\right)^2}$$

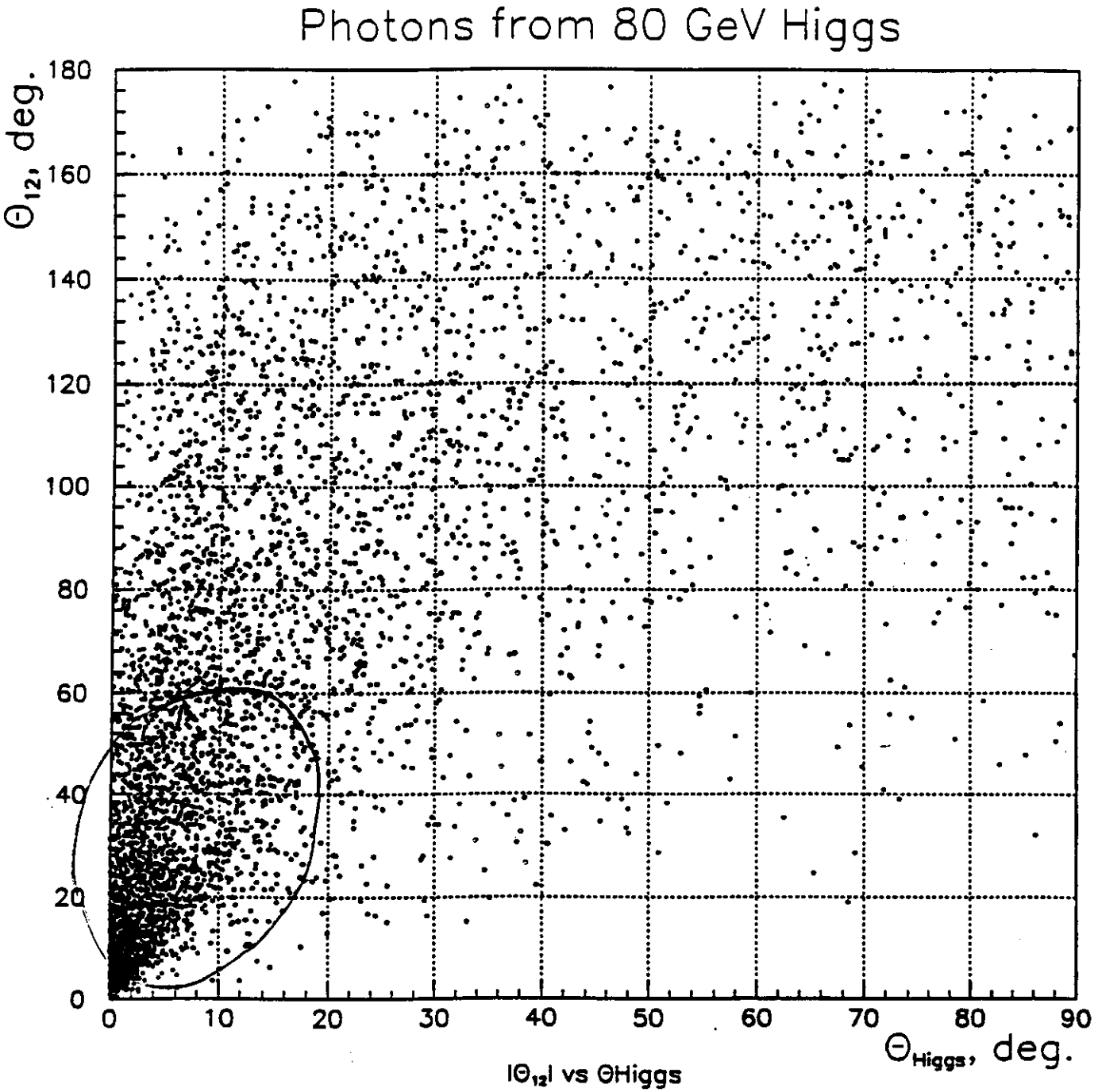
Photons from 80 GeV Higgs
Θ_{12}, deg.
180
160
140
120
100
80
60
40
20
0
0
10
20
30
40
50
60
70
80
90
Θ_{Higgs}, deg.
$|\Theta_{12}|$ vs ΘHiggs

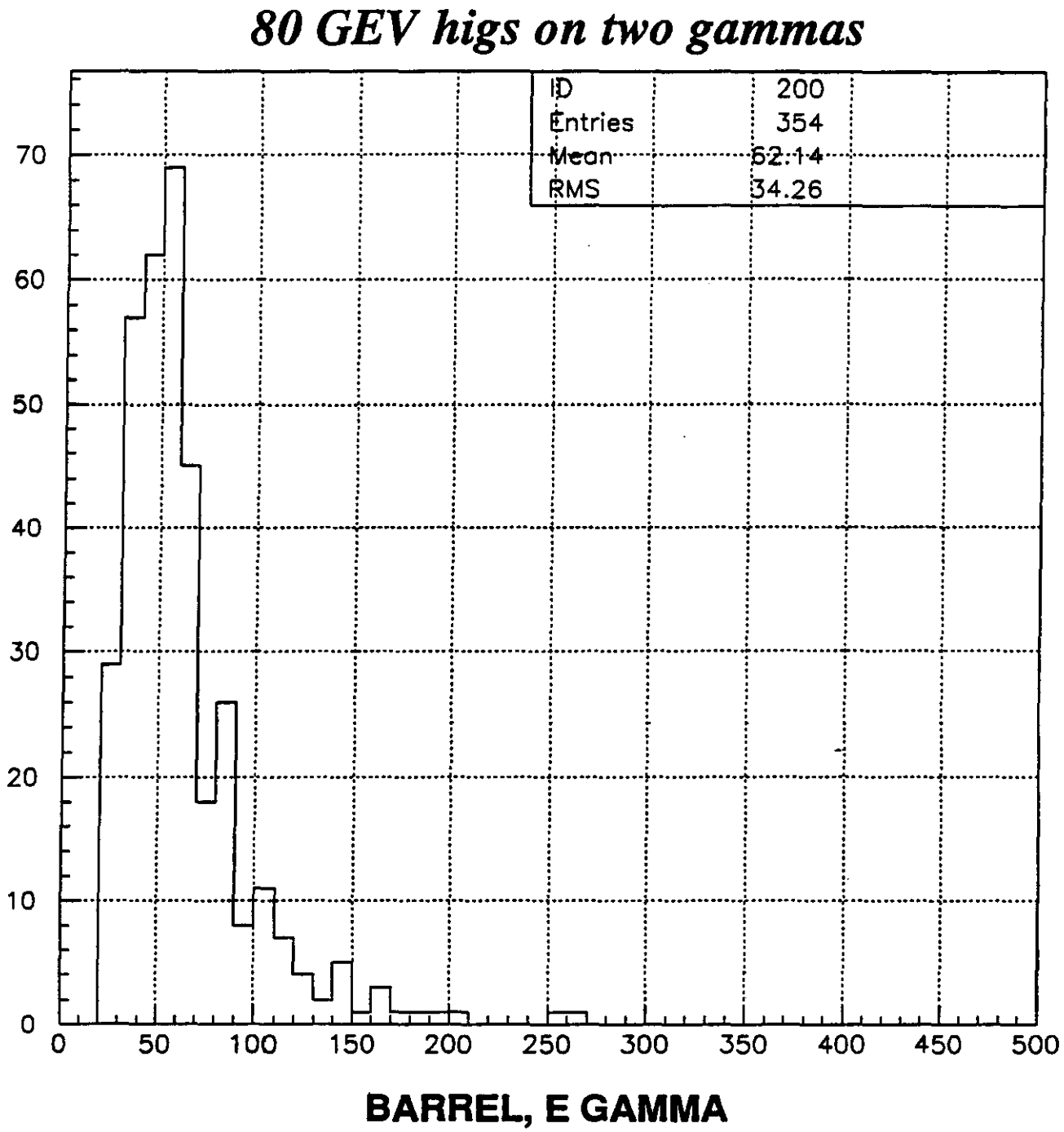
80 GEV higs on two gammas
ID 200
Entries 354
Mean 62.14
RMS 34.26
0
10
20
30
40
50
60
70
0
50
100
150
200
250
300
350
400
450
500
BARREL, E GAMMA

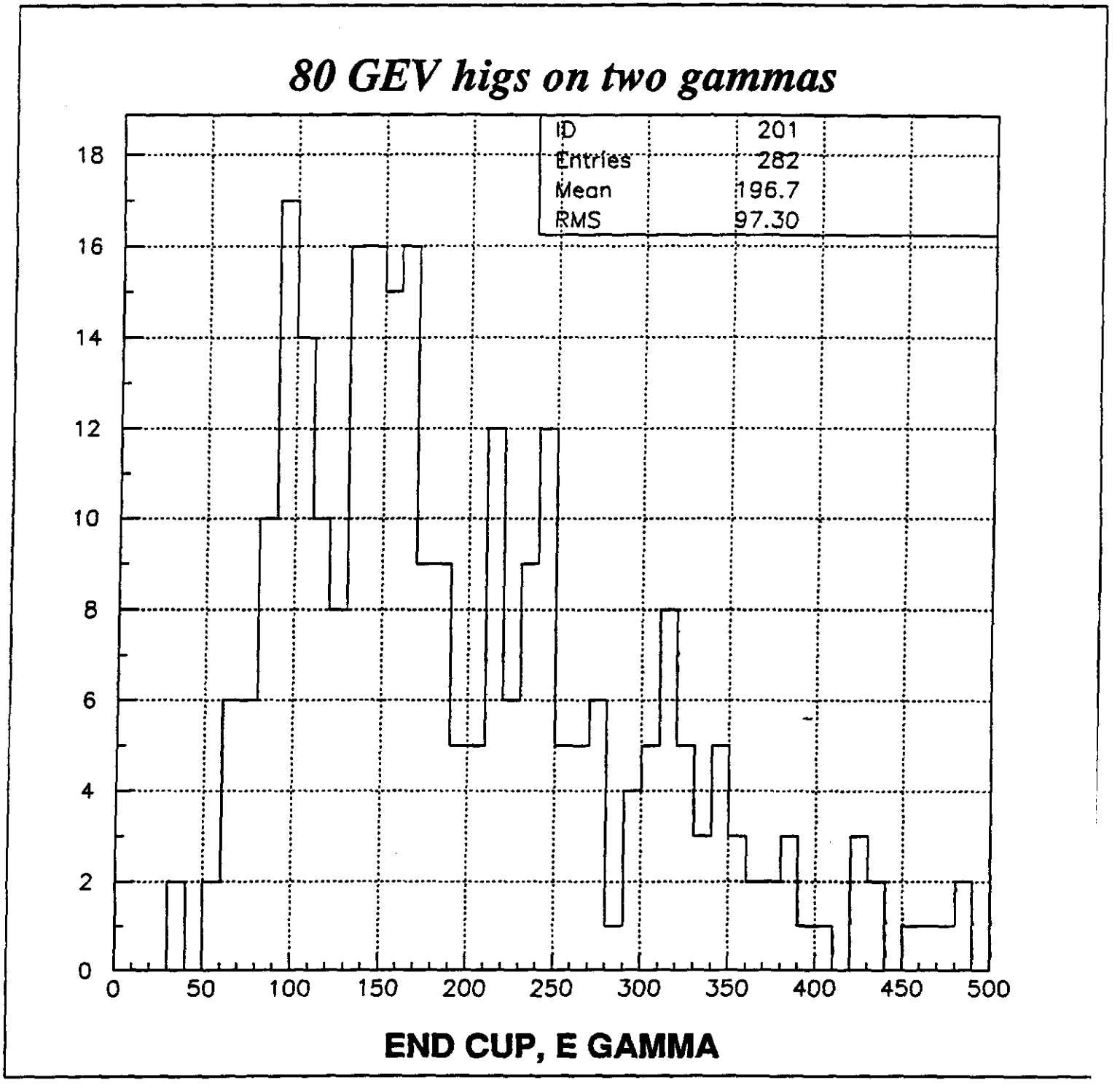
80 GEV higs on two gammas
ID 201
Entries 282
Mean 196.7
RMS 97.30
0
2
4
6
8
10
12
14
16
18
0
50
100
150
200
250
300
350
400
450
500
END CUP, E GAMMA

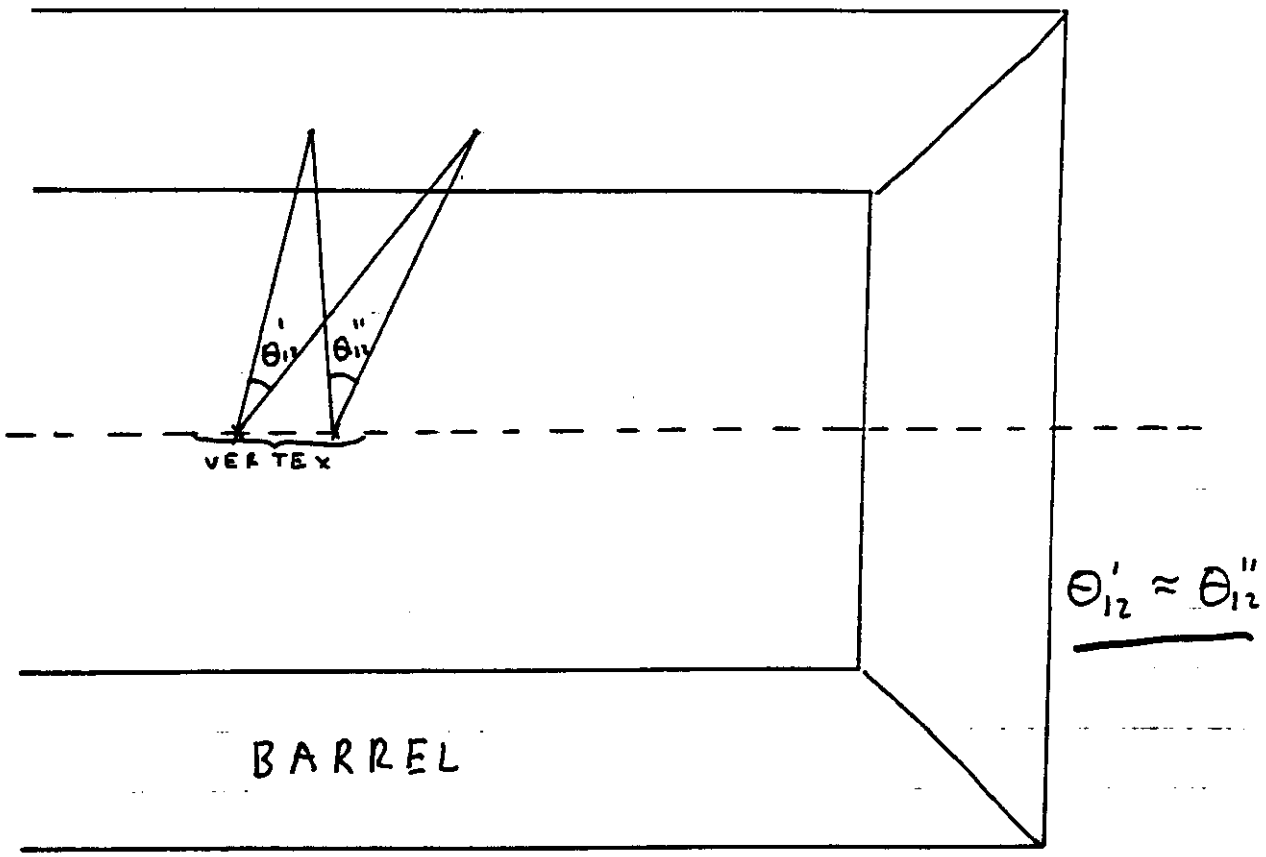
θ'_{12}
θ''_{12}
VERTEX
BARREL
$\theta'_{12} \approx \theta''_{12}$

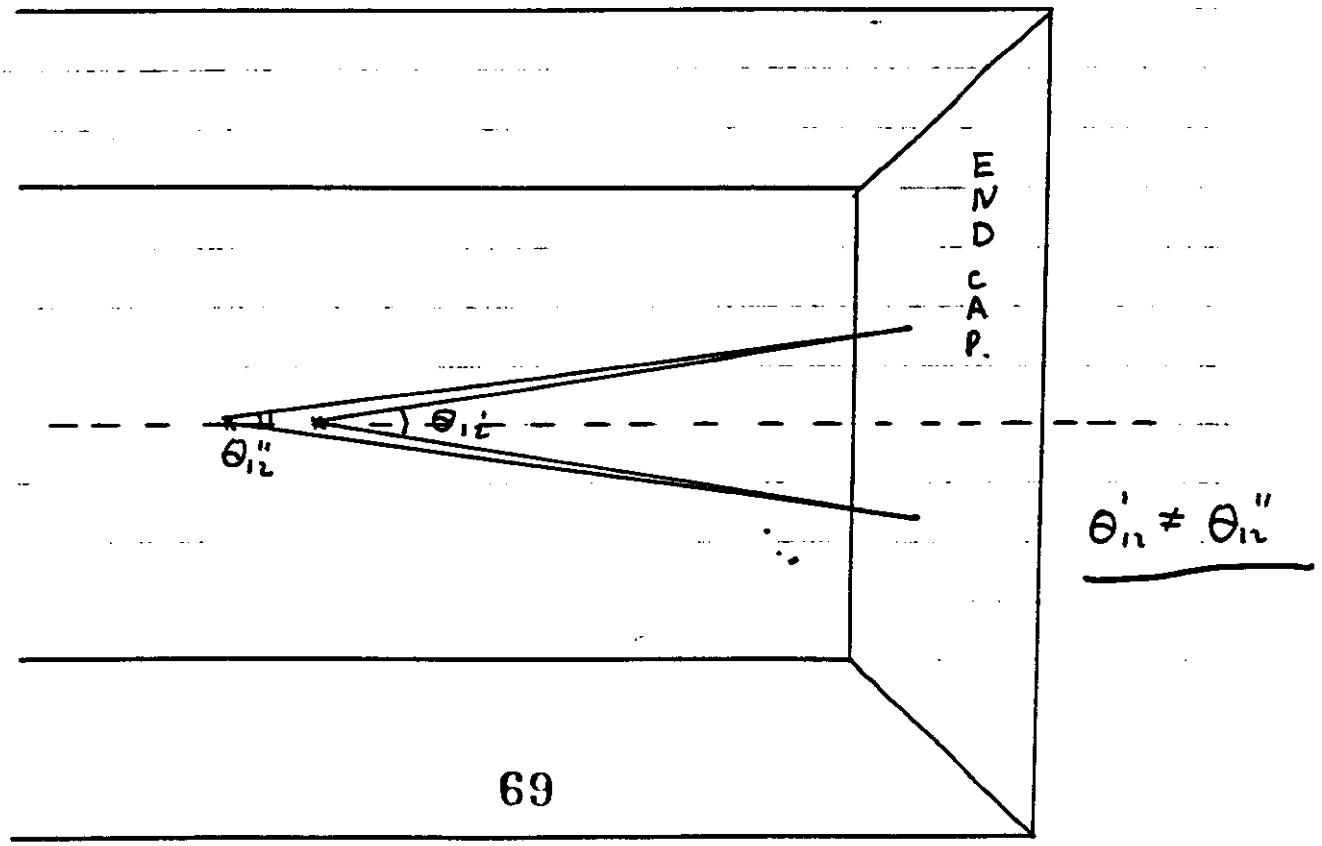
END CAP.
θ'_{12}
θ''_{12}
$\theta'_{12} \neq \theta''_{12}$

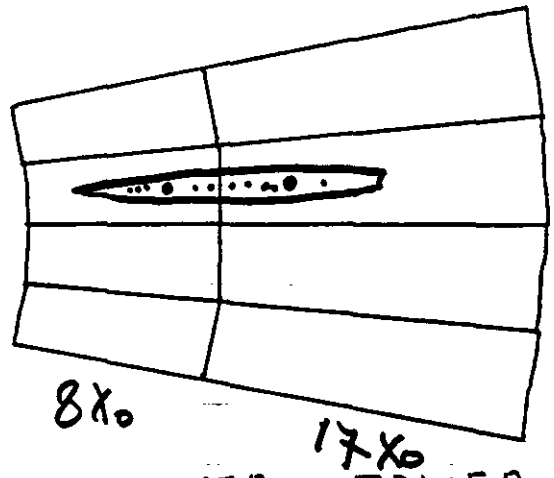

1

TOWER - TOWER
$8X_0$ $17X_0$

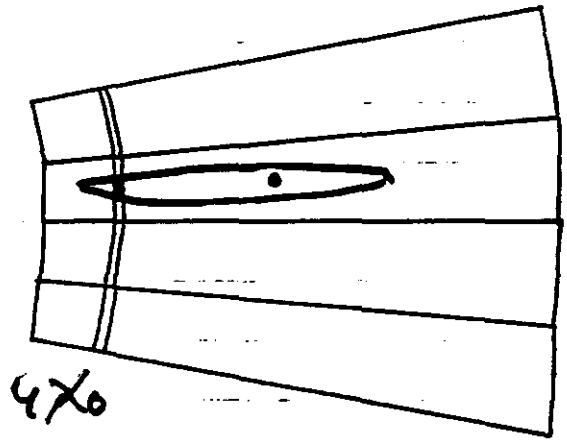

2

STRIPS - TOWER
STRIPS- AFTER $4X_0$

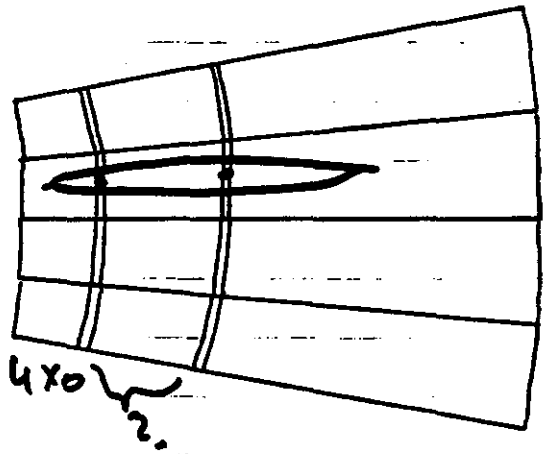

3

STRIPS- STRIPS.

$\sigma_z = 4.2$ cm.

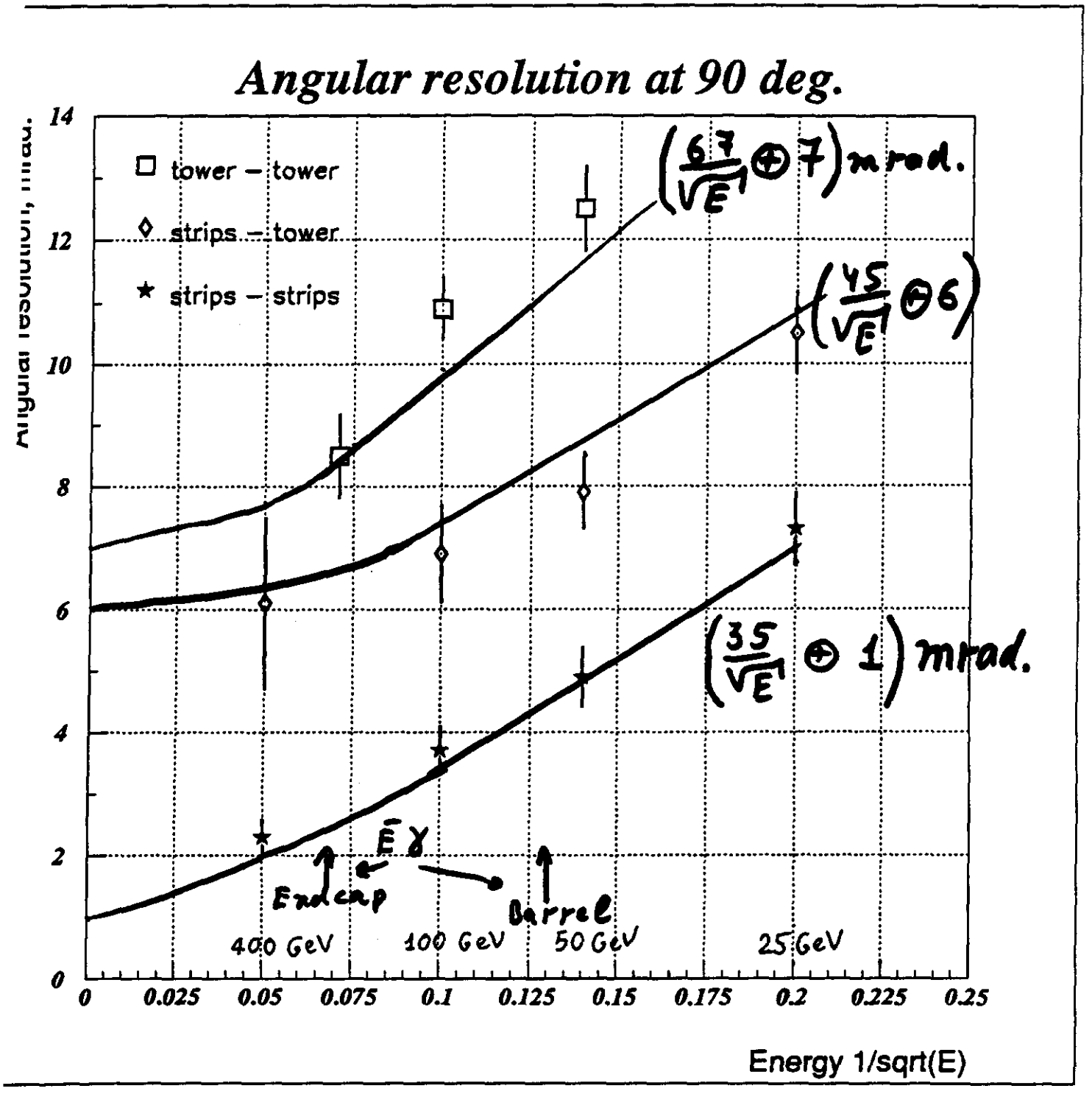
Angular resolution at 90 deg.
Angular resolution, mrad.
tower – tower
strips – tower
strips – strips
$\left(\frac{67}{\sqrt{E}} \oplus 7\right)$ mrad.
$\left(\frac{45}{\sqrt{E}} \oplus 6\right)$
$\left(\frac{35}{\sqrt{E}} \oplus 1\right)$ mrad.
$\bar{E}\gamma$
Endcap
Barrel
400 GeV
100 GeV
50 GeV
25 GeV
0
2
4
6
8
10
12
14
0
0.025
0.05
0.075
0.1
0.125
0.15
0.175
0.2
0.225
0.25
Energy 1/sqrt(E)

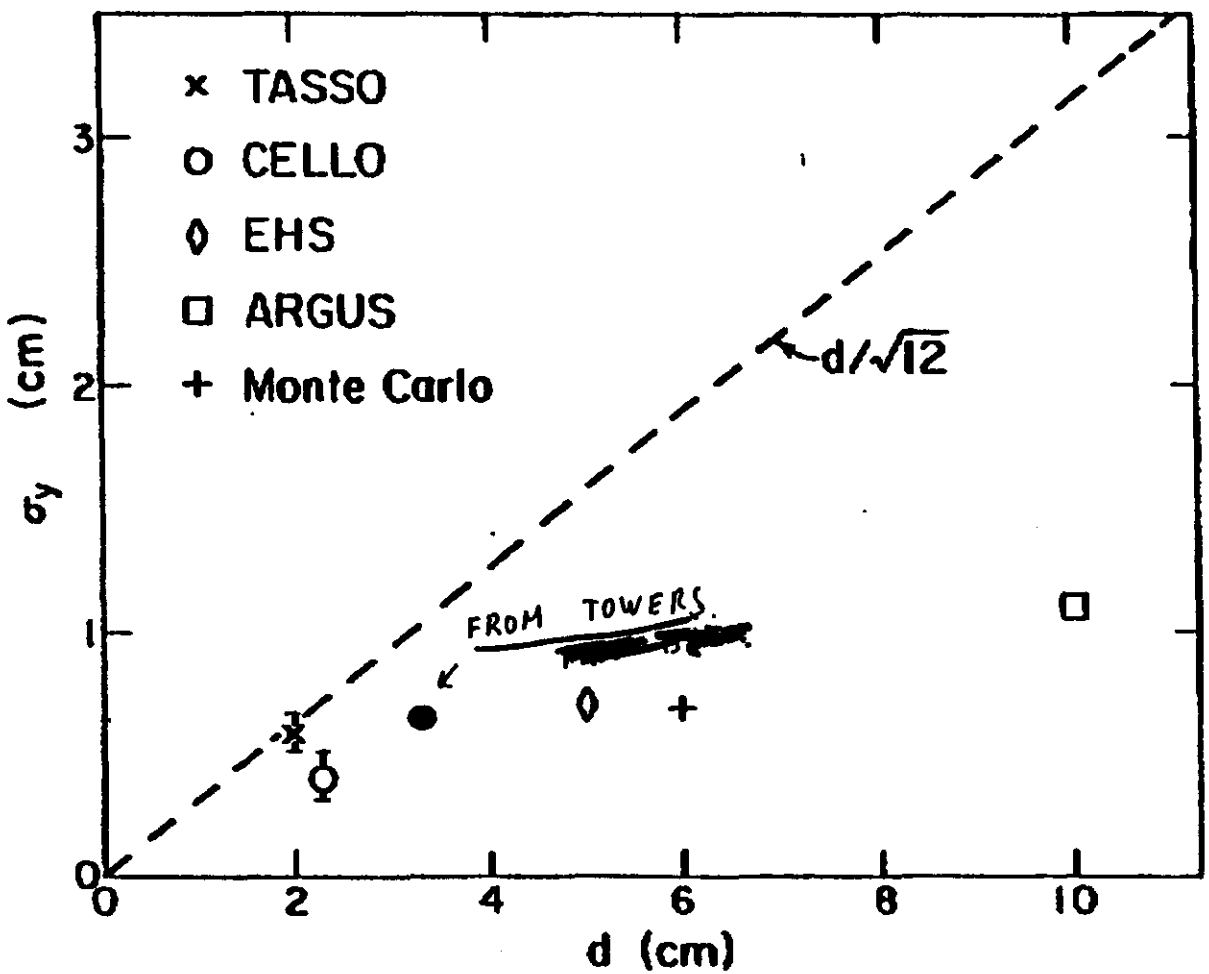

$$\sigma_y(E) = \frac{\sigma_y}{\sqrt{E}}$$

Fig. 29. Compilation of the position resolution for several segmentation values. Included (+) is the Monte Carlo result for 6 cm strips (both boundaries are used).

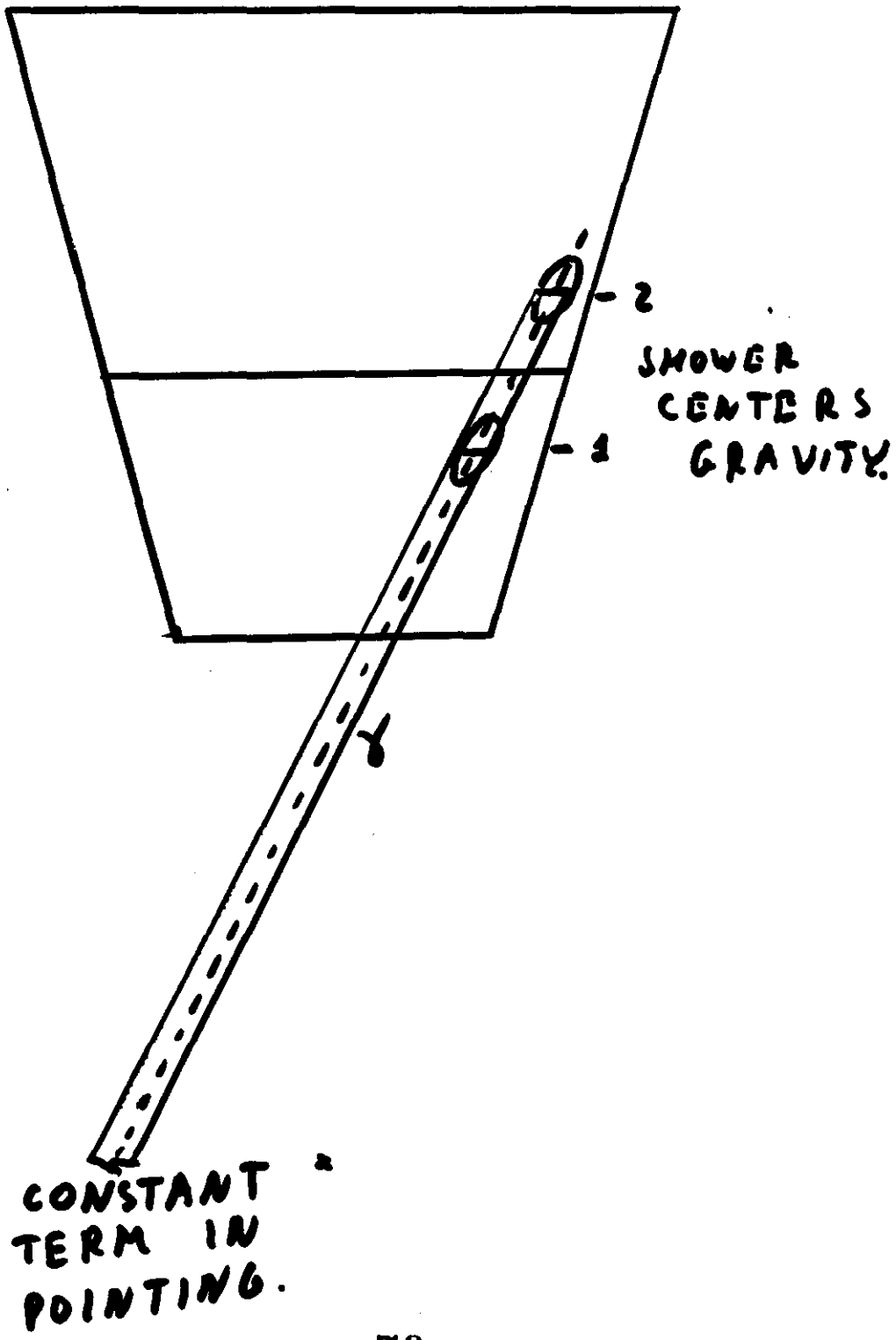
2
1
SHOWER
CENTERS
GRAVITY.
γ
CONSTANT
TERM IN
POINTING.

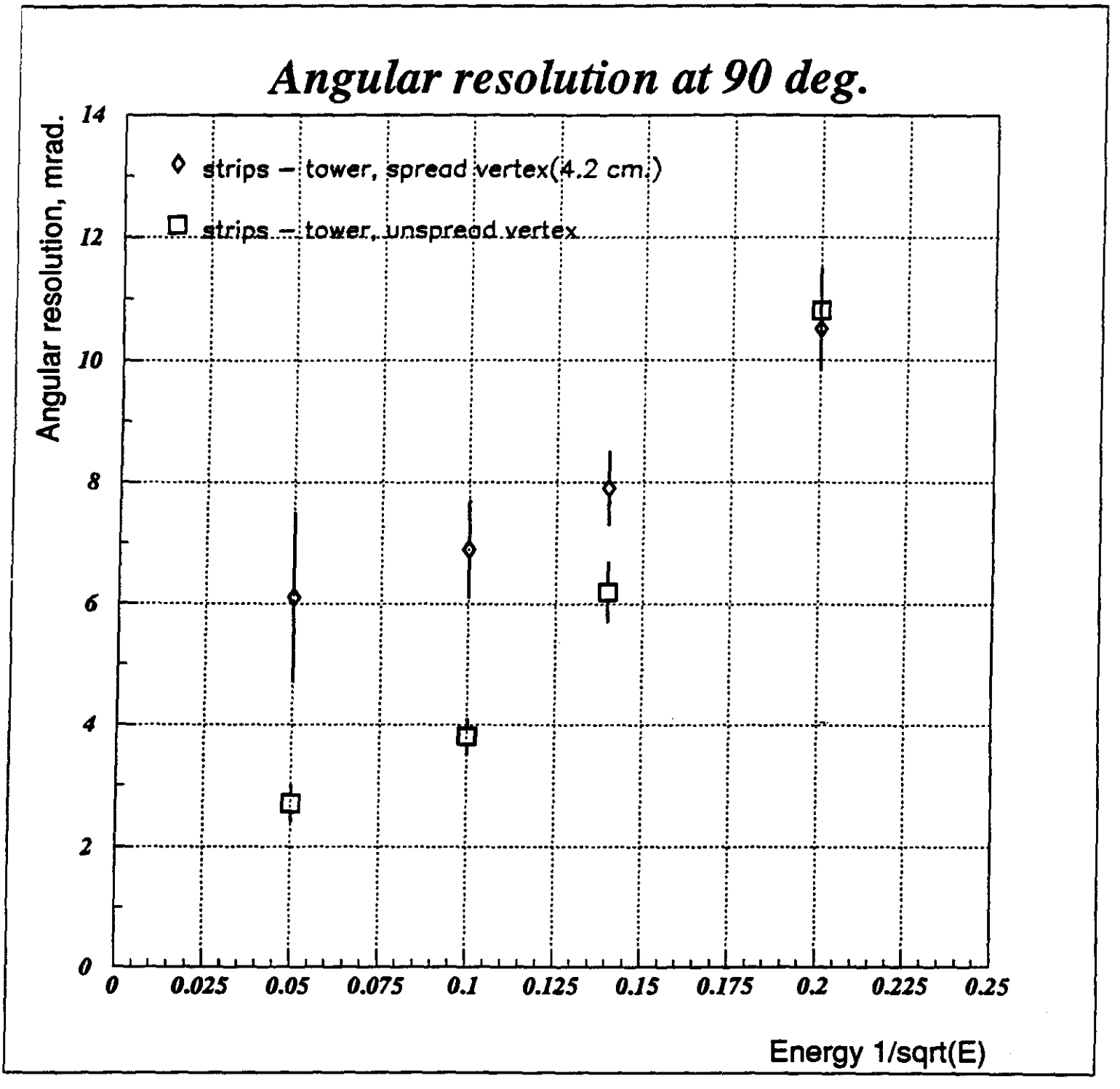
Angular resolution at 90 deg.
Angular resolution, mrad.
strips – tower, spread vertex(4.2 cm.)
strips – tower, unspread vertex
0
2
4
6
8
10
12
14
0
0.025
0.05
0.075
0.1
0.125
0.15
0.175
0.2
0.225
0.25
Energy 1/sqrt(E)

100 GEV, LKr Par Plate, 1mm strips, 0.029 towers

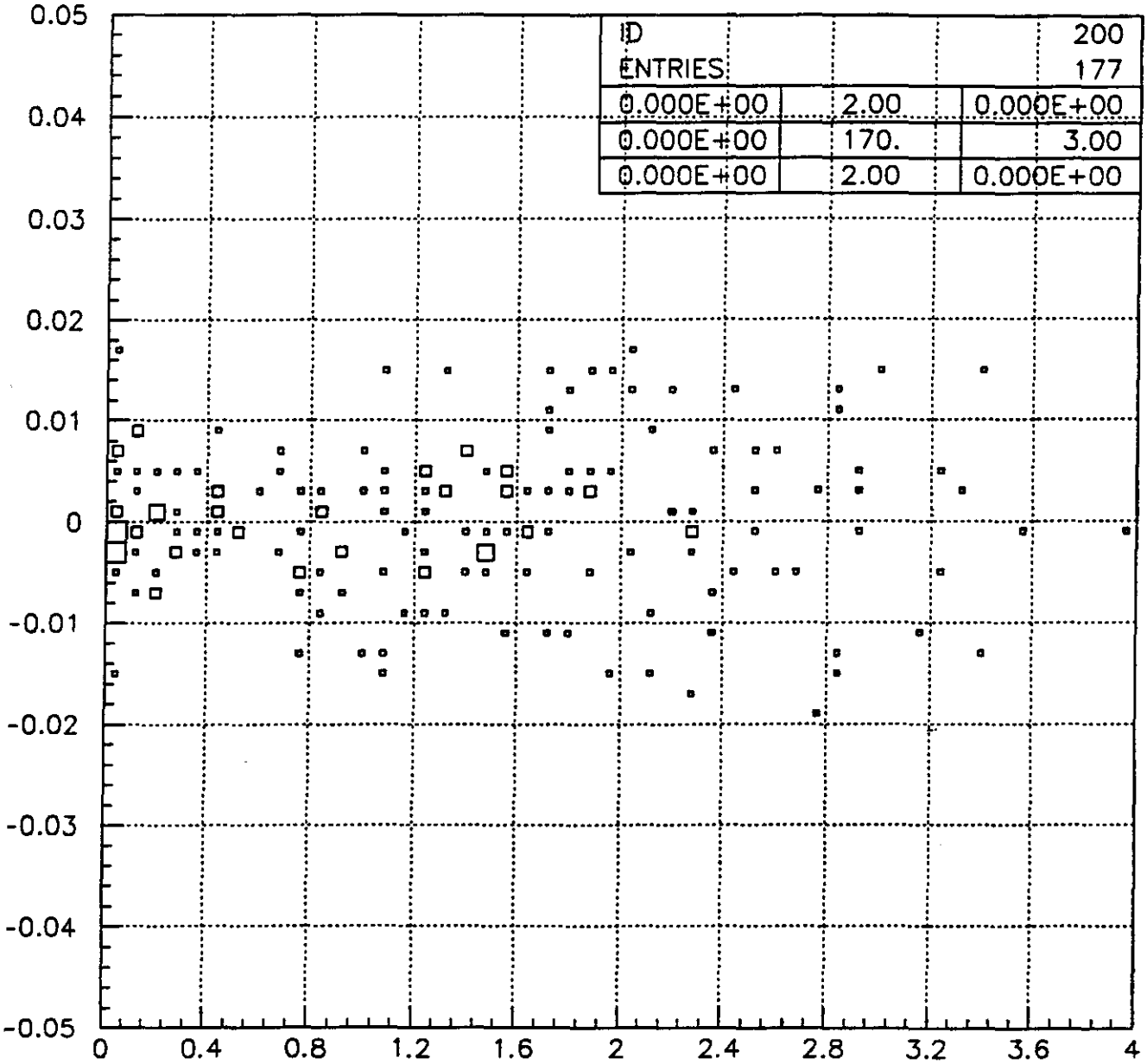

Energy in preradiator vs. pointing accuracy

STRIPS- STRIPS. $\delta_z = 4.2$ cm.

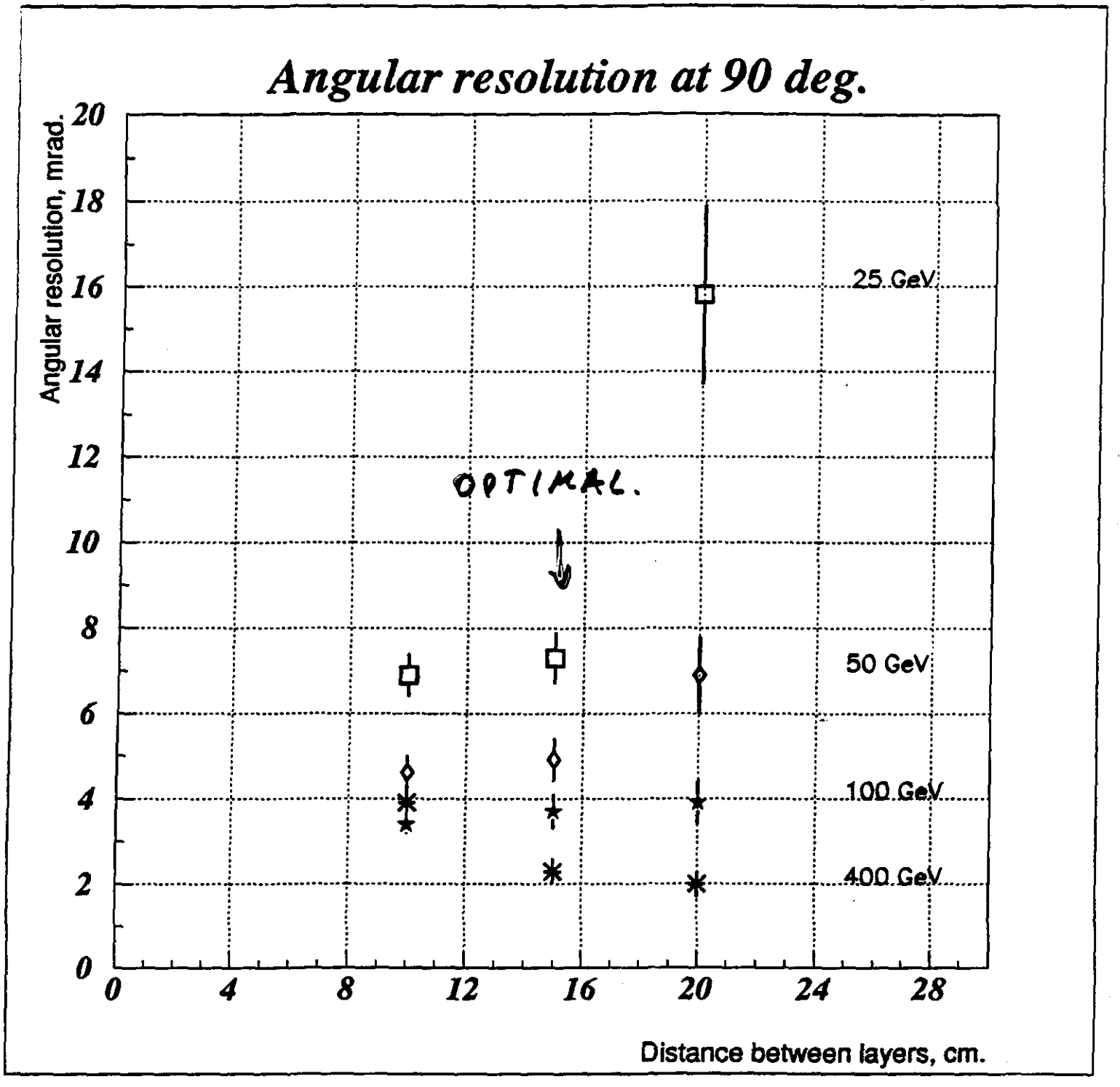

$\sigma_z = 4.2$ cm

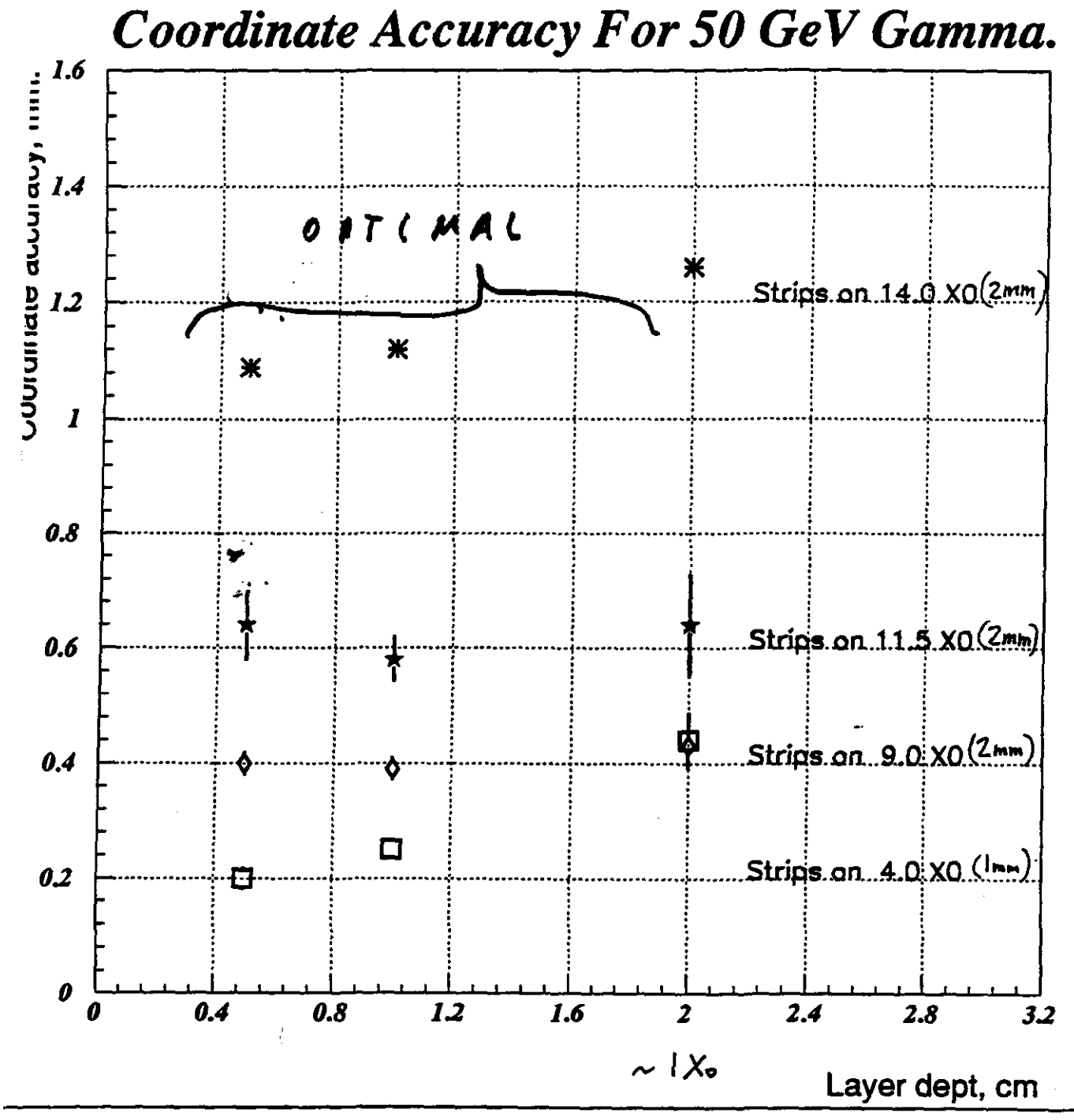
Coordinate Accuracy For 50 GeV Gamma.
Coordinate accuracy, mm.
1.6
1.4
1.2
1
0.8
0.6
0.4
0.2
0
0
0.4
0.8
1.2
1.6
2
2.4
2.8
3.2
OPTIMAL
Strips on 14.0 X0 (2mm)
Strips on 11.5 X0 (2mm)
Strips on 9.0 X0 (2mm)
Strips on 4.0 X0 (1mm)
~ 1 X₀
Layer dept, cm

$\sigma_z = 4.2$ cm

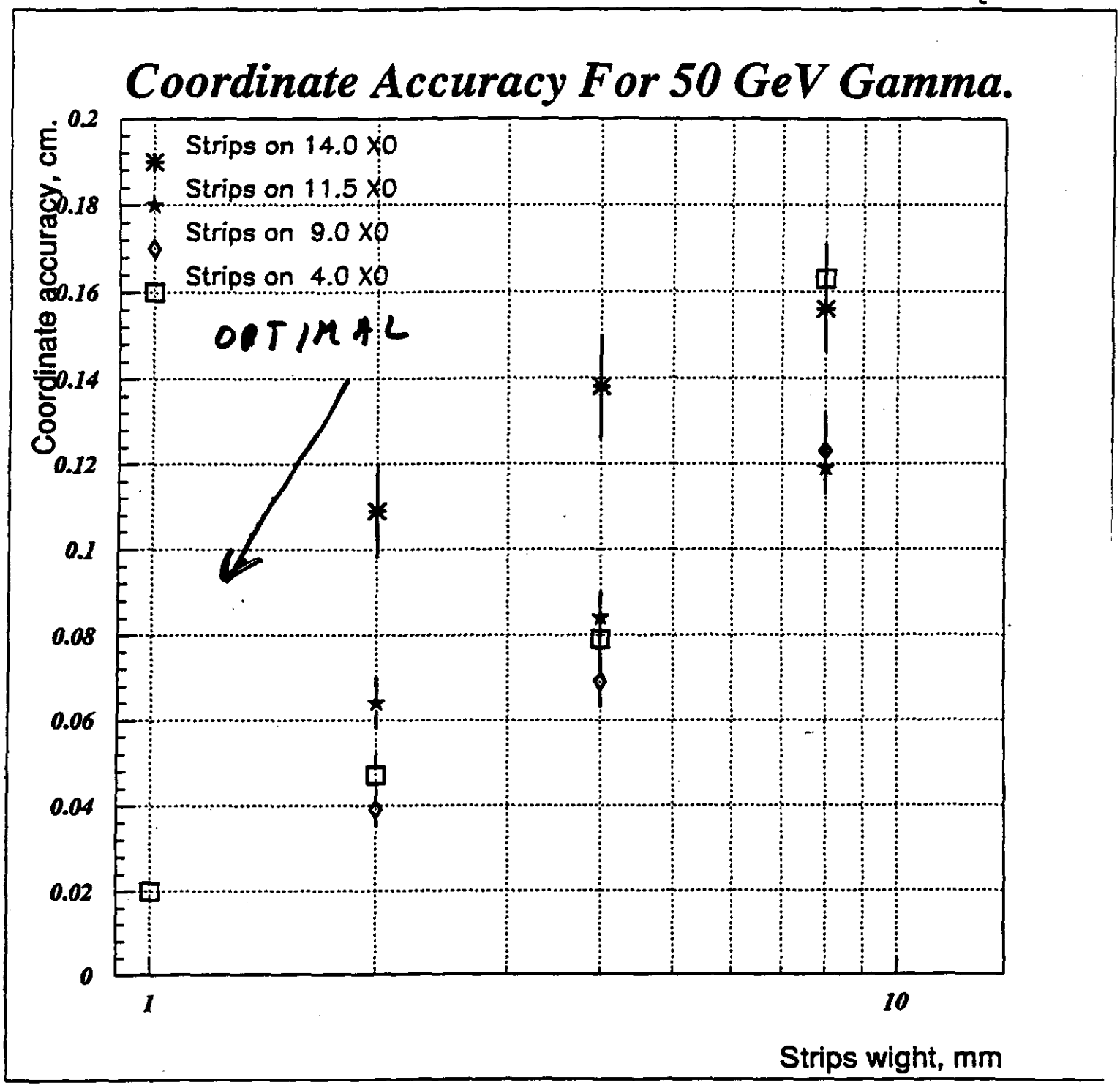
Coordinate Accuracy For 50 GeV Gamma.
Strips on 14.0 X0
Strips on 11.5 X0
Strips on 9.0 X0
Strips on 4.0 X0
OPTIMAL
Coordinate accuracy, cm.
0.2
0.18
0.16
0.14
0.12
0.1
0.08
0.06
0.04
0.02
0
1
10
Strips wight, mm

CONCLUSION

* WE MUST IMPROVE POINTING
* WE KNOW HOW TO DO IT
* THE MOST PROMISING WAY IS NARROW STRIPS
* POINTING IS MOST IMPORTANT IN ENDCAP

Yu.Efremenko

Presentation by:

R. McNeil

Muon Considerations

MUON ISSUES

Besides measuring the Jet Energy and determining $\not{E}_T$, The Calorimeter serves to

- Suppress hadron punchthrough
  - # λ
  - Compactness $\Rightarrow$ Level arm for muon system

- Measure Muon Energy loss
  - Materials $\Rightarrow$ $\langle E_{LOSS} \rangle$, σ_{ELOSS}, # Catastrophic E_{LOS}
  - σ_E/E for muon E_{LOSS} measurement
    noise terms (neutrons)
  - isolation cuts (segmentation)
  - Passive vs Active Calorimetry
  - Tagging Catastrophic Energy loss

- Induce the Muon to shower and exit with numerous γ, e^+e^- which obscure the muon in the muon system.
  - final layers of the calorimeter (mat'ls, dens.)
  - Space between calorimeter and muon system

- Neutron shield
  - final layers
  - Space for poly

Comparison GEANT vs Data ZEUS BCAL HAC Section

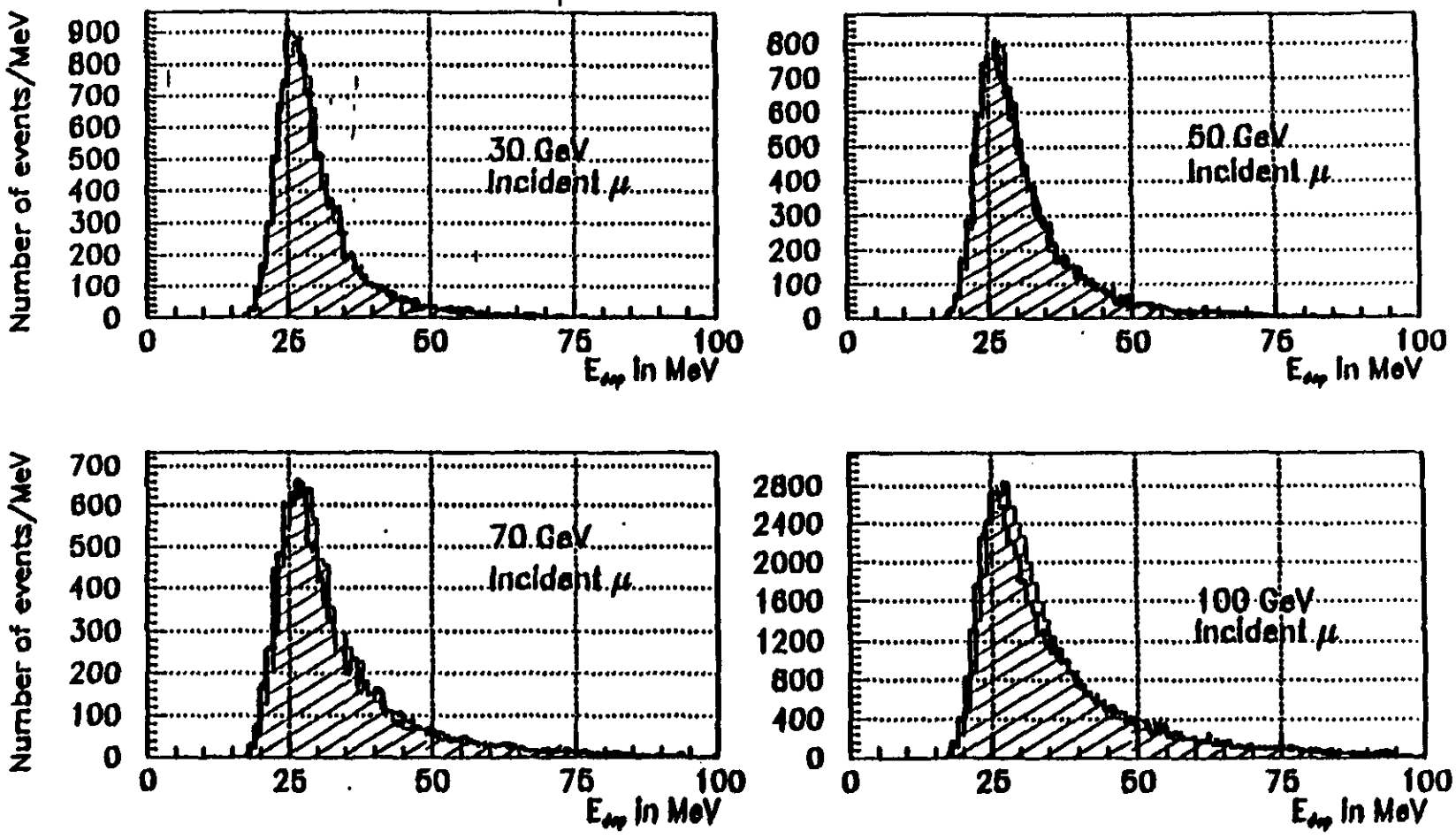

13cm of Scintillator in 50 layers 2λ absorbe

Figure 1 GEANT Simulation of Energy Deposited in scintillator of hadronic section #1 (HAC 1) of ZEUS Barrel Calorimeter compared with experimental data from 1991 FNAL test beam run. Solid histogram is data, dashed histogram is GEANT Simulation.

GEANT Simulation of 100 GeV ν
through 12λ of Cu/scint Calorimeter

Reconstruct E_ν assuming perfect measurement of E_ν^{OUT}

Active Calorimeter resolution: $\frac{\sigma_E}{E} = \frac{35\%}{\sqrt{E}}$

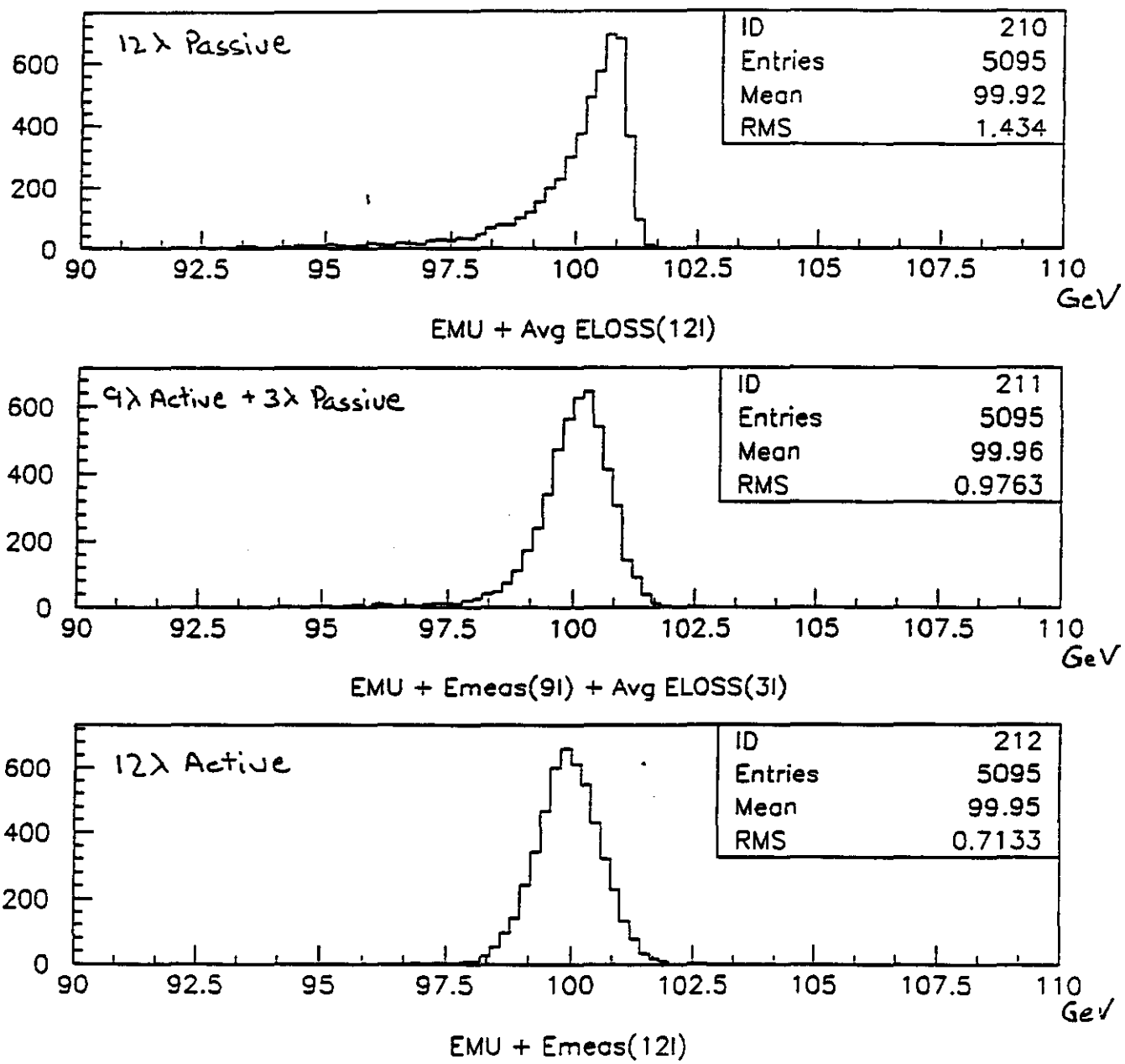

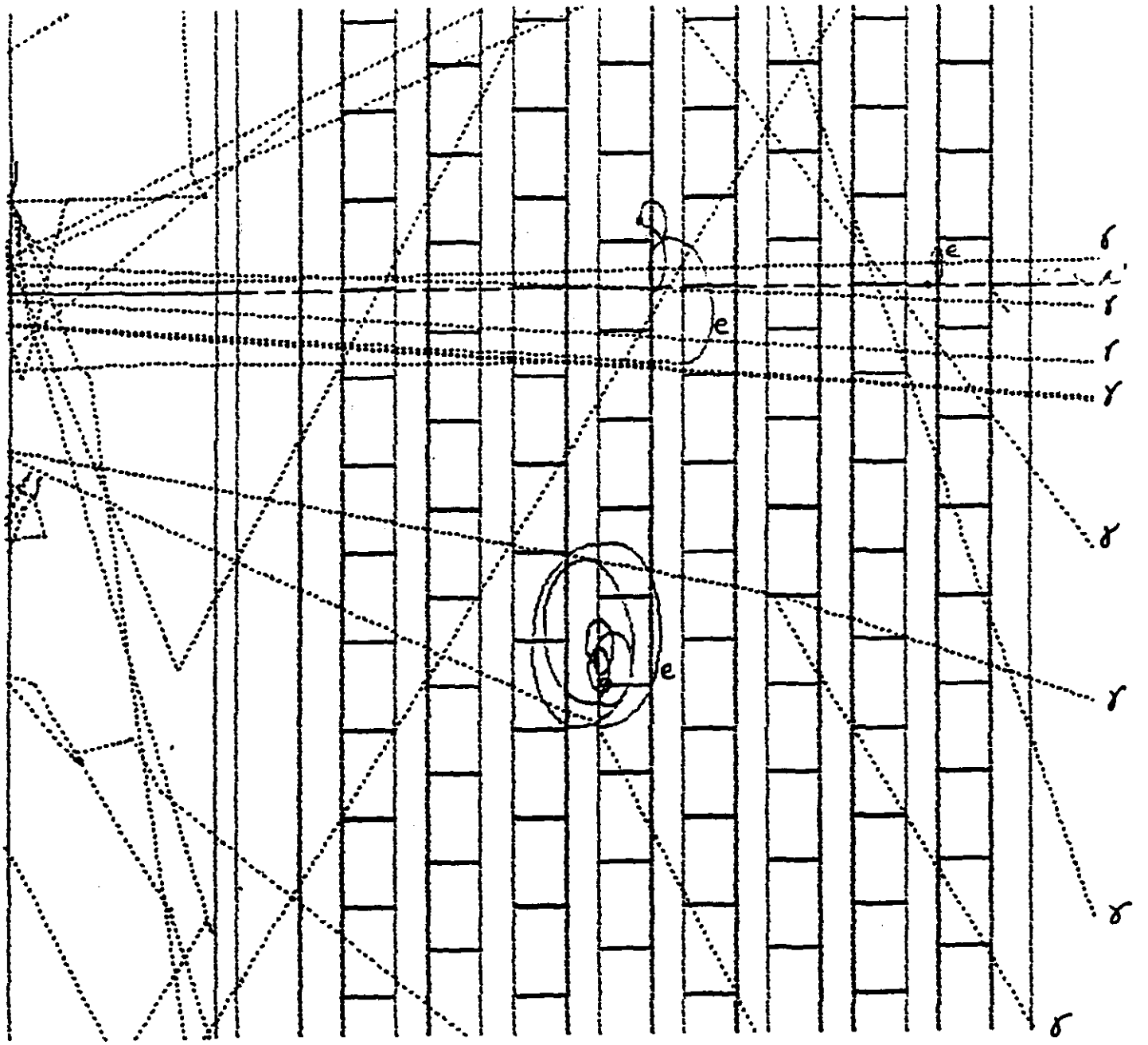
e
e
e
e
γ
γ
γ
γ
γ
γ
γ

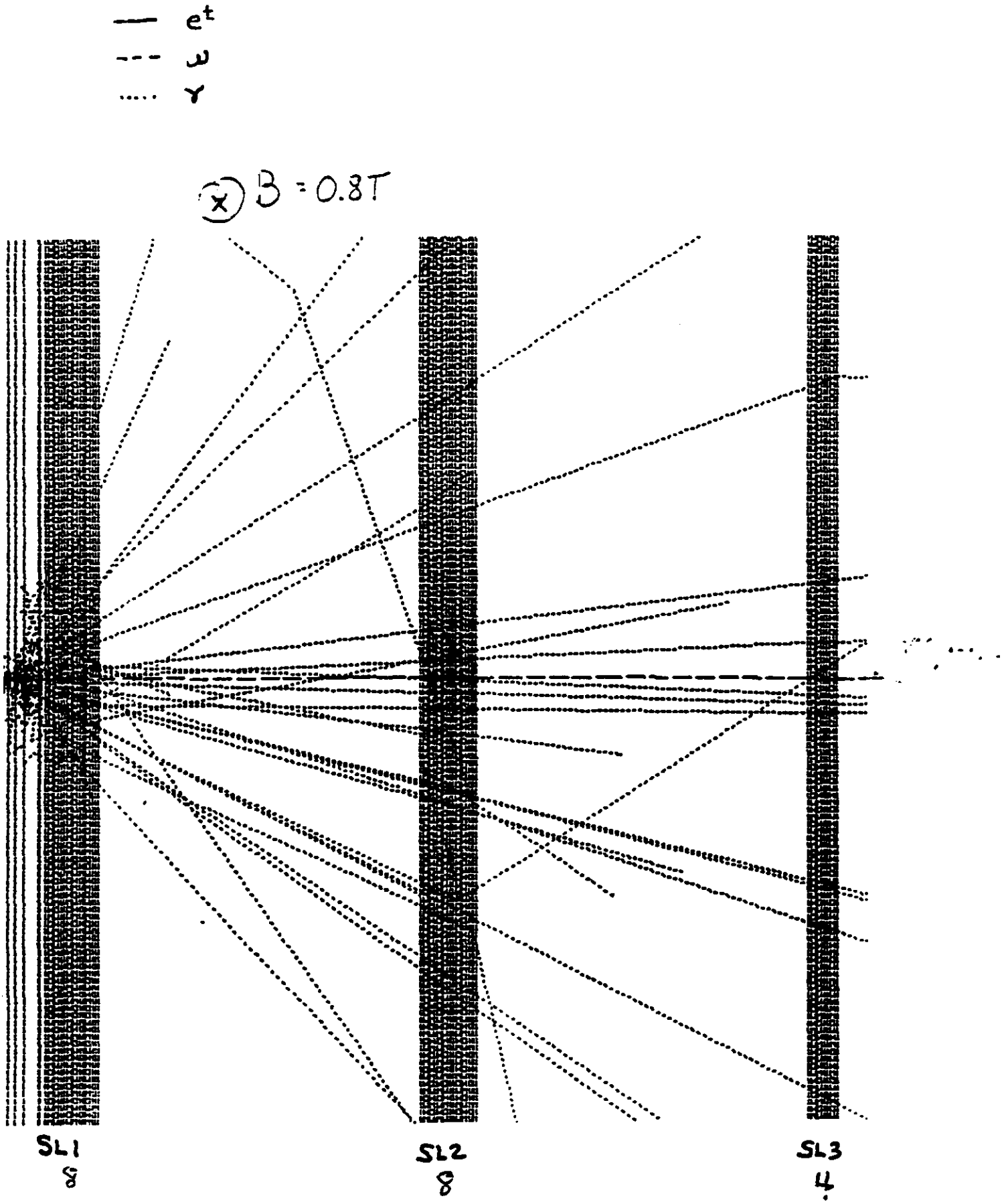
e+
ω
γ
B = 0.8T
SL1
8
SL2
8
SL3
4

GEANT Simulation of 10GeV ν
through 12λ of Cu/Scint Calorimeter

Reconstruct E_ν assuming perfect measurement of E_ν^{OUT}

Active Calorimeter resolution: $\frac{\sigma_E}{E} = \frac{35\%}{\sqrt{E}}$

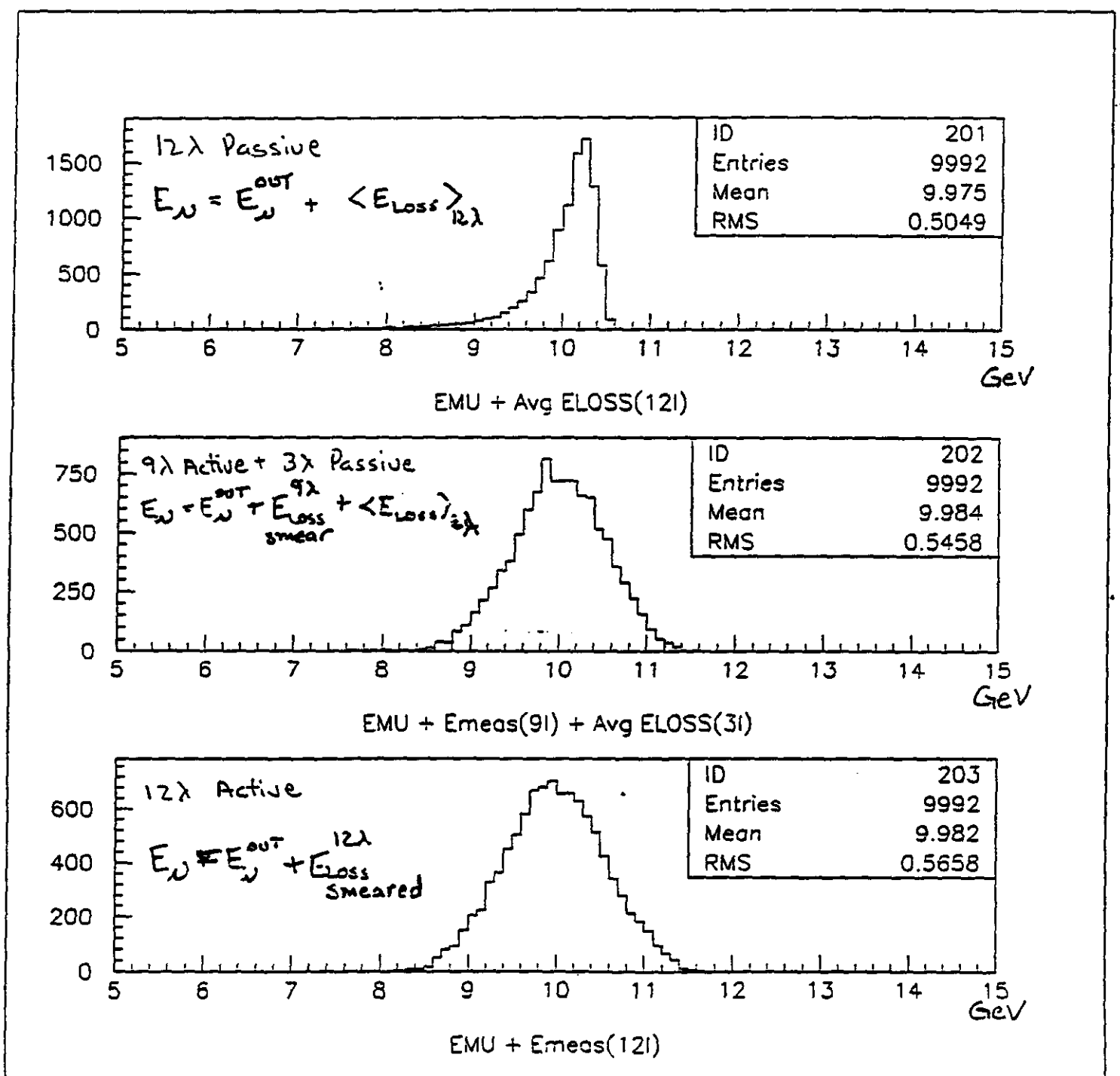

How Close can 1ST μ Layer be to Calorimeter?

$$R = \frac{P_T}{0.3\,9\,B}$$

Put air gap to curl up low momentum particles

Low momentum particles exiting with muon
Avg 2-3 electrons per 1TeV/c μ

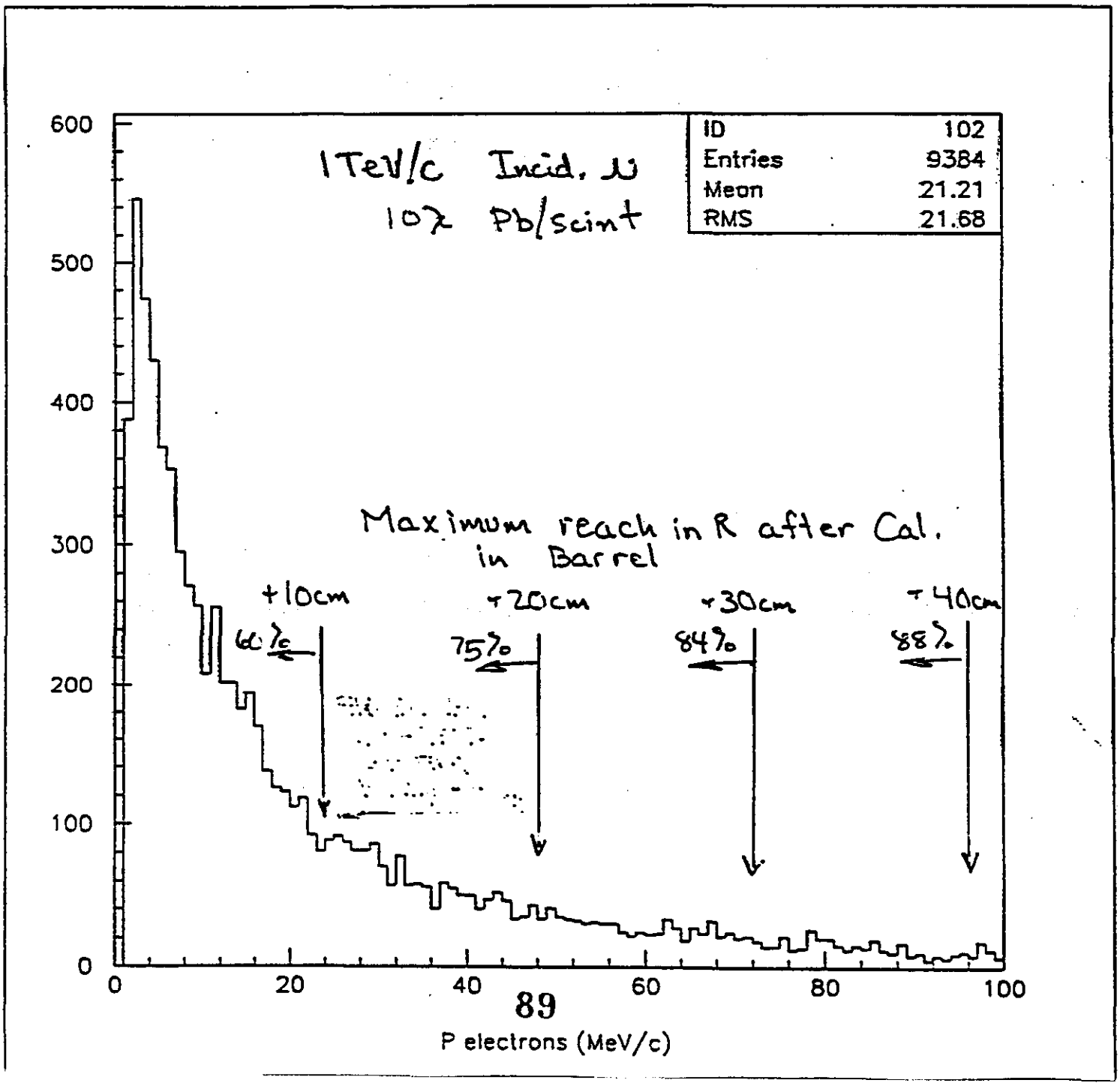

gem

γeμ

Presentation by:

R. Wigmans

e / h

LONGITUDINAL LEAKAGE AS FUNCTION OF CALORIMETER DEPTH

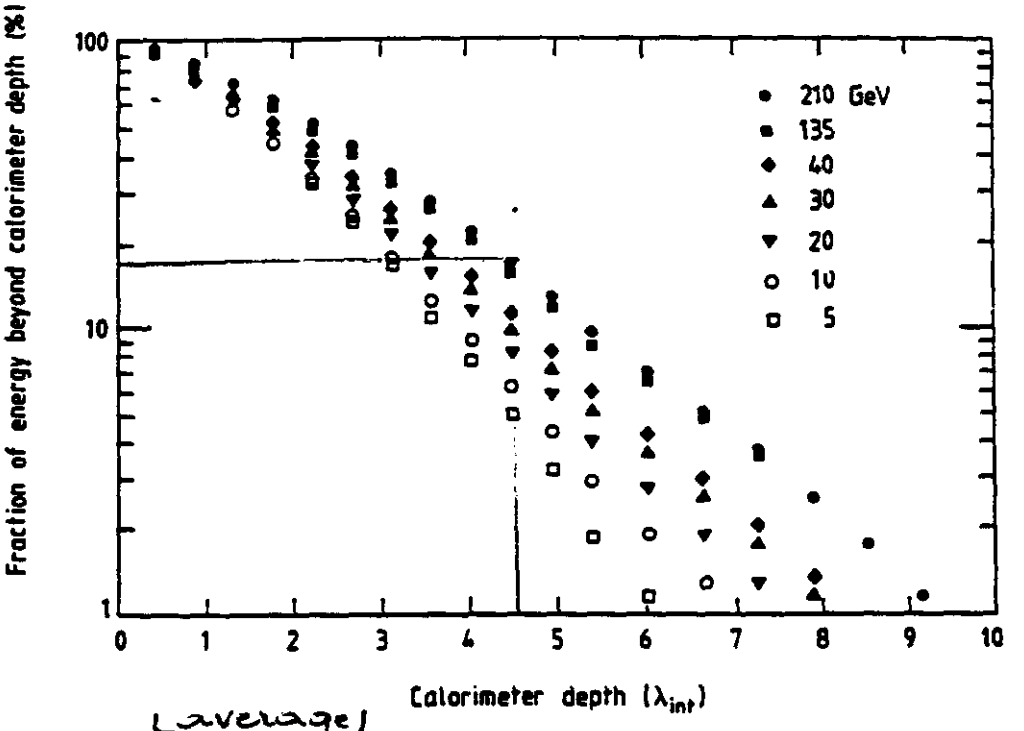

(average)

Figure 7. The leakage as a function of the detector depth, for pions of 5–210 GeV, measured in a uranium/plastic-scintillator calorimeter. Data from Catanesi *et al* (1987).

What is e/h?

e/h is the ratio of the calorimeter responses to the e.m. and non-e.m. components of hadron showers.

e/h is - independent of energy (f_{π^0} E-depende

- figure of merit for a particular combination of active + passive material

e/h cannot be measured directly
can be derived from $e/\pi\,(E)$

$$e/\pi\,(E) = \frac{e/h}{1 - (1 - e/h)\, f_{\pi^0}(E)}$$

Only if $e/h \equiv 1 \longrightarrow$ linearity

RELATION e/h vs e/π

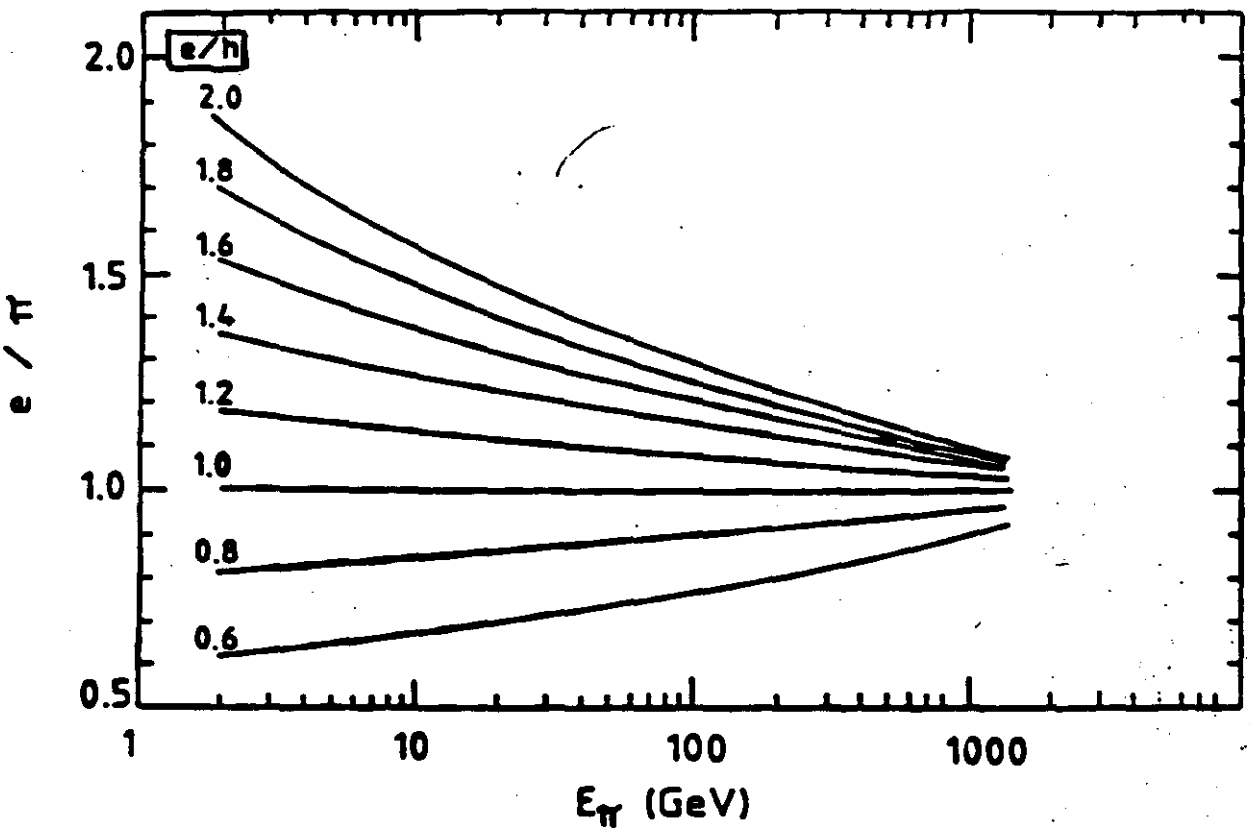

Measurement e.m. component of hadronic showers

(NIM A 316 [1992] 184)

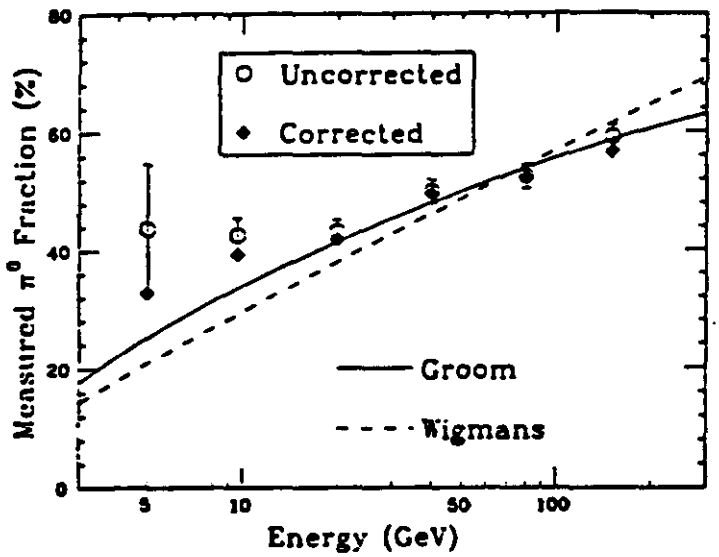

Fig. 20. The estimated π^0 fraction of hadronic showers in the SPACAL calorimeter as a function of the pion energy, as determined by the method described in the text. The two curves are calculations taking into account the noncompensation of the detector (see text).

LATERAL PROFILE HADRONIC SHOWERS

From NIM A 316 (1992) 184 (SPACAL)

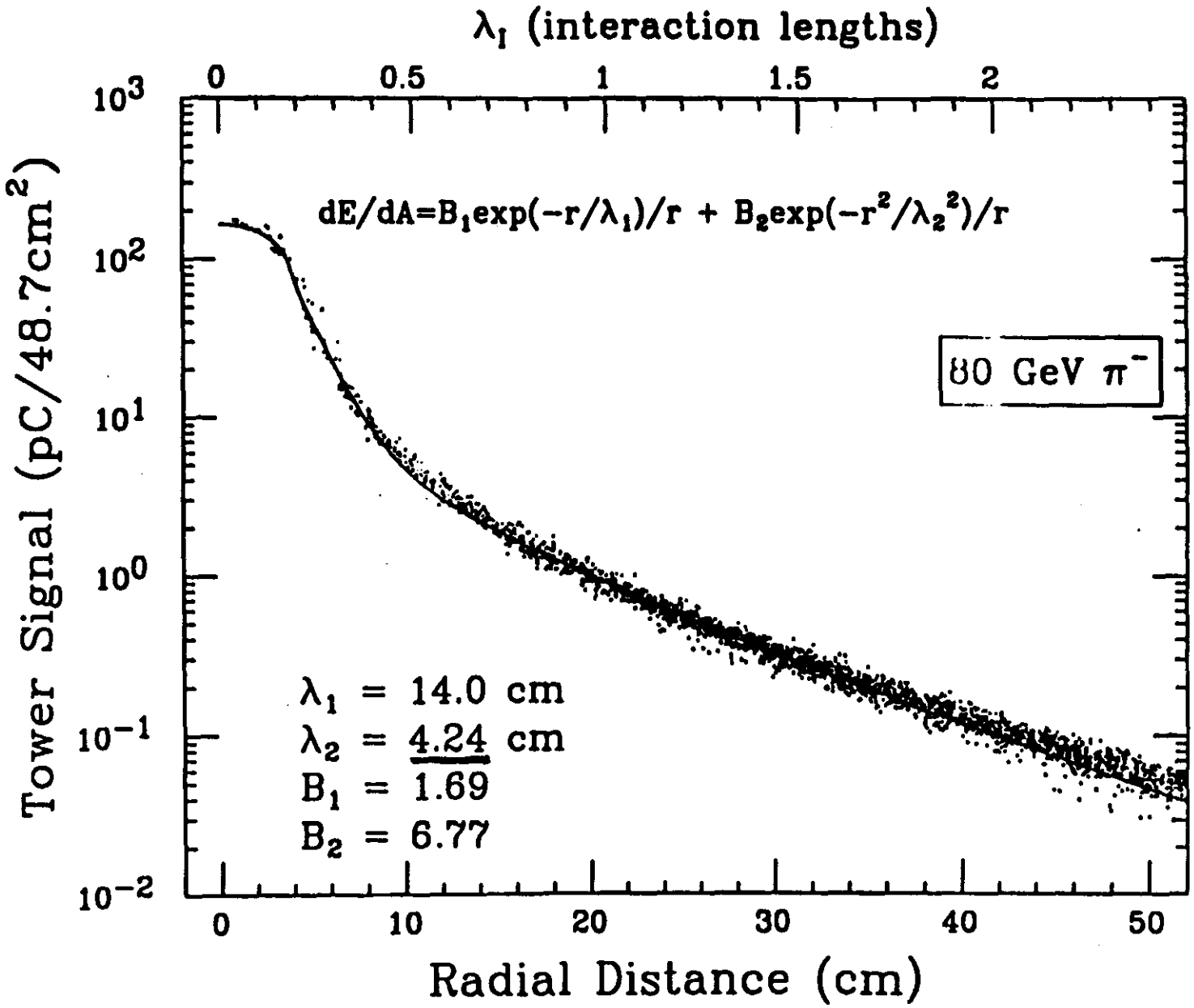

Where does the non-e.m. energy go?
(simplified)

	Pb calorimeters	Fe (Cu calorimeters
Ionizing particles	41%	51%
Neutrons	12%	8%
Binding energy losses		

Pb calo

$$e/h = \frac{e/mip}{0.41 + 0.12\ n/mip}$$

Cu (Fe) calo

$$e/h = \frac{e/mip}{0.51 + 0.08\ n/mip}$$

→ Compensation depends on the response to e.m. showers and response to neutrons

NUCLEAR INTERACTION INDUCED BY 3.8 GeV π

Early example of the nuclear interaction of a π-meson of energy 3·8 BeV

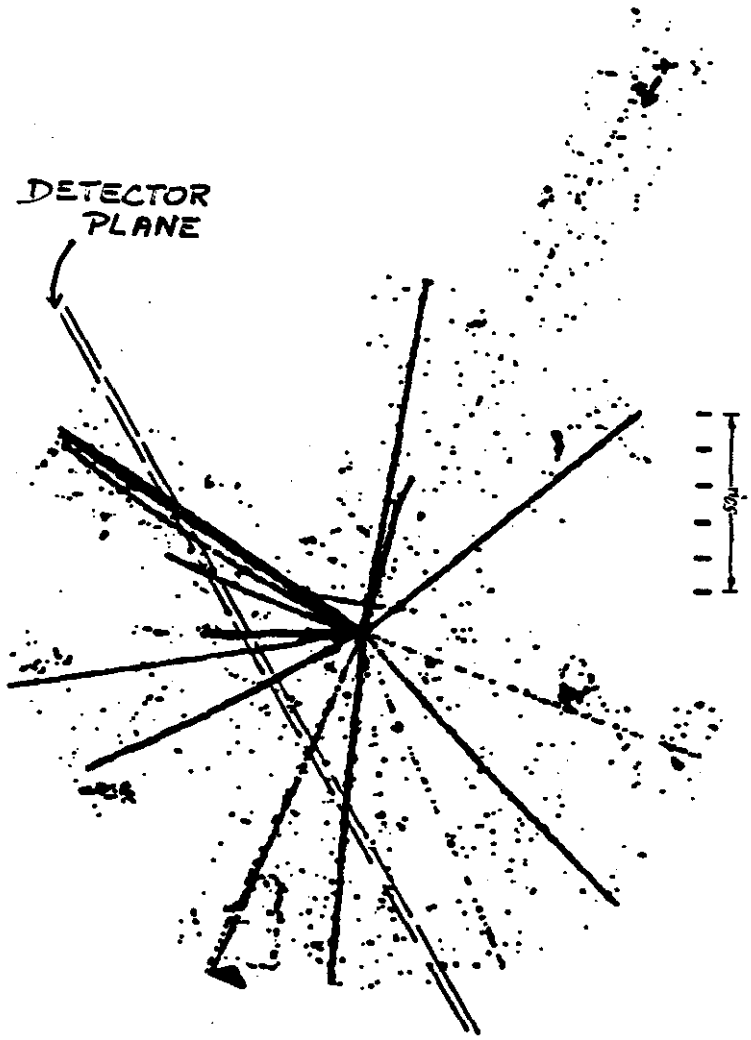

PLATE 11—9

Dford G5 emulsion. Lock and Yekutieli (1952), unpublished.

A π-meson of energy 3·8 BeV, emitted from a disintegration of type 7 – 10 μ, produces a secondary disintegration of type 18 – 1 π. It is probable, but not established, that several of the lightly ionising secondary particles are π-mesons.

Figure 30

What is e/mip ?

e/mip = sampling fraction e.m. showers relative to sampling fraction min. ion. partic

mip → given by PDG and calo composition

e → EGS 4

→ e/mip precisely and reliably calculable

e/mip is difficult to determine <u>experimentally</u>, since mip's do not exist (use μ response at different energies – NIM A 320 [1992] 128)

30 - 40% of e.m. signal comes from electrons <u>below 1 MeV</u> (photoelectrons)

e/mip depends on :
- $Z_{passive}$
- Z_{active}
- thickness absorber layers

ENERGY DEPOSIT IN 10 GeV e^- SHOWER (EGS 4)

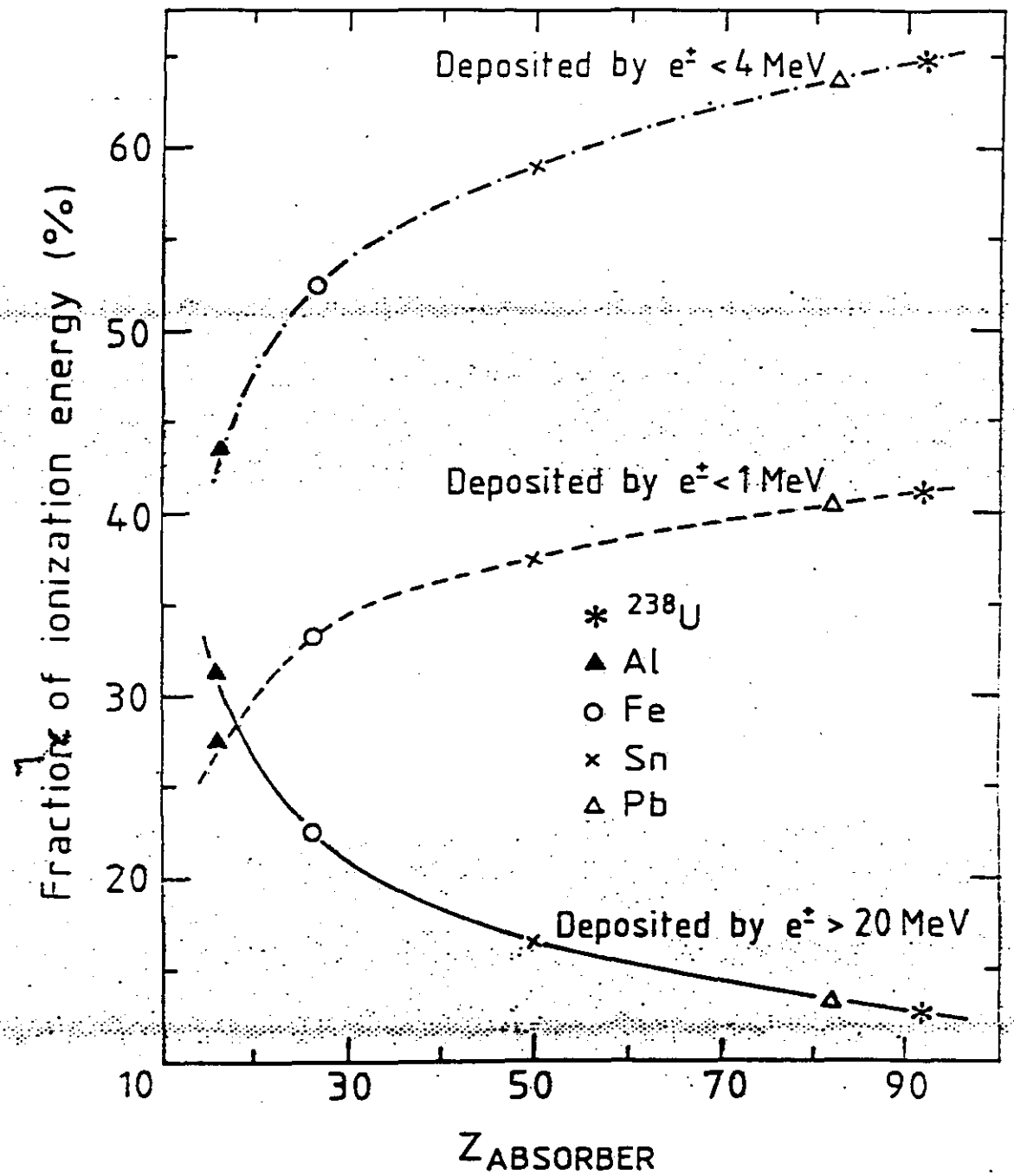

Figure 13

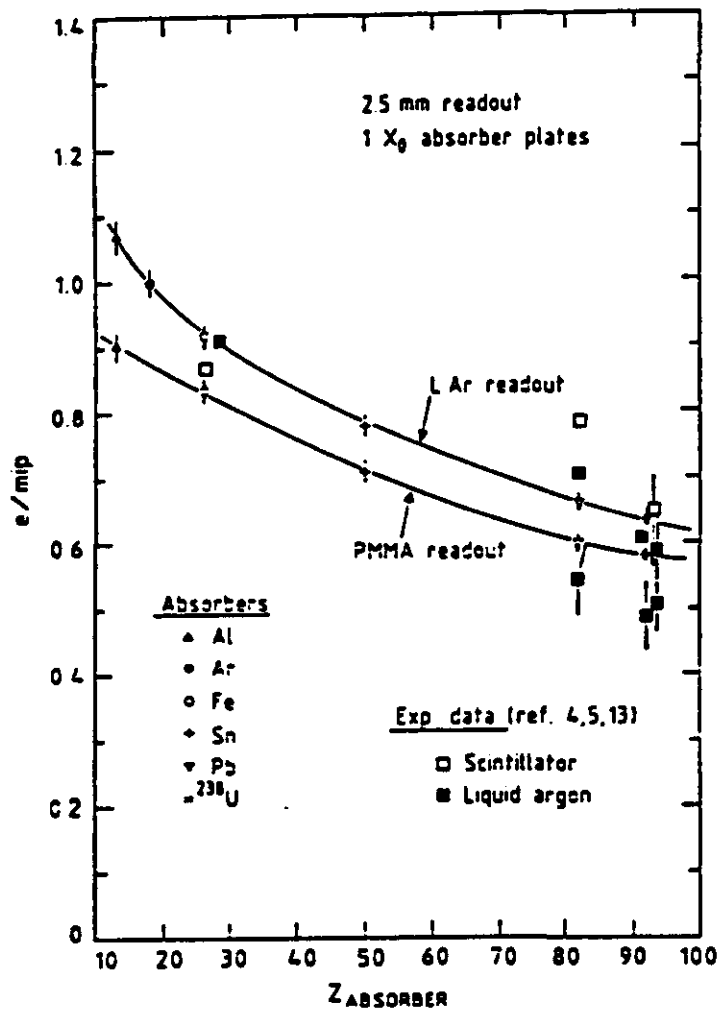

Fig. 5. The $e/$mip signal ratio for sampling calorimeters as a function of the Z-value of the absorber, for 2.5 mm liquid-argon and plastic scintillator readout. The absorber layers are $1X_0$ thick. Results from EGS4 Monte Carlo simulations

COMPENSATION

SUPPRESSION OF e.m. RESPONSE (π^0 COMPONENT)

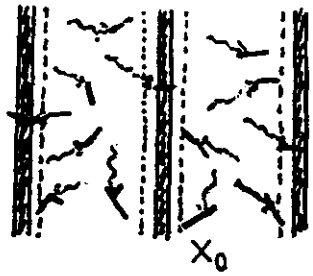

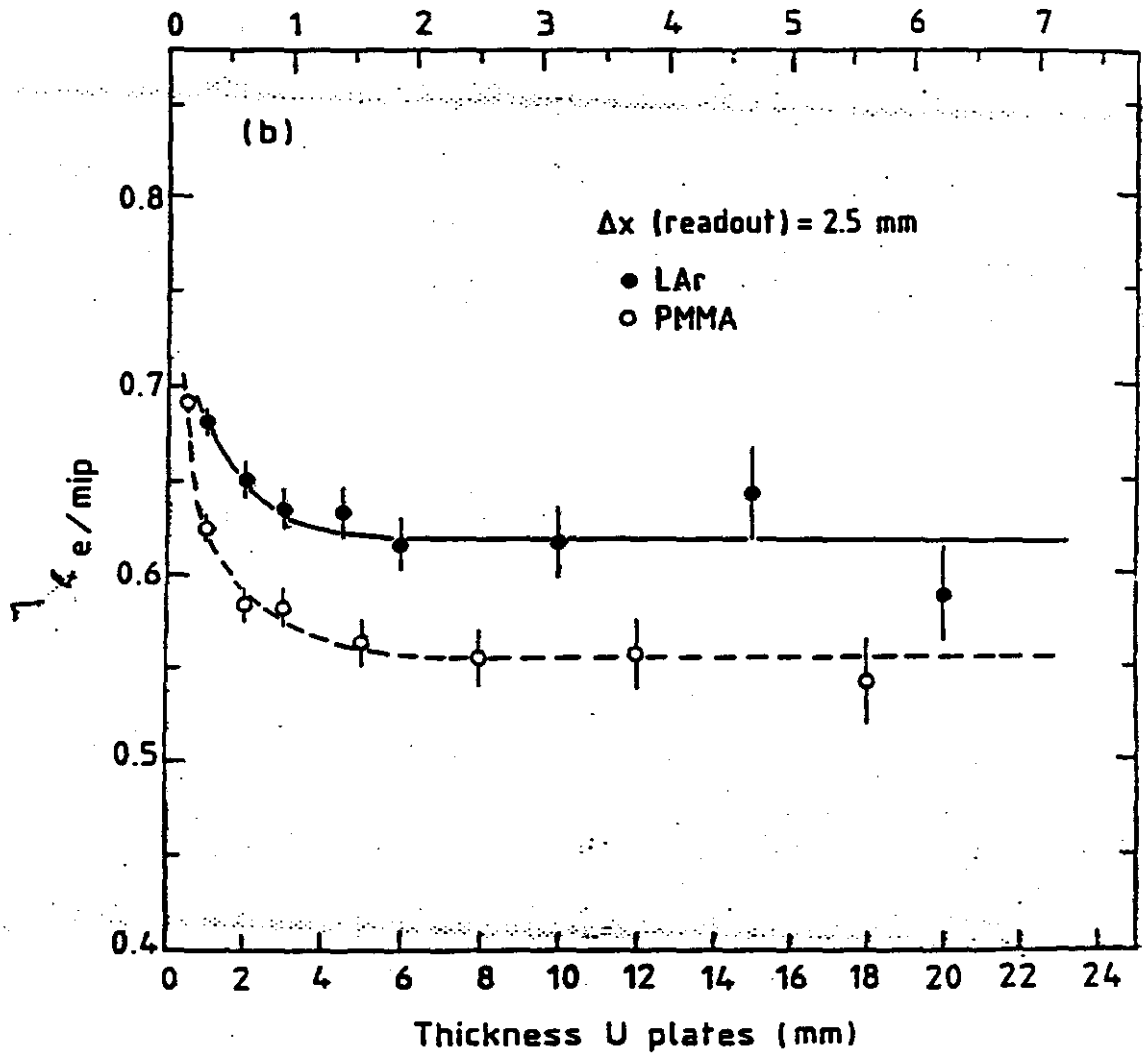

e/mip SPACAL = 0.71 (measured)

e/mip ACCORDION = 0.78 (EGS/GEANT)

(1 mm Pb → 0.36)

e/h and e/mip values for several Pb calorimeters

Table 1 The calculated values of the e/h value, using the formula from eq. (2), and the e/mip (EGS4) and n/mip[14] values for some calorimeters considered for future experiments. Where possible, the results of experimental measurements are given as well.

Table 1 The (expected) e/h value of some calorimeters						
Configuration	Reference	$(e/mip)_{calc}$	$(e/mip)_{meas}$	$(n/mip)_{calc}$	$(e/h)_{calc}$	$(e/h)_{meas}$
Pb/scint. tiles 10/2.5 mm	ZEUS[14]	0.62	0.63 ± 0.05	1.7	1.01	1.05 ± 0.04
Pb/scint. fibers 4/1 mm	SPACAL[6]	0.69	0.71 ± 0.05 *)	1.7	1.12	1.15 ± 0.02
2 mm Pb/Lar 20 ns	RD3[16]	0.78	-	< 0.5	> 1.6	-
1 mm Pb/LAr 20 ns	GEM[16]	0.86	-	< 0.5	> 1.8	-
3+12 mm Pb/LAr 2 μs	SLD[17]	0.69	-	0.7	1.40	1.37 ± 0.12 **)
BaF_2 crystals	GEM[16]	1.0	-	< 0.5	> 2.1	-

*) Preliminary result, Published 0.72 ± 0.03 (NIM A320 [1992] 128)
**) Based on a measurement of $e/\pi = 1.24 \pm 0.10$ at 11 GeV, using eqs. (1)

$$e/h = \frac{e/mip}{0.41 + 0.12\, n/mip}$$

n/mip

Neutrons are predominantly from nuclear evaporation $\langle E_n \rangle \sim 2\text{-}3$ MeV

They mainly lose energy through
- inelastic scattering $(n,n'\gamma)$
- elastic scattering (n,n')
- nuclear capture (n,γ)

	$(n,n'\gamma)$	(n,n')	(n,γ)
me scale	10 ns	10 ns	1 μs
action of E^n_{kin} deposited	~ 50%	~ 50%	up to 300%
ontribution to calo signal	all calo's	only if H_2	all calo's

→ n/mip ≤ 0.5 in LAr/LKr with short gate

n/mip $\sim 0.7\text{-}0.8$ in LAr/LKr with long gate

n/mip tuneable in calorimeter with hydrogenous readout.

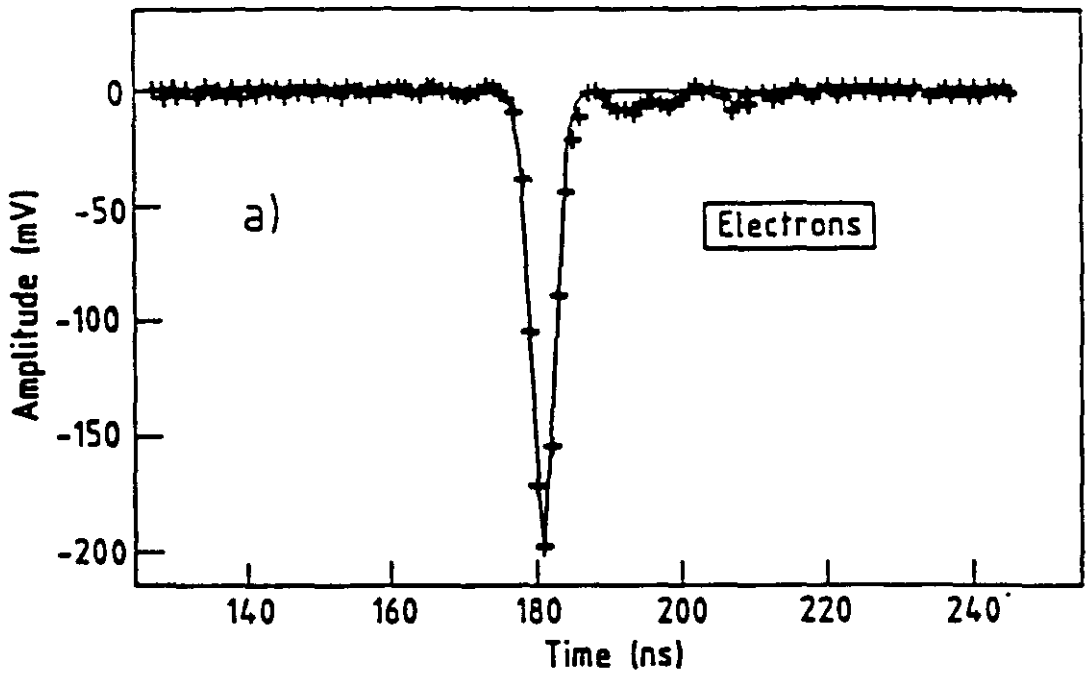
a)
Electrons
Amplitude (mV)
0
-50
-100
-150
-200
140
160
180
200
220
240
Time (ns)

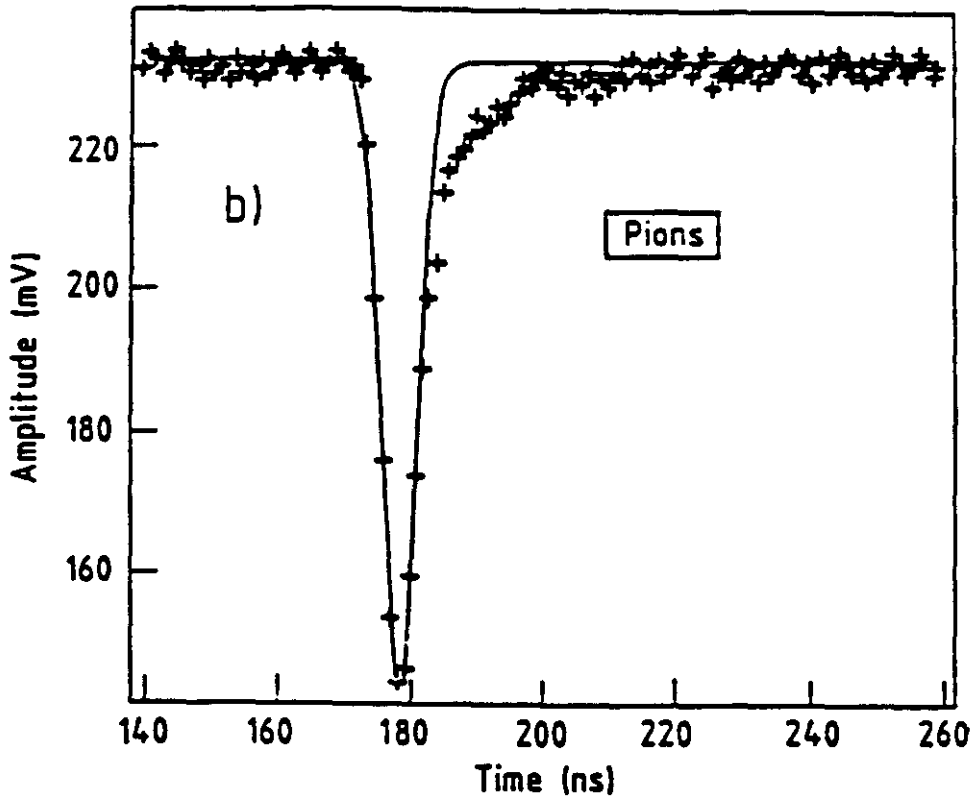
b)
Pions
Amplitude (mV)
220
200
180
160
140
160
180
200
220
240
260
Time (ns)

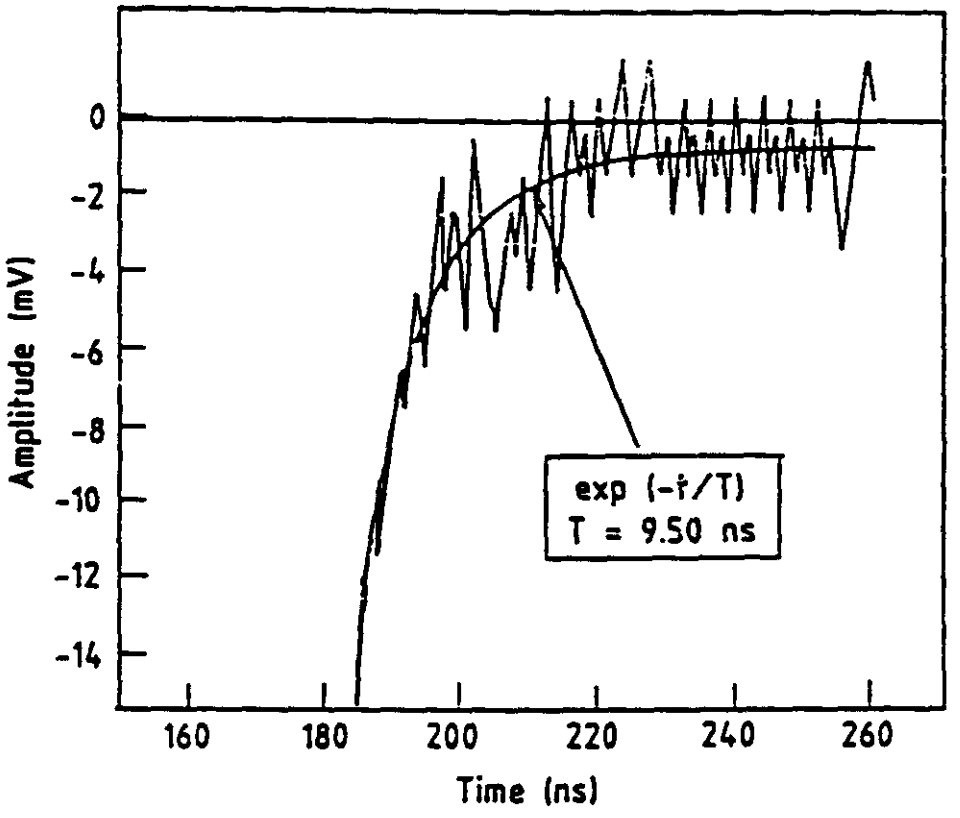
0
-2
-4
-6
-8
-10
-12
-14
Amplitude (mV)
160
180
200
220
240
260
Time (ns)
exp (-t/T)
T = 9.50 ns

RELATIVE CONTRIBUTION
neutrons TO CAL. SIGNAL

e/h SIGNAL
RATIO

^{238}U : ~ 60 n/GeV

ΔB_n ~ 5 MeV

→ from (n,γ) :
300 MeV/GeV

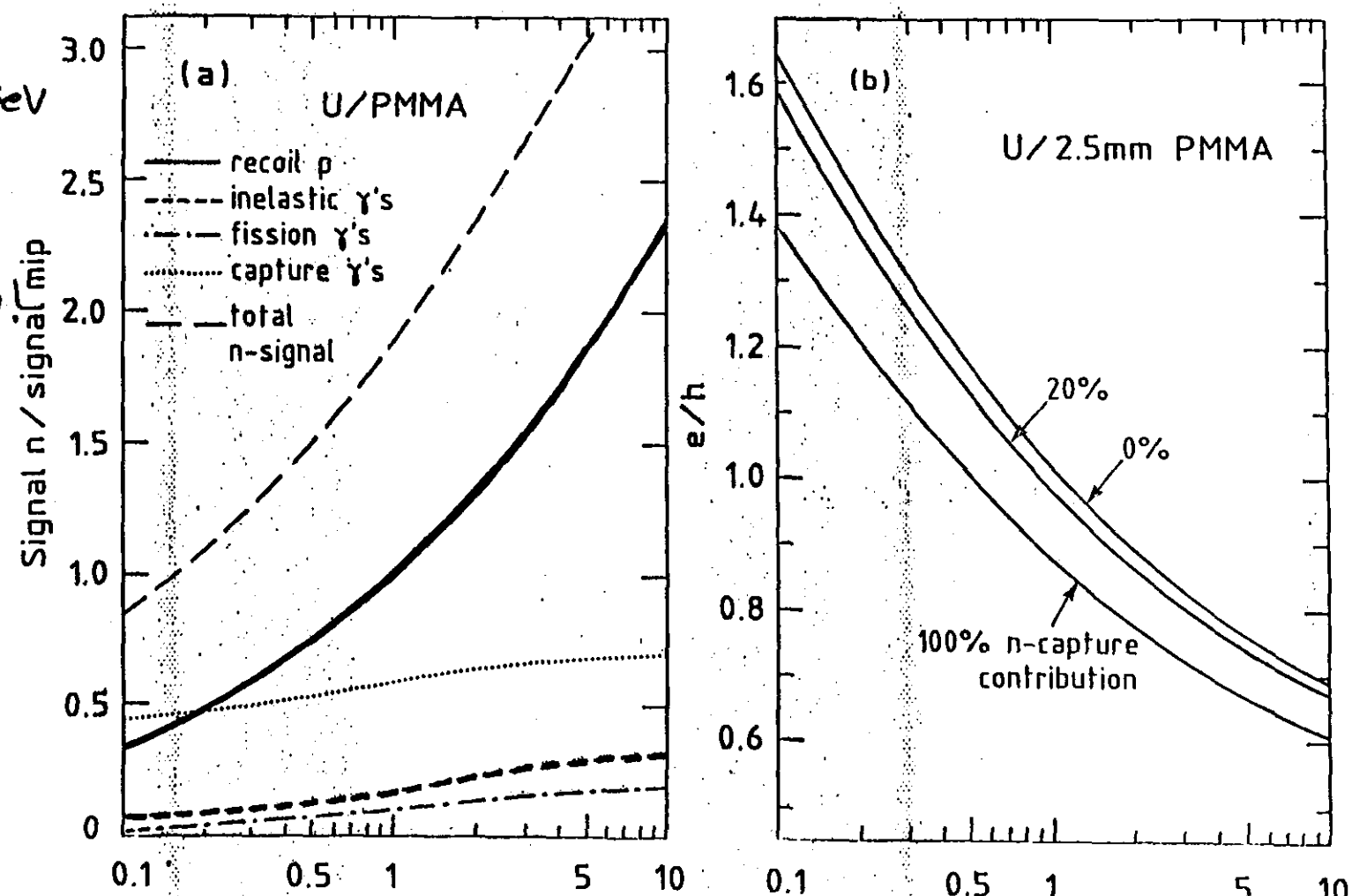

$R_d = \frac{\text{passive material}}{\text{active material}}$ → R_d

← sampling fraction —

Figure 36

RELATIVE CONTRIBUTION
neutrons TO CAL. SIGNAL

e/h SIGNAL
RATIO

^{238}U : ~60 n/GeV
ΔB_n ~ 5 MeV
→ from (n,γ) :
300 MeV/GeV

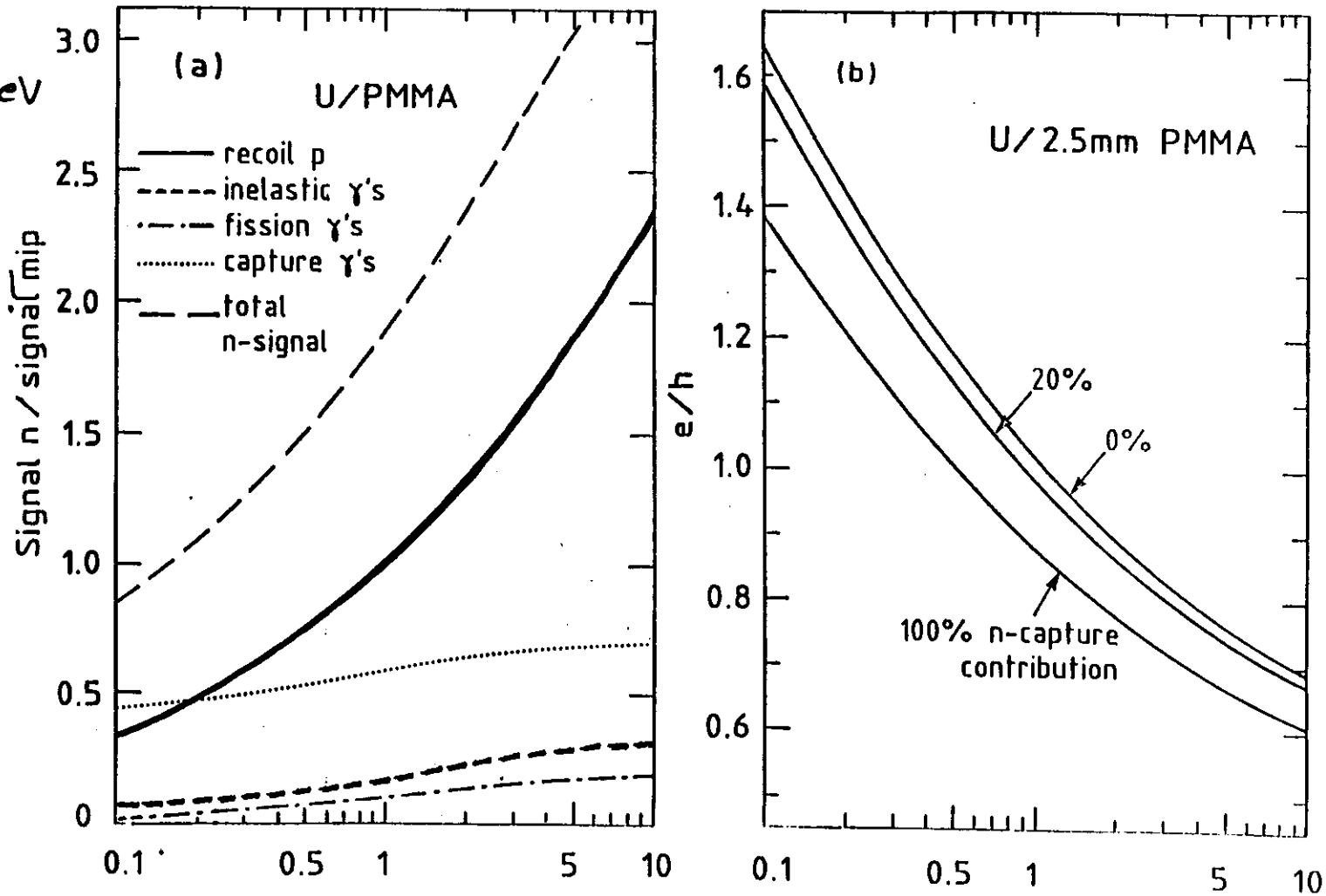

$R_d = \frac{\text{passive material}}{\text{active material}}$ → R_d

← sampling fraction —

Figure 36

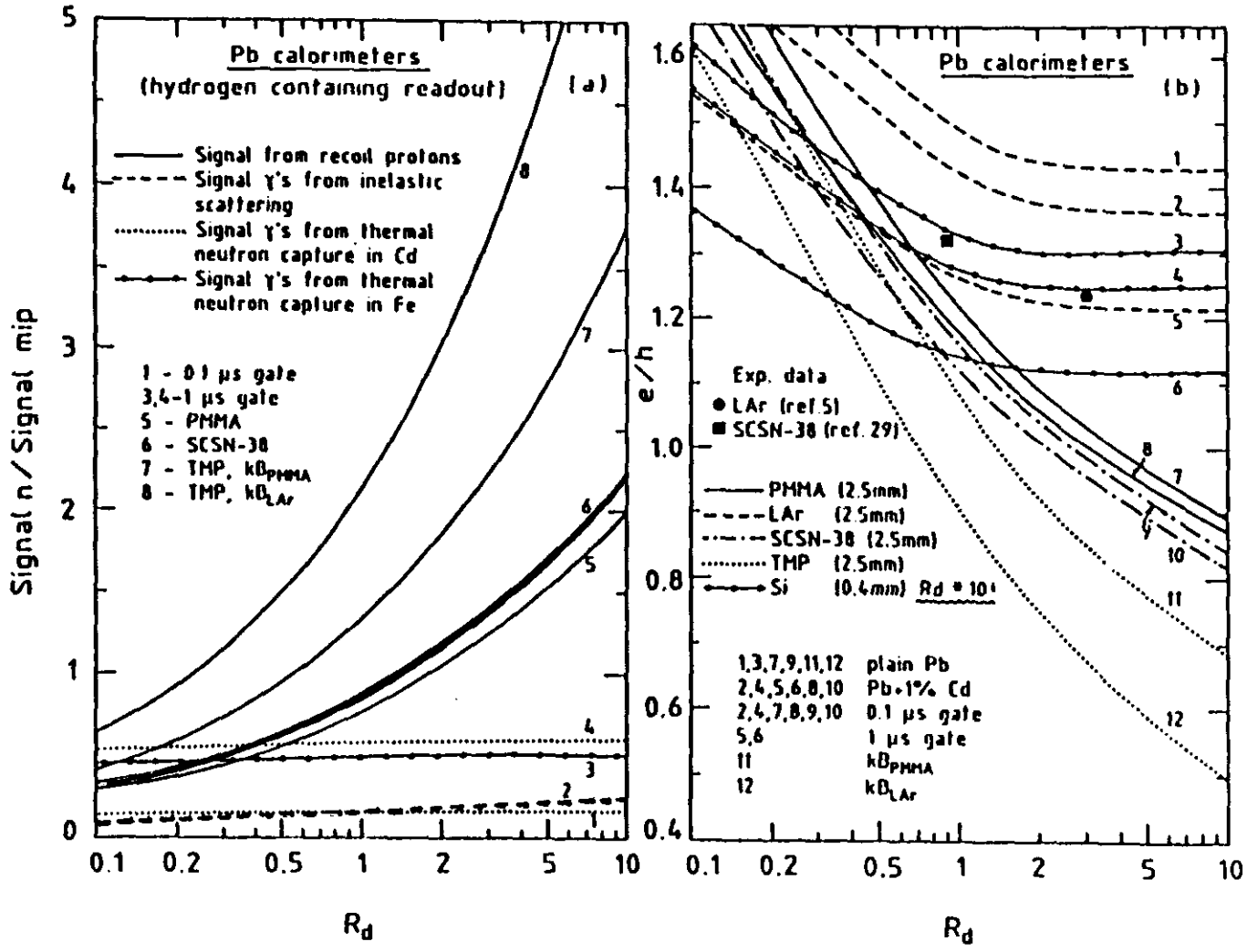

Fig. 19. (a) The signal ratio neutron/mip for lead calorimeters using various readout media, as a function of the ratio of the thicknesses of the absorber and readout layers. The full lines give the contribution of recoil protons. The other lines give the contribution of excitation and capture γ's for SCSN readout, assuming that capture takes place in iron or cadmium (see text). (b) The signal ratio e/h for lead calorimeters employing different readout materials, as a function of the ratio of the thicknesses of the absorber and readout layers. For Si readout the horizontal scale should be read multiplied by 10. See text for details.

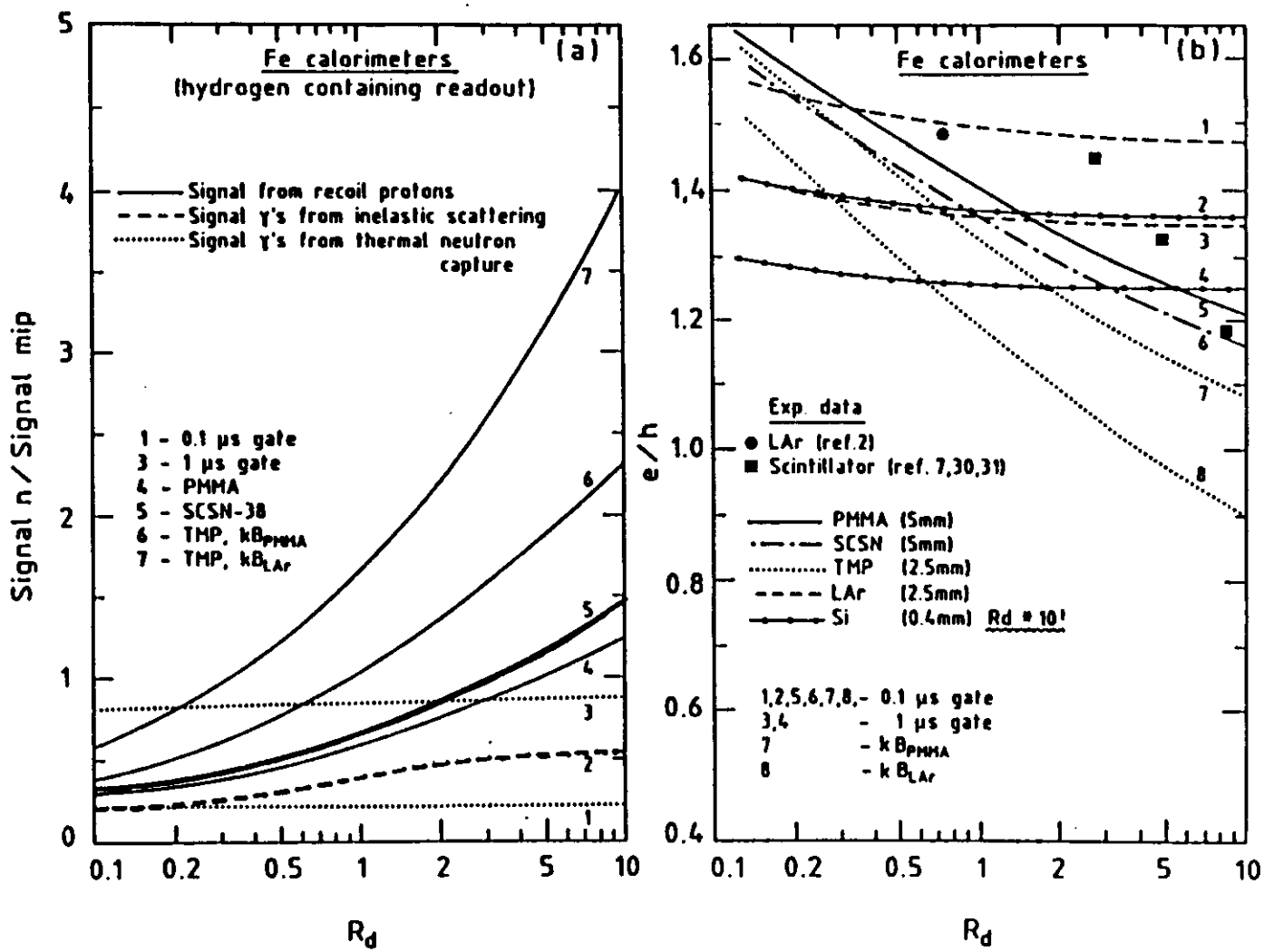

Fig. 20. (a) The signal ratio neutron/mip for iron calorimeters using various readout media, as a function of the ratio of the thicknesses of the absorber and readout layers. The full lines give the contribution of recoil protons. The other lines give the contribution of excitation and capture γ's for SCSN readout. See text for details. (b) The signal ratio e/h for iron calorimeters using different readout media, as a function of the ratio of the thicknesses of the absorber and readout layers. For Si readout the horizontal scale should be read multiplied by 10. See text for details.

e/h Cu calorimeters

$$e/h = \frac{e/mip}{0.51 + 0.08\ n/mip}$$

Configuration	e/mip	n/mip	e/h
Cu/fibers (5 vol %)	0.82	2.5	1.15
Cu/LAr	0.91	0.5	1.65
Cu/LKr	1.05	0.5	1.90

Experimental:

Fe/LAr : $e/\pi = 1.4$

Cu/fiber : $e/h \sim 1.2$

What are consequences of this
for calorimeter performance?

Only devices with comparable e/h values are homogeneous hadron calorimeters:

Liquid scintillator (NIM 125, 447)

- σ/E essentially constant for $E = 20 - 150$ GeV (12%)
- 15% signal nonlinearity
- non-Gaussian response

NaI (NIM 75, 130)

- $\sigma/E \sim 25\%$ at 8 GeV

Particle Data Booklet (p. 137)

constant term = 14% $[|1 - e/h|]$

↳ for hadronic energy measurements
(single hadron AND JETS)

Fluctuations in the π^0 fraction of hadron showers (σ_{RMS})

from NIM A316 (1992) 124

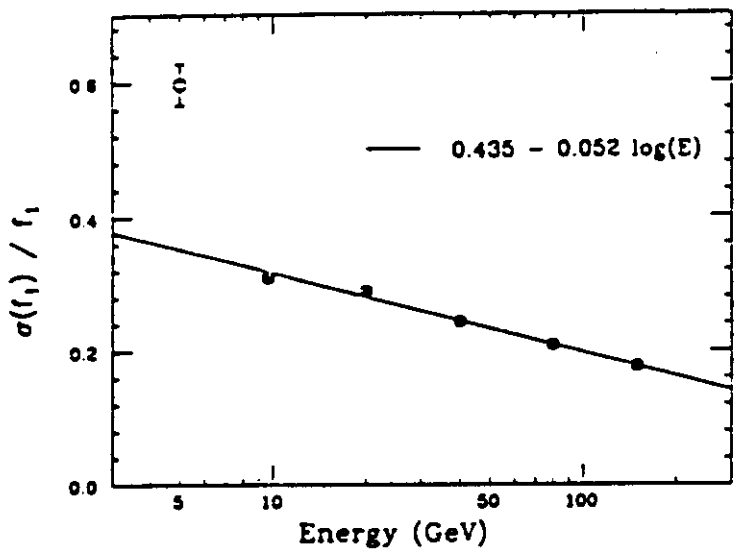

Fig. 22. The relative width $\sigma_{rms}(f_1)/f_1$ of the fraction of the hadronic shower energy contained in the central tower of the calorimeter as a function of the shower energy. The point at 5 GeV was not included in the fit. Data for pions entering this tower perpendicularly in its center.

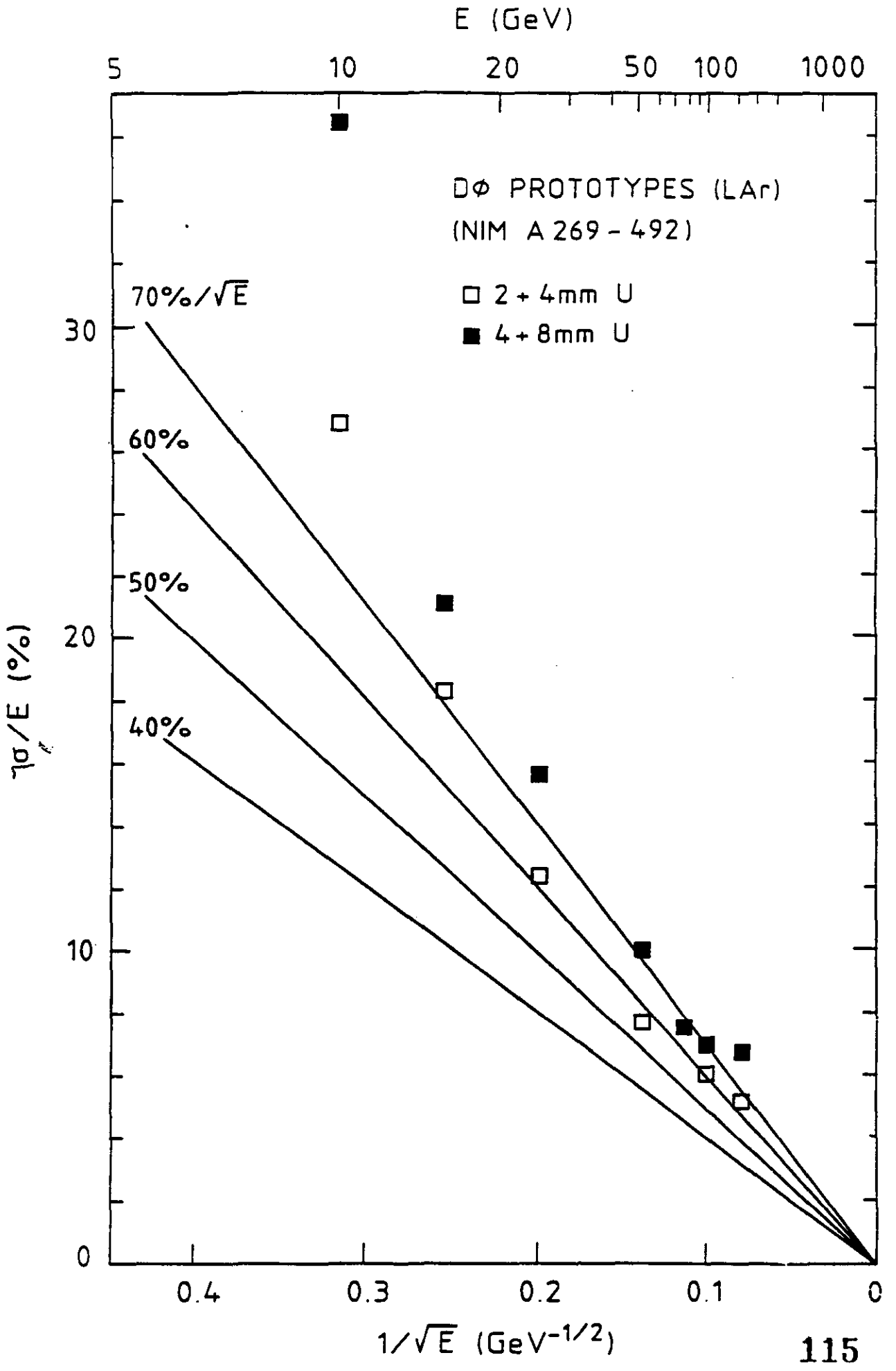
E (GeV)
5
10
20
50
100
1000
DØ PROTOTYPES (LAr)
(NIM A 269 - 492)
2 + 4mm U
4 + 8mm U
70%/√E
60%
50%
40%
30
20
10
0
σ/E (%)
0.4
0.3
0.2
0.1
0
1/√E (GeV^-1/2)

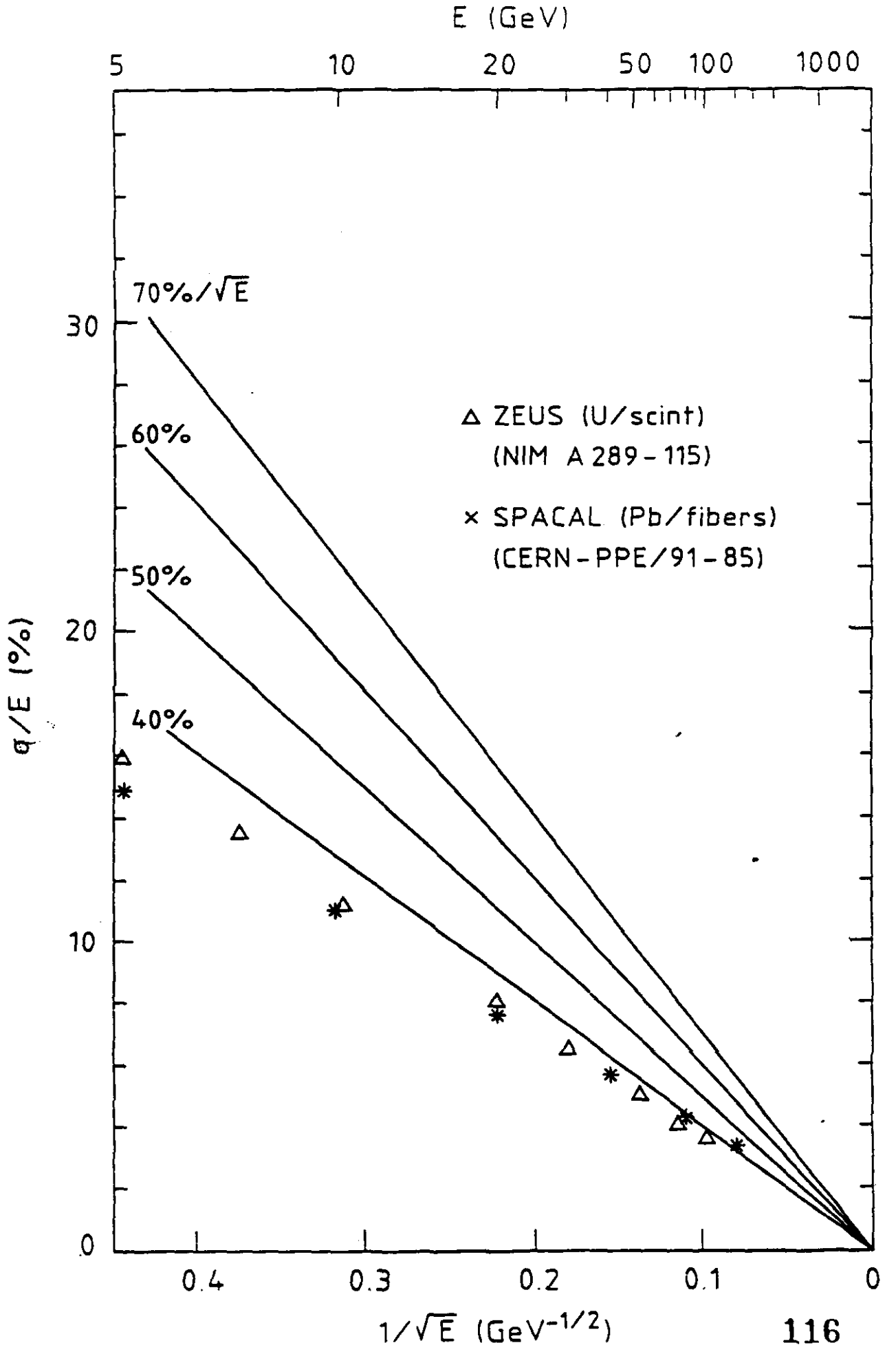
E (GeV)
5
10
20
50
100
1000
70%/√E
60%
50%
40%
30
20
10
0
σ/E (%)
△ ZEUS (U/scint)
(NIM A 289-115)
× SPACAL (Pb/fibers)
(CERN-PPE/91-85)
0.4
0.3
0.2
0.1
0
1/√E (GeV^-1/2)

gem

γeμ

Presentation by:

Bill Worstell

Bill Worstell

Energy (GeV)	Hybrid Resolution(%)	Integrated Resolution (%)
50	6.26	5.56
100	4.99	4.45
200	3.65	3.43
500	2.51	2.91
1000	1.90	2.96
2000	1.48	2.82
5000	0.99	2.63
10000	0.91	2.90

Table 1: $\alpha = 4$ Jet Energy Resolution

Energy (GeV)	Hybrid Resolution(%)	Integrated Resolution (%)
50	6.30	5.17
100	5.15	4.34
200	3.62	3.31
500	2.55	2.79
1000	1.90	2.39
2000	1.35	2.21
5000	0.98	2.04
10000	0.72	2.05

Table 2: $\alpha = 6$ Jet Energy Resolution

Energy (GeV)	Hybrid Alpha=4	Hybrid Alpha=6	Integrated Alpha=4	Integrated Alpha=6
50	.9966	.9960	.9943	.9920
100	1.0000	1.0000	1.0000	1.0000
200	1.0095	1.0090	1.0074	1.0065
500	1.0168	1.0175	1.0201	1.0187
1000	1.0240	1.0240	1.0375	1.0282
2000	1.0285	1.0280	1.0489	1.0398
5000	1.0342	1.0350	1.0616	1.0530
10000	1.0375	1.0380	1.0740	1.0634

Table 3: Jet Linearity vs. α

the signal and no backgrounds for the Z', the worsening of the resolution from 2.9% to 3.5% with a 2% additional constant term was deemed acceptable.

At the risk of being considered a partisan, however, one might well note that the hybrid:

1. Has better resolution at high energies (here it is argued that this makes only marginal improvement in the physics capability, as above)